UNIVERSITY OF COPENHAGEN
FACULTY OF SCIENCE

MSc. Thesis in Quantum Physics

Non-standard Neutrino Interactions in Compact Binary Merger Remnants

Samuel J. P. Bensted

Advisors: Dr. Irene Tamborra

Submitted: May 22, 2023

Abstract

The aim of this thesis is to find the effects of Non-Standard Interactions (NSIs) on the flavour evolution of neutrinos, in particular in the context of neutrino-rich Compact Binary Mergers (CBM). CBMs and their remnants are rich in both neutrinos and neutrons, and the neutron-rich ejecta are thought to be possible locations for heavy element production through the r-processes. In many hydrodynamical simulations of both the CBMs and their remnants, a common approximation is that neutrinos do not flavour oscillate. However, electron neutrinos in the CBM system may impact the proton-to-neutron ratio in the r-process region, and so the flavour evolution is very important. In particular, CBMs are rich in antineutrinos, so the neutrinos may experience a Matter-Neutrino Resonance (MNR), which may produce strong flavour conversions. Additionally, the neutrinos are an area of the Standard Model (SM) where new physics may appear and because of their small interaction rate, such new physics is relatively unconstrained. Therefore this thesis considers the effects that NSIs, below current experimental bounds, may have on the flavour evolution in a CBM at the boundary to the r-process region.

I consider only the outer regions of the CBM system, as the densities in the inner regions become so high as to trap the neutrinos and scatter them incoherently. I therefore study a Hamiltonian comprised of coherent matter neutrino-neutrino scatterings. On top of these effects, I add NSIs to the Hamiltonian and evolve the neutrinos under a mean-field approximation. I evolved the neutrino ensembles in two different systems. First, I considered a toy-model system to study the possible effects of the NSIs on well-known resonances, and found the NSIs to change resonance locations and the adiabaticity needed for resonances. The second system is a simulation of a BNS merger remnant by Ref. [1]. A few trajectories are picked out which represent the SM resonances that the system experiences. Indeed, both MNRs and MSW resonances are experienced with SM physics, although their occurrence is very trajectory dependent. In particular, MNRs only occur for trajectories which a close to the torus plane. Therefore averaging many trajectories decrease the effect of such resonances at different points in the system. Including NSIs changes the na-

ture of the oscillations quite dramatically. In particular, a new MSW-like resonance appears which is possible for both neutrinos and antineutrinos at the same location, even with a large background neutrino potential. This resonance can convert flavours maximally and has a steep cut-off in terms of adiabaticity. This also allows MNRs for positive neutrino potential. This means that the final flavour evolution in the SM trajectories can become completely inverted. This is very NSI parameter-dependent, and so a different set of parameters can yield a result where the averaged flavour conversion is dramatically different from the no-oscillation case. Additionally, the neutrino flavour evolutions may be decomposed in terms of variations of a subset of trajectories, meaning that it is the initial region and direction which is important for the flavour evolution. The rich parameter space of NSIs provide ample examples of the many possible impacts of NSIs on neutrino flavour conversions in a BNS merger remnant. In particular, NSIs may drive a new symmetric MSW resonance, which changes the final flavour evolution significantly as compared to SM evolutions. On the other hand, the possible flavour conversions of SM evolutions are suppressed by averaging over many trajectories. A parameter scan reveals that the NSIs can have a large impact on the final flavour, even when averaging over contribution from many trajectories.

Abbreviations

SM - Standard Model

NSI - Non-Standard Interactions

BNS - Binary Neutron Star

BH - Black Hole

CCSNe - Core Collapse Supernovae

NC - Neutral Current

CC - Charged Current

MSW - Mikheyev-Smirnov-Wolfenstein

MNR - Matter-Neutrino Resonance

Acknowledgements

I would like to thank Irene Tamborra for supervising and guiding this thesis and for inclusion into her group at the NBIA. I wish to also thank Shashank Shalgar for the many discussions, always being up for a discussion, and challenging me to become a better physicist. I want to thank Amit Singh, Pedro Dedin, Marie Cornelius, Annika Rudolph and Ersillia Guarini for discussions and broadening my view of physics. Lastly I want to thank Laura Rysager for helping me and encouraging me so much during my thesis time.

Contents

Introduction

The development of quantum field theory has been through a reconciliation of the principles of special relativity with those of quantum mechanics, whilst preserving the axioms of each theory [48]. In the 1960s and 70s, a lot of ideas were put forth, discussions had, and experiments were probing the edge of our understanding, which ended up formulating the Standard Model (SM) of particle physics. The Standard Model was written as an $SU(3) \otimes SU(2) \otimes U(1)$, a gauge symmetry, and in addition, one needs empirical evidence in order to constrain the parameters of the model [49]. The core of the model is a set of particles, 12 fermions, 4 vector bosons and single scalar bosons, as well as their antiparticle counterparts. The vector bosons are 4 gauge bosons, the photon, the W and Z bosons, and the gluons, which all mediate interaction and are known as "force carriers". The scalar boson is the Higgs boson. Of the fermions, there are the 6 quarks, and lastly, there are the 6 leptons, electrons, and neutrinos. The discovery of beta electrons in beta decay produced an anomaly in the 1930s, as the kinetic energy of the electrons varied. Fermi proposed that perhaps there was an additional, undetectable particle emitted, which he named the neutrino, the 'little neutral one'. These particles were discovered in weak interaction, and since then the bounds still suggest that they interact only weakly, leaving one neutrino type for each charged lepton: electron-, muon-, and tau-neutrinos. Since the weak interaction maximally violates parity, only left-chiral neutrinos needed to be included in the SM. This also suggested that the particle did not have a mass, as these are generated through a Dirac mass, which couples left- and right-chiral particles. Therefore they were characterised by their weak isospin, spin, lepton number and masslessness. An example of this is beta minus decay, where a neutron decays to a proton, an electron, and an electron antineutrino, where the electron antineutrino makes up for the electron's positive lepton number. In the 1980s it was also established that the neutrino may be massive, meaning they interact with gravity, but gravity is not a part of the SM. However, the upper bound on their mass scale is of the order 10^{-37} [kg], meaning that this interaction is incredibly weak [47].

Neutrinos 1. are electrically neutral, 2. do not participate in strong interactions, 3.

have extremely small mass (from upper bounds), and 4. have short-ranged, weak interaction, and so neutrinos are largely free-streaming for most of their propagation throughout the universe. Omitting the well-known photons, they are the most abundant particles in the universe [43]. In this way they are good candidates for astronomical signatures, as they provide a large amount of direct data from their source, whereas light is more easily absorbed on their path, cosmic rays/ions are dispersed by magnetic fields and gravitational waves are hard to detect for all but the heaviest cosmic mergers. However, this non-interaction feature, which is so good for astronomical signatures, is quite a hindrance when it comes to observations. Neutrino interaction cross-sections are generally so small that it takes either a large volume of material or incredibly dense materials, in order to actually observe the neutrinos. Hence we have huge experiments, like the IceCube collaboration, which uses 1 km^3 worth of ice nuclei[1] as targets for neutrino interactions. The interactions produce charged leptons, generating Cherenkov radiation which is detected by a photodetector. However, one can use all of the astronomical methods mentioned above in a combined 'multi-messenger' view of astronomy, where each provides a piece of the puzzle, such as a possible neutrino prompt emission of Gamma-Ray Bursts being useful for setting the photon telescopes to a particular region [42].

Neutrinos are part of any weak interaction involving charged leptons, and so they also affect any nucleosynthesis (the production of new materials) which involves beta reactions. An atomic nucleus may capture a number of neutrons until it becomes unstable and decays into another element, emitting a neutrino in the process. The rate of the process gives the range of possible initial conditions from which these processes may occur. If there exist stable heavy elements already (seeds), the neutron capture may be slow and decay to heavier elements. If there are no seeds, then the capture must be fast, such as to create the seeds from which to create heavy elements. These elements also tend to be the neutron-rich stable isotopes of the elements. These two regimes are known as the s- and r-processes, for 'slow' and 'rapid'. The r-process needs a large number of neutrons and so the expected production sites are core-collapse supernovae (CCSNe) or the envelope of a Compact Binary

[1] at the South Pole!

Merger (CBM) Remnant. Such CBM Remnants might be from the merger of a Neutron Star (NS) and a Black Hole (BH), a merger of a binary NS (BNS) system or a BH-BH merger, resulting in either a BH or hypermassive NS. The CCSNe and BNS mergers are both neutron-rich environments. The CCSNe is neutron-rich due to the compression of electrons and protons, forming a neutron star at its core, and the BNS system is already a system of neutron stars, which are 90% neutrons.

In this thesis, I will focus on a BNS merger remnant simulation performed by [1]. The BNS merger may end in a torus-like object surrounding a black hole. As the remnant cools, it ejects much of its mass into the outer shell, meaning the nuclei capture the neutron-rich material and undergoes r-processes to generate heavier elements. However, the decompression of the neutrons in the torus produces protons, electrons, and antineutrinos again. In addition, the overall temperature of the event also produces electron neutrino-antineutrino pairs. As these neutrinos enter the outer shell they may impact the proton-to-neutron ratio, as they go through inverse beta reactions (see fig. 1). If the ratio of antineutrinos to neutrinos is large, then the r-processes are increased, due to the increase in abundance of neutrons, leading to an overall increase in heavier, neutron-richer elements. The reverse gives a decrease in the r-processes and fewer neutron-rich, heavy elements. The impact of neutrinos in such environments is therefore an important area of study.

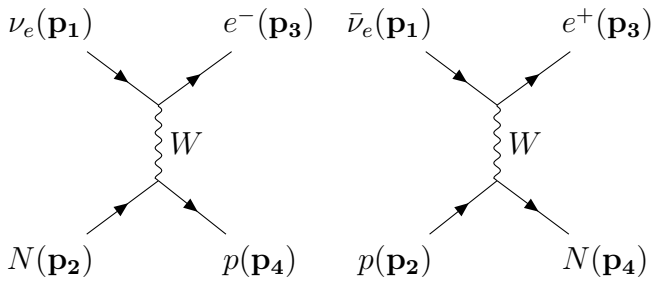

Figure 1: Inverse beta decays. The left diagram shows an electron neutrino-neutron interaction producing electrons and protons. The right diagram shows a proton-electron antineutrino interaction producing a positron and neutron.

As neutrino interactions are very rare, most neutrino detection experiments are hosted underground. The reasoning behind having the experiments underground, or under large

amounts of water, is that most other particles will be scattered by the time they reach the detector, reducing the background. These experiments mostly consist of large volumes which either detect Cherenkov light, use a scintillator or by looking at how the composition of the material changes. Given that neutrinos are produced as flavours in weak interactions, and that their subsequent interaction is limited, one might expect that any neutrinos produced in the sun will be detected as the same flavour in the underground detectors here on Earth. To begin with, the experiments checked the theoretical predictions of solar neutrinos, as this was the largest natural neutrino production site which might produce a detectable signal. The Homestake experiment [28] detected a discrepancy in the expected number of flavour states along the neutrino propagation line. They saw fewer electron neutrinos than expected and then the SNO experiment [29] was able to detect both the electron flux and combined flux of all flavours. The electron flux was indeed lower, but the total flux predicted for the neutrinos was as expected, indicating that the neutrinos were just of a different flavour. Years prior, Pontecorvo [27] postulated that neutrinos might experience an oscillation and build a model for the oscillations. Over the years he made different models, for neutrino-antineutrino oscillations and neutrino-sterile neutrino oscillations, but they could be adapted to another model. One could view the oscillations to have two implications: neutrinos are actually massive, and there is a misalignment between the mass states and flavour states. That the neutrinos are massive is implied by the fact that, in order to oscillate the states must experience time. If they experience time, then they must be going slower than the speed of light, which is true of massive objects. Both the Dirac and Klein-Gordan eqs. [49] imply that the massive states are eigenstates of propagation. Given that this oscillation between flavours is something which occurs during propagation from the production site to the detection site, then they cannot be eigenstates of propagation. Hence the flavour states are not aligned with the massive states, and there must exist some mixing matrix which relates the flavour states to the mass state. So it is an empirical fact of oscillations which implies that neutrinos are massive. The SM does not contain massive neutrinos, but the mass terms can be generated with either Dirac or Majorana masses. The implications of the mass type are manifold, affecting everything

from Leptogenesis (see below) to Dark Matter candidates. Luckily, the character of the mass does not affect the nature of the neutrino flavour oscillation, and I will disregard it for the purpose of this thesis.

That the neutrinos oscillate between flavours has a possible impact on the r-process outside of the CCSNe and BNS mergers. The energy scale of the BNS merger is still such as to produce standard matter (first generation particles) and if the electron neutrino now oscillates away to a muon or tau flavour, then the inverse beta decay may not occur anymore. Hence looking at the effects of neutrino flavour oscillations will be an important aspect of the neutrino impact on r-processes happening in the outer shell of the BNS merger.

The SM produces incredibly accurate predictions in the domain of particles which should exist, such as the W- and Z-bosons, up- and down-quarks, and famously the Higgs in 2012. However, in some areas, the model falls short. There is to date no implementation of gravity which can be experimentally verified. Baryogenesis, there seems to be more matter than antimatter around, is also unexplained. Therefore there are proposed extensions to the SM, which go from minimal extension, such as adding an additional neutral particle like a right-handed neutrino, or families of new particles in the supersymmetric (SUSY) extensions. There are, for example, proposed solutions to Baryogenesis, which involve the neutrino sector. Their role may be in explaining such an asymmetry through a process known as Leptogenesis [25]. This process can, formally, occur for both Dirac and Majorana neutrinos. The extension into Majorana neutrinos is minimal, as these neutrinos are their own antiparticles but imply lepton number non-conservation. This gives way to an asymmetry in the baryon sector through the neutrino weak interactions. The Dirac neutrinos may also provide Leptogenesis through a combination of sphalerons and neutrino equilibration in the early universe, due to a discrepancy between left and right Yukawa couplings [25].

The SM needs to be extended in order to account for neutrino masses, whose form is still undecided. The neutrinos masses may also point in the direction of extension of the SM, an effective theory in the low energy sector. Here new mediators could give rise to

new interactions which change the production, detection and propagation of the neutrinos. The specific form of the general extension differs and the constraint is typically model dependent, but in general, one can write point-like interactions for the neutrino. For this thesis, I consider Non-Standard Interactions (NSIs) which consist of Fermi point interaction with common matter, meaning electrons, up- and down-quarks.

The main goal of this thesis is to find the impact of these NSIs on the flavour oscillations of neutrinos, but in particular, I will consider the NSI effects on neutrinos (and antineutrinos) in a BNS system. This is to see the effects of NSIs on the flavour evolution, as the neutrinos propagate into the r-process region, because as stated earlier, the neutrinos impact the neutron-to-proton ratio, thereby affecting the r-process and, finally, change the element composition synthesized. The way in which I will do this is by building up the theory for neutrino propagation. I'll start by explaining what the neutrinos are and what SM interactions they experience as well as give examples of how the flavours oscillations are changed by these. To finish the theory section I introduce NSI interactions.

With the theory done, I go to the numerical part of the thesis. I numerically solve the flavour evolutions in two different systems: A toy-model system, and a simulated BNS system. In these systems, I then go through the possible flavour oscillations, first due to SM physics, and then due to NSIs. I finish off the numerical section with a parameter scan of possible NSI configurations and provide an analysis of the different sectors within the parameter space, in particular how the trajectories decompose into just a handful of archetypical trajectories.

Therefore I will slowly put together the theoretical parts needed to explore the effects of non-standard neutrino interactions on the neutrino flavour oscillations in the BNS system. I'll start by reviewing the theory of the Standard Model and what neutrinos are.

Theory of Neutrino Flavour Evolution

Standard Model Neutrinos

In the Standard Model, as mentioned above, the neutrinos identified as flavour states, which are split into three generations, each associated with a charged lepton: $\nu_e,\ \nu_\mu,\ \nu_\tau$ couple to $e,\ \mu,\ \tau$ in SU(2) doublets, $L_\alpha = \begin{pmatrix} \alpha \\ \nu_\alpha \end{pmatrix}$. These are known as the neutrino *flavour* states. The neutrinos basically only interact weakly, meaning that their interaction vertices in the SM Lagrangian can be written as follows,

$$\mathcal{L}_{SM} \supset \mathcal{L}_\nu = \sum_{\alpha=e,\mu,\tau} \left[\left(\frac{g}{\sqrt{2}} \bar{\nu}_\alpha \not{W} P_L \alpha + h.c. \right) + \frac{g}{2\cos\theta_W} \bar{\nu}_\alpha \not{Z} P_L \nu_\alpha + i\bar{\nu}_\alpha \not{\partial} \nu_\alpha + \mathcal{L}_{mass} \right] \quad (1)$$

where g is the weak coupling constant, the feynman slashed $\not{W},\ \not{Z}$ are the weak interaction bosons, $\gamma^\mu W^\pm_\mu,\ \gamma^\mu Z^0_\mu$, θ_W is the Weinberg angle, P_L is the projection operator[26]. Examples of these interaction vertices can be seen in fig. (2). The W interactions are known as Charged Current (CC) interactions and the Z are known as Neutral Current (NC). The (chiral) projection operator P_L is there because the weak interaction maximally violates parity, only affecting left-chiral states. The mass Lagrangian is unspecified, as it might be a Dirac type or Majorana type mass, but one might write a general Lagraganian as,

$$\mathcal{L}_{mass} \sim \sum_{\alpha,\beta} \bar{\nu}_\alpha M_{\alpha\beta} \nu_\beta + h.c. \quad (2)$$

In particular, the mass matrix M may not be diagonal, meaning that lepton flavour number coudl be violated, and experiments seem to point this way, as we will now explore.

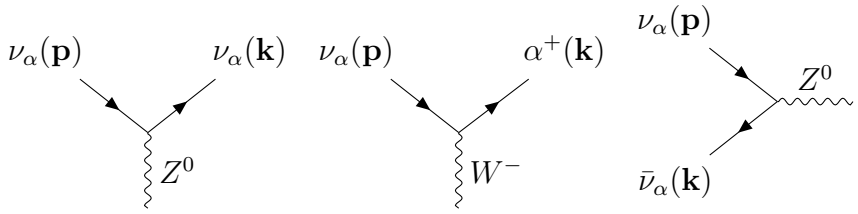

Figure 2: Standard Model Neutrino interaction vertices. The left most diagram is an example of a Neutral Current interaction. The middle is an example of a Charged Current interaction. The last is a Neutral Current annihilation.

Vacuum oscillation

Neutrinos are produced as flavour states in weak interactions and propagate throughout the universe, but due to the weak coupling being, well, weak, the neutrinos rarely interact with anything. Therefore one might imagine that a neutrino flavour produced in, say, a fusion process in the Sun, might then propagate all the way down to the Earth and be detected in one of the underground detectors set up. However, these underground experiments detected a discrepancy in the expected number of flavour states along the neutrino propagation line. First the Homestake experiment [28] saw fewer solar electron neutrinos than expected and then SNO [29] detected a similar amount of solar electron neutrinos, but from neutral currents that could also see that the total flux was as expected. This indicates that the solar electron neutrinos must have changed their flavour during their propagation. Years prior, Pontecorvo [27] postulated that the then-known electron neutrino might oscillate into a sterile (0 weak isospin) neutrino [26]. This framework was readopted when muon neutrinos were discovered and it was postulated that neutrinos are actually massive and that there was a misalignment between the mass states and flavour states. Assuming that the neutrinos are oscillating in vacuum, this misalignment is implied by the massive states being the eigenstates of the propagation of the neutrino, due to being solutions to the Dirac and Klein-Gordan eqs. [49]. Since the flavour states are oscillating, they cannot be simultaneous eigenstates of the propagation or their flavour would be conserved. Therefore it makes sense to postulate the relation following relation between flavour states $\nu_{\mathbf{F}}$, made

of α flavours, and mass states $\nu_{\mathbf{M}}$, containing j massive states,

$$\nu_F = U\nu_M \qquad \Longrightarrow \qquad |\nu_\alpha(\mathbf{x},t)\rangle = \sum_j^N U_{\alpha j}\,|\nu_j(\mathbf{x},t)\rangle \tag{3}$$

Where N is the number of orthogonal massive states $|\nu_j(\mathbf{x},t)\rangle$, U is a unitary mixing matrix. The probability of an initial α flavour becoming a γ flavour at times t is $P_{\nu_\alpha\to\nu_\gamma}(\mathbf{x},t) = |\,\langle\nu_\gamma|\nu_\alpha(\mathbf{x},t)\rangle\,|^2 = |\psi_{\gamma\alpha}(\mathbf{x},t)|^2$. Since the massive states are eigenstates of the Dirac equation, they have plane wave solutions and I can write,

$$|\nu_\alpha(\mathbf{x},t)\rangle = \sum_j^N U_{\alpha j}e^{-i(p_j)^\mu x_\mu}\,|\nu_j\rangle = \sum_j^N U_{\alpha j}e^{-i\phi_j}\,|\nu_j\rangle \tag{4}$$

where $|\nu_j\rangle = |\nu_j(\mathbf{0})\rangle$ for simplicity. Finding the wave function coeffficient then becomes easy enough, by transforming to and from the mass states,

$$\psi_{\gamma\alpha}(\mathbf{x},t) = \langle\nu_\gamma|\nu_\alpha(\mathbf{x},t)\rangle = \sum_k^N\sum_j^N e^{-i\phi_j}\,\langle\nu_k|\,U^*_{\gamma k}U_{\alpha j}\,|\nu_j\rangle \tag{5}$$

Squaring the coefficient gives me the transition probability,

$$P_{\nu_\gamma\to\nu_\alpha}(\mathbf{x},t) = |\psi_{\gamma\alpha}(\mathbf{x},t)|^2 = \sum_{kljn}^N e^{-i(\phi_j-\phi_n)}\,\langle\nu_n|\,U^*_{\alpha n}U_{\gamma l}\,|\nu_l\rangle\,\langle\nu_k|\,U^*_{\gamma k}U_{\alpha j}\,|\nu_j\rangle \tag{6}$$

$$= \sum_{jn}^N e^{-i(\phi_j-\phi_n)}U^*_{\alpha n}U_{\gamma n}U^*_{\gamma j}U_{\alpha j} \tag{7}$$

In general the transition probability can be written as [26],

$$P_{\nu_\gamma\to\nu_\alpha} = \delta_{\alpha\gamma} - \sum_{j>n}^N\left(4Re\left[U^*_{\alpha n}U_{\gamma n}U^*_{\gamma j}U_{\alpha j}\right]\sin^2\left(\frac{\phi_j-\phi_n}{2}\right) - 2Im\left[U^*_{\alpha n}U_{\gamma n}U^*_{\gamma j}U_{\alpha j}\right]\sin(\phi_j-\phi_n)\right) \tag{8}$$

So we see that $P_{\nu_\gamma \to \nu_\alpha}$ is governed by the phase of the plane waves. This phase can be found either via simplistic arguments, or one can consider the wave packet nature of the particles [30]. In the cases of complete coherence and complete incoherence, one arrives at the same result, although the physical assumptions are markedly different. In the simplistic argument the wavefunctions are plane waves, and the phase is given by $\phi_j = p_j^\mu x_\mu = E_j t - \mathbf{p}_j \cdot \mathbf{x}$. Assuming the energies are equal $\Delta \mathbf{E}_{jn} = 0$ and the planes waves travel along the same line, the difference must be due to the momenta,

$$\phi_j - \phi_n = \Delta E_{jn} t - \Delta \mathbf{p}_{jn} \cdot \mathbf{x} = \Delta p_{jn} x \tag{9}$$

Letting the energy of the states be the same ($\mathbf{E}_j = \mathbf{E}_n$), the first term dies away and the momenta can be expanded $p_j = |E|\sqrt{1 - \frac{m^2}{E^2}}$. In the ultrarelativistic limit limit of $m_j << E$,

$$\Delta p_{jn} \simeq E_j(1 + \frac{m_j^2}{2E_j}) - E_n(1 + \frac{m_n^2}{2E_n}) = \frac{\Delta m_{jn}^2}{2E} \tag{10}$$

Where $\Delta m_{jn}^2 = m_j^2 - m_n^2$. So to first order the phase difference between the neutrino states is due to the difference in the masses of the massive states. If one took the wavepacket approach, one would arrive at the phase difference being due to the overlap of the wavefunctions, and the oscillation would attenuate as the wavepackets separate and consequently decohere [30].

Now I have established the general form of the transition probability and found that the phase difference is due to a difference in mass between the neutrino states, we can narrow our view to that of the Standard Model. Here $N = 3$, and the mixing parameters have been measured as in Table 1.

Mixing Parameters	Normal Ordering (90% CL)	Inverted Ordering (90% CL)
Δm^2_{21}	$(7.53 \pm 0.18) \cdot 10^{-5}$ $[eV^2]$	$7.53 \pm 0.18 \cdot 10{-}5$ $[eV^2]$
$\sin^2(\theta_{12})$	$0.307^{+0.0013}_{-0.012}$	$0.307^{+0.0013}_{-0.012}$
Δm^2_{23}	$(2.453 \pm 0.033) \cdot 10^{-3}$ $[eV^2]$	$-2.536 \pm 0.034 \cdot 10^{-3}$ $[eV^2]$
$\sin^2(\theta_{23})$	0.546 ± 0.021	0.539 ± 0.022
$\sin^2(\theta_{13})$	$(2.20 \pm 0.07) \cdot 10^{-2}$	$2.20 \pm 0.07 \cdot 10^{-2}$
δ (CP-phase)	$1.36^{0.20}_{-0.16} \cdot \pi$	$1.36^{0.20}_{-0.16}\dot{\pi}$

Table 1: Best fit values from the Particle Data Group in 2022 [31].

Because of the large separation between the mass differences, the oscillations can be split into different regimes. The vacuum oscillations wavelength in the Δm^2_{21} sector is two orders of magnitude above the wavelength of Δm^2_{32}. Therefore I'll consider a two-level system, i.e. $N = 2$, so that I can identify how the neutrino oscillations occur in this simplified system. Figure (3) shows this to be a fine approximation, since the oscillations do not interfere, if I consider just a few oscillation lengths.

For $N = 2$, U is a 2×2 matrix with four independent variables, however, three of these can absorbed as global phases into the lepton states of the charged current interaction, $j_{CC} = 2\sum_{\alpha,j} \bar{\alpha}_L \gamma_\nu U_{\alpha j} \nu_{j_L}$ [26], by rewriting $(\bar{\alpha}_L, \nu_{j_L}) \longrightarrow (\bar{\alpha}_L exp(i\epsilon), \nu_{j_L} exp(i\beta))$. This can be done in 3 independent ways, for 4 states. Therefore the mixing matrix becomes just a rotation matrix, described by the mixing angle θ,

$$U = \begin{pmatrix} \cos(\theta) & \sin(\theta) \\ -\sin(\theta) & \cos(\theta) \end{pmatrix} \tag{11}$$

I will be working with an ultra relativistic neutrino state composed of an electron neutrino and a heavy 'x' flavour, which could, for example, be a linear superposition of the muon and tau neutrinos, $\nu_x = \frac{1}{\sqrt{2}}(\nu_\mu + \nu_\tau)$, $\nu_F = (|\nu_e\rangle, |\nu_x\rangle)$. The massive states, $\nu_M = (|\nu_1\rangle, |\nu_2\rangle)^T$, obey the Schrödinger equation,

$$\frac{\partial \nu_M(\mathbf{x}, t)}{\partial t} = -\frac{i}{\hbar}\mathcal{H}_M \nu_M(\mathbf{x}, t), \qquad \mathcal{H}_M = \frac{1}{2E}\begin{pmatrix} m_1^2 & 0 \\ 0 & m_2^2 \end{pmatrix} \tag{12}$$

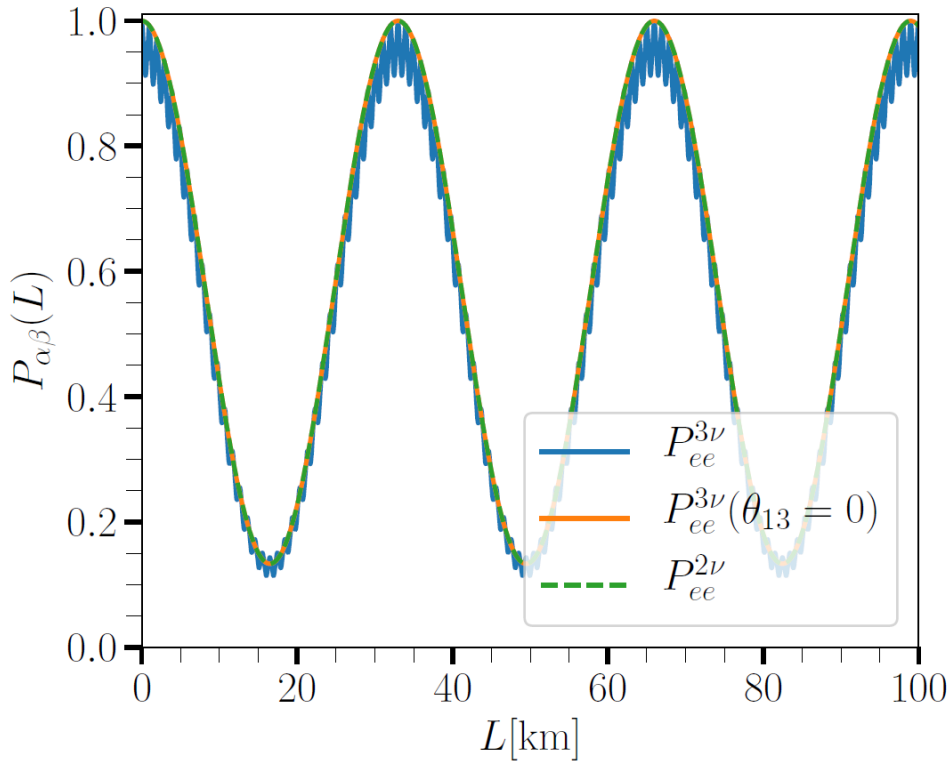

Figure 3: Three neutrino oscillations and two neutrino oscillations. $P^{n\nu}_{ee}$ refers to the oscillation survival probability of the 'n' neutrino system. As one can see, the oscillation of one sector happens at a completely different length scale compared to the other sector. Figure taken from Ref. [32]

A global phase does not affect oscillations, therefore I remove something proportional to unity, in order to symmetrize the problem a bit (and setting $\hbar = 1$ for simplicity),

$$\mathcal{H}_M - \frac{tr(\mathcal{H}_M)}{2} = \frac{\omega}{2}\begin{pmatrix} -1 & 0 \\ 0 & 1 \end{pmatrix}, \qquad \omega = \frac{\Delta m^2}{2E}, \qquad \Delta m^2 = m_2^2 - m_1^2 \tag{13}$$

Using eq. (3) and U, I can rewrite eq. (12) in terms of flavour,

$$\frac{\partial \nu_F(\mathbf{x},t)}{\partial t} = -iU\mathcal{H}_M U^\dagger \nu_{\mathbf{F}}(\mathbf{x},\mathbf{t}) = -i\mathcal{H}_F = -\frac{i\omega}{2}\begin{pmatrix} -\cos(2\theta) & \sin(2\theta) \\ \sin(2\theta) & \cos(2\theta) \end{pmatrix}\nu_F(\mathbf{x},t) \tag{14}$$

where $\mathcal{H}_F = U\mathcal{H}_M U^\dagger$ is known as the flavour *vacuum Hamiltonian*. Looking at the time evolution of an electron neutrino it becomes even more readily apparent that the neutrino flavours evolve into one another due to a phase difference between the mass states,

$$|\nu_e(\mathbf{x},t)\rangle = \left(\cos^2(\theta)e^{i\phi_1} + \sin^2(\theta)e^{i\phi_2}\right)|\nu_e\rangle + \sin(\theta)\cos(\theta)\left(e^{i\phi_2} - e^{i\phi_1}\right)|\nu_\alpha\rangle \tag{15}$$

Having established how flavour oscillations happen in vacuum and that it is due to a phase difference due to the neutrino masses, I switch to the (flavour) density matrix (ρ) formalism. For each neutrino state of initial flavour δ, $|\nu_\delta(\mathbf{x},\mathbf{p},t)\rangle$, I can define the single particle density matrix operator, which is given by,

$$\hat{\rho}(\mathbf{x},t) = \sum_\delta |\nu_\delta(\mathbf{x},t)\rangle\langle\nu_\delta(\mathbf{x},t)| \tag{16}$$

where the expectation values with respect to the flavour states describe the configuration of the neutrino state,

$$\langle\rho_{\alpha\beta}(\mathbf{x},t)\rangle = \sum_\delta \langle\nu_\alpha|\nu_\delta(\mathbf{x},t)\rangle\langle\nu_\delta(\mathbf{x},t)|\nu_\beta\rangle \tag{17}$$

The diagonal entries gives the occupation number of the state, which may be a mix of possible initial flavours and the off-diagonal gives the level of coherency or correlation

between the flavours. The sum over δ is implied by the flavour oscillation since the states may oscillate into one another, changing the occupation numbers. From here on I will be referring to the expectation value of the density operator when I refer to the density matrix, as I am interested in how the configuration of the state changes. Furthermore, I will use population and occupation number interchangeably for the diagonal entries. The time evolution of the single-particle density matrix is found by expanding $\frac{\partial \rho_{\alpha\beta}}{\partial t}$, yielding the Liouville Von Neumann eq.,

$$\frac{\partial \rho(\mathbf{x}, t)}{\partial t} = -i \left[\mathcal{H}_F, \rho(\mathbf{x}, t)\right] \tag{18}$$

All of the above treatment for oscillations and density matrices is the same for the antineutrinos ($\bar{\rho}$), and so,

$$\langle \bar{\rho}_{\beta\alpha}(\mathbf{x}, t)\rangle = \langle \bar{\nu}_\alpha | \bar{\nu}_\delta(\mathbf{x}, t)\rangle \langle \bar{\nu}_\delta(\mathbf{x}, t) | \bar{\nu}_\beta\rangle \tag{19}$$

where the reversed flavour structure guarantees that both ρ and $\bar{\rho}$ transform the same way under U [33].

This formalism becomes especially useful when considering large ensembles neutrinos. For this large ensemble of neutrinos, the system should be described by a total density matrix of entangled neutrinos for each momentum mode, equivalent to an m-particle Green's function. However, I can approximate the evolution of the ensemble, by identifying each singular neutrino and let all other neutrinos act as a background medium. This is known as the *mean-field approximation* [43]. The system is then decoupled from non-local interactions with each other and each neutrino can be described by the time evolution of single particle density matrix [16],

$$\frac{\partial P(\mathbf{x}, \mathbf{p}, t)}{\partial t} = -i \left[\mathcal{H}_F, P(\mathbf{x}, \mathbf{p}, t)\right] \tag{20}$$

where $P(\mathbf{x}, \mathbf{p}, t) d^3\mathbf{p} = dn_{\nu_\mathbf{p}}(\mathbf{p}, t)\rho(\mathbf{x}, \mathbf{p}, t)$ is the single particle density matrix weighted by the differential number density $n_\nu(\mathbf{p}, t)$ due to the mean field of other neutrinos contained

in the differential momentum volume $d^3\mathbf{p}$.

This approximation is justified in the many-body theory [33]. By only considering (physical) bilinears, the free (no interaction) Green's function can be found by using Wick's theorem. This can then be used to find the interacting m-particle Green's function by looking at perturbative expansion of the number operators $a_k^\dagger a_k$ (with $a_k^\dagger$ the creation operator for a neutrino of quantum numbers k). Truncating the expansion after the first term, keeping the terms linear in the interaction, and taking the expectation value with respect to the (pure) initial state, yields a Hamiltonian modified by the interaction for eq. (18) in the limit of infinitesimal interaction time. This is exactly the mean-field approximation.

Therefore eq. (18) is the governing equation I will be using, where the Hamiltonian will change as I include more and more effects, as needed to model the propagation through out of the BNS torus to the outer shell. The form means that the total coherency of the system is conserved, i.e. there is no damping term which is reducing the population. In addition, all the evolution I will be considering always start as electron neutrinos and electron antineutrinos.

Considering a generic hermitian Hamiltonian, I can write out the change in the density matrix elements as,

$$\frac{\partial \rho_{ee}}{\partial \mathbf{x}} = -i\left[(\mathcal{H}_F)_{ex}\rho_{ex}^* - (\mathcal{H}_F)_{ex}^*\rho_{ex}\right], \quad \frac{\partial \rho_{ex}}{\partial \mathbf{x}} = -i\left[\left((\mathcal{H}_F)_{ee} - (\mathcal{H}_F)_{xx}\right)\rho_{ex} + (\mathcal{H}_F)_{ex}\left(\rho_{xx} - \rho_{ee}\right)\right] \tag{21}$$

For the vacuum case, the Hamiltonian is constant, so there is no change in the derivatives. However, what may be noticed is that in order to change the populations, one needs to have a large imaginary part on the off-diagonal. I will therefore turn to what contributions to the neutrino Hamiltonian may arise from the surrounding medium.

Standard Model Interactions

During the propagation of the neutrino through the interior of the Sun, it encounters such high densities that it becomes likely that a weak interaction occurs. In general, any likely detectable signal will be influenced by such celestial bodies, as many, many neutrinos are required to observe a neutrino signal, implying in turn that the density must have been large initially. Such interactions can lead to the so-called Mikheyev-Smirnow-Wolfenstein (MSW) effect, which may alter the flavour evolution significantly. In addition, our detectors are not placed in empty space, but on the Earth, and depending on the origin of the neutrino it becomes necessary to take into account the effects of scattering. By looking at the MSW effect which emerges in this in-medium propagation, the sign of Δm^2_{21} was determined. The size of Δm^2_{23} is too large, and so the MSW effect is too small to be observed in the Earth, leaving this as an open question for future experiments.

Although the neutrinos barely interact, it very much depends on the density of the medium and the energy of the neutrino, as the (center-of-mass) cross section σ_{com} grows as $\sigma_{com} = G_F s$ with the center of energy, s and Fermis constant G_F. In the lab frame $s = 2EM$, with M the mass of the target nuclei and E the neutrino energy. This gives a mean-free path l in a medium of number density N with target particles,[26],

$$l \sim \frac{1}{N\sigma} \sim \frac{10^{-38} cm^2}{(N cm^3)(\frac{EM}{GeV^2})} \tag{22}$$

In particular, for neutron stars and supernovae cores (number density $\sim 10^{36}/cm^3$) and neutron-rich material (mass $\sim$ 1 [GeV]), the mean free path of a 1 [MeV] neutrino is of the order of a kilometre, which is about the size of such an object. Hence the neutrino will interact with the medium and be scattered. In the very dense region of a CCSNe or torus of the BNS merger remnant, the neutrino mean free path is so small that in general they are considered to be in a 'trapped region' where they scatter back and forth, until they either reach the surface of the trapping region or the system cools enough to let them escape.

The region which I am interested in is outside of the dense torus region and black hole formed in a BNS merger, so I will not consider these very dense region effects, where the scattering makes the medium opaque, since the scattering changes the neutrino energy, changes the neutrino population, and makes the neutrino deviate from its path. The reasoning is that I wish to follow the neutrino ensemble from their production point to the outer shell, and including inelastic scatterings may greatly change the flavour evolution [34]. In addition, if the neutrinos scattered in a medium and changed momentum, I would be able to locate exactly which particle scattered the neutrino, thereby knowing about the medium collapses the superposition. Instead I consider such interactions which do not change the momenta of the neutrinos, the so-called *Coherent Forward Scatterings*.

Coherent Forward Scattering

Since I am considering celestial systems, the matter will be dominated by the first generation SM matter, i.e. electrons, up- and down-quarks (u and d). Therefore the interactions I am considering are of the type seen figure (4), where whatever states come in also come out. The 'coherent' part of the interaction refers to the fact that the scatterings only change the phase of the scattered state, which means that the state may interfere with itself. This is how the flavour oscillations may be enhanced or decreased. To begin with I will see what part of the coherent forward weak interactions affect the system, because if it is the phase which changes, then it has to be that the phase difference must not be the same for all of the neutrinos, otherwise there would be no effect.

For Charged Current (CC) interactions, any interaction with a u- or d quark necessarily only has a single neutrino involved, as the lepton number must be conserved ($\nu_\alpha \to \alpha$). These scatterings I do not consider and so I am left with a soup of electron interaction. All of the astronomical environments under consideration are electrically neutral, and in the SM neutrino NC scattering from electrons and protons are equal in magnitude but opposite in sign, so they cancel each other out and what is left are the neutron NC interactions [26]. These are equal for all of the neutrino flavours, which means that every interaction gives

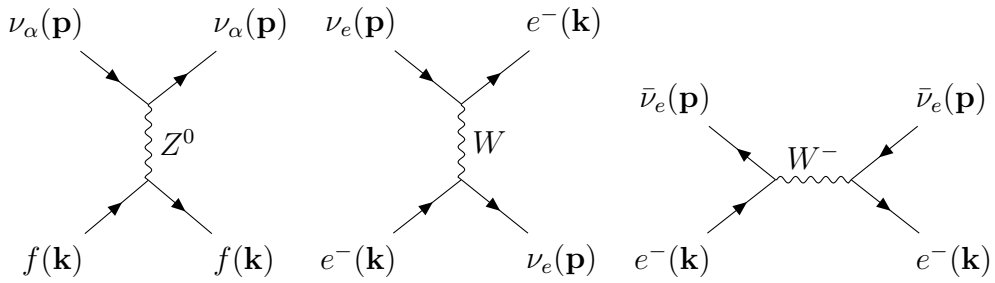

Figure 4: Coherent neutrino-matter Interactions. These interactions do not change the momenta of the neutrino, or only do so for indistinguishable particles. $f = \{e, u, d\}$ is a first generation fermion.

the same phase, essentially a global phase, and so the NC interactions may be neglected for flavour oscillations in this case. The only relevant interaction from coherent forward scattering through a common matter medium is therefore the contribution from the electron soup, so let me expand on these diagrams.

By Legendre transforming eq. (1) I find the CC Hamiltonian,

$$\mathcal{H}_{(\text{coherent CC})} \simeq -\left[\frac{g}{\sqrt{2}}\bar{\nu}_e \not{W} P_L e + h.c.\right] - \frac{g}{2\cos\theta_W}\bar{\nu}_\alpha \not{Z} P_L \nu_\alpha \tag{23}$$

Now I can write up the Hamiltonian amplitude for the center Feynman diagram in fig. (4),

$$\mathcal{A}_{\text{coherent CC}} = \left(\bar{e}(i\frac{g}{\sqrt{2}}\gamma^\nu P_L)\nu_e\right)\left[i\frac{-\eta_{\mu\nu} + \frac{p_\mu p_\nu}{M_W^2}}{p^2 - M_W^2 + i\epsilon}\right]\left(\bar{\nu}_e(i\frac{g}{\sqrt{2}}\gamma^\mu P_L)e\right) \tag{24}$$

where $\gamma^u = (\gamma^0, \boldsymbol{\gamma})$ are matrices which obey the Clifford Algebra [49]. In the limit of $E_\nu \ll \frac{M_W^2}{4m_e} \sim 1.6$ [PeV], which would be the high-tail of neutrinos in BNS mergers, this amplitude can be approximated with the effective Fermi 4-fermion interaction. The Hamiltonian can therefore be expressed by the 4-current, j_μ [26],

$$\mathcal{H}_{\text{CC}} = \frac{G_F}{\sqrt{2}} j^\dagger_{W_\mu} j^\mu_W \tag{25}$$

A Fierz transformation [26] rewrites the currents to same-fermion currents. This gives the

effective CC Hamiltonian,

$$\mathcal{H}_{\text{CC}} = 2\sqrt{2}G_F \left(\bar{\nu}_e \gamma^\mu P_L \nu_e\right) \left(\bar{e}\gamma_\mu P_L e\right) \tag{26}$$

where $G_F = \frac{g^2}{8M_W^2}$. Taking the medium to be static and unaffected during the propagation (since the scattering is not changing momentum), one can average over the electron soup, keeping only their thermal average value,

$$\mathcal{H}_{\text{CC}} = 2\sqrt{2}G_F \left(\bar{\nu}_e \gamma^\mu P_L \nu_e\right) \langle e \rangle \tag{27}$$

The thermal average $\langle e \rangle$ is given by [32],

$$\langle e \rangle = \int d^3 p_e f(E_e, T) \left(\gamma^0 - \frac{\mathbf{p} \cdot \boldsymbol{\gamma}}{E_e V}\right) \cdot \frac{1}{V} \tag{28}$$

where $f(E_e, T)$ is the statistical distribution of energy (normalized to $n_e V$), p_e is the 3-momentum of the electrons, and E_e is the energy of the electron. If $f(E_e, T)$ is symmetric in momentum space, then the entire thing becomes,

$$\langle e \rangle = n_e \gamma^0 \tag{29}$$

and so the thermal average is proportional to the density of electrons,

$$\mathcal{H}_{\text{CC}} = 2\sqrt{2}G_F n_e \left(\bar{\nu}_e \gamma^0 P_L \nu_e\right) = \sqrt{2}G_F n_e \left(\bar{\nu}_{e_L} \gamma^0 P_L \nu_{e_L}\right) \tag{30}$$

with the opposite sign interaction for electron antineutrinos. Calculating the shift in energy of a neutrino travelling through this potential shows that the shift for left-chiral neutrinos is proportional to $\sqrt{2}G_F n_e$ [26]. I should actually have a contributions from positrons so that the potential is the difference between the number of electrons and positrons. The number of positrons in the systems I will consider is negligible, so this is left out.

This matter interaction can be rewritten in terms of the Baryon number density (n_B)

and electron fraction (Y_e), rather than the electron number density,

$$n_e = n_B Y_e = \frac{\rho_B}{m_N + m_P} Y_e \tag{31}$$

with ρ_B the baryon density and m_N, m_P the masses of protons and neutrons. The matter interaction under consideration only affects the electron neutrino, so the matter interaction Hamiltonian for the 2-level system becomes a shift in energy,

$$\mathcal{H}_{\text{CC}} = \lambda Y_e \begin{pmatrix} 1 & 0 \\ 0 & 0 \end{pmatrix} \tag{32}$$

where $\lambda = \sqrt{2} G_F n_B$, but since a global phase can be removed from the Hamiltonian, we can remove the trace (as in the vacuum case),

$$\mathcal{H}_{\text{CC}} = \frac{\lambda(\mathbf{r})}{2} \begin{pmatrix} Y_e(\mathbf{r}) & 0 \\ 0 & -Y_e(\mathbf{r}) \end{pmatrix} \tag{33}$$

where $\boldsymbol{r}$ has been put in for clarity, since it can influence the diagonal of the Hamiltonian as function of distance, which is the basis for the following section on the first matter resonance.

Mikheyev-Smirnov-Wolfenstein Resonance

The Mikheyev-Smirnov-Wolfenstein (MSW) [4] resonance occurs when a neutrino ensemble is propagating through matter and can *coherently* scatter forward in the medium. This scattering generates additional phases and the scattered ensemble is superposed on the non-scattered ensemble. This coherent scattering has the possibility of enhancing the flavour conversion to such an extent that it may become maximal, i.e. that the population of the neutrino completely flips flavour, so all electron neutrinos become x neutrinos. The MSW affects the diagonal part of the total flavour Hamiltonian, which can take the density matrix time evolution to completely be in the off-diagonal components, driving the resonance, as

we will find shortly.

The Hamiltonian in the flavour basis can be found by combining the vacuum and matter results, eq. (14) and eq. (33),

$$\mathcal{H}_F = \mathcal{H}_{\text{vacuum}} + \mathcal{H}_{\text{CC}} = \frac{\omega}{2}\begin{pmatrix} -\cos(2\theta) + \frac{Y_e(\mathbf{r})\lambda(\mathbf{r})}{\omega} & \sin(2\theta) \\ \sin(2\theta) & \cos(2\theta) - \frac{Y_e(\mathbf{r})\lambda(\mathbf{r})}{\omega} \end{pmatrix} \tag{34}$$

However, in general there also exists instantaneous matter (or medium) mass eigenstates of the propagation, ν_I, which are rotated away from the vacuum states by U_I and are described by a Hamiltonian[2],

$$H_I = \frac{\omega_I}{2}\begin{pmatrix} 1 & 0 \\ 0 & -1 \end{pmatrix} \tag{35}$$

with ω_I as the in-medium frequencies, where the masses are modified by the matter scattering. This must be related to $\mathcal{H}_F$ by a rotation, the way that the vacuum flavour Hamiltonian related to the vacuum mass Hamiltonian[3],

$$\mathcal{H}_F = U_I H_I U_I^\dagger \qquad\qquad U_I = \begin{pmatrix} \cos(\theta_I) & \sin(\theta_I) \\ -\sin(\theta_I) & \cos(\theta_I) \end{pmatrix} \tag{36}$$

Equating eq. (36) and eq. (34) gives the following relation between the matrix components,

$$\tan(2\theta_I) = \frac{\sin(2\theta)}{\cos(2\theta) - \frac{Y_e(\mathbf{r})\lambda(\mathbf{r})}{\omega}} \tag{37}$$

This relation shows that there may exist a radius R where the electron number density is such that the flavour mixing becomes maximal and this is known as the MSW resonance.

[2]This diagonalisation is allowed for matrices being Hermitian, as the spectral theorem says that any normal matrix A is related to a diagonal matrix D by $A = UDU^*$.

[3]In general there may be additional phases [36], but I neglect these here as they do not affect the resonance location.

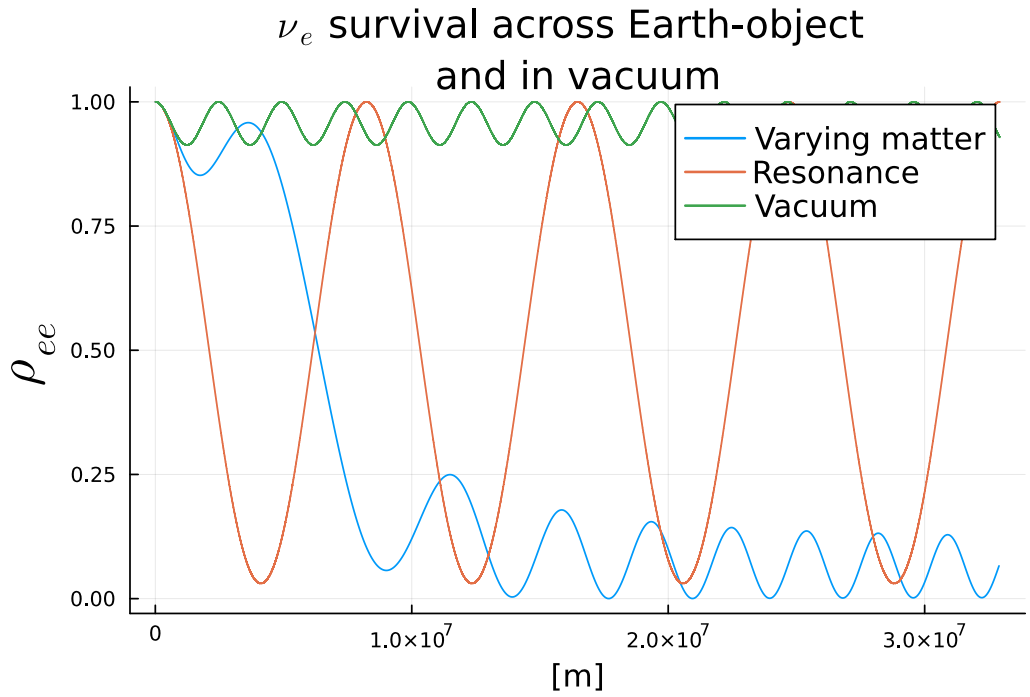

Figure 5: The electron neutrino population, ρ_{ee}, as a function of distance for varying matter profile (blue), resonance matter (orange), and vacuum (green) for reference. The varying matter profile shows the MSW Resonance for Earth-like object. The electron neutrino was $E = 2.5$ [GeV] with the mass splittingΔm_{23}. The matter profile was $2\rho_B \cdot exp(-6x)$, with $\rho_B = 24\left[\frac{gm}{cm^3}\right]$ (Earth has an avg. core density $\rho_{earth} = 12\frac{gm}{cm^3}$). 'Resonance' refers to N_R, the resonance density, which drives the MSW resonance to maximal mixing and this line is the theoretical prediction.

If I let $n_e(R) = N_R = \frac{\omega\cos(2\theta)}{2\sqrt{2}G_F}$, then $\theta_I \longrightarrow \frac{\pi}{4}$, and the matter mixing matrix becomes,

$$U_I(R) = \frac{1}{\sqrt{2}}\begin{pmatrix} 1 & 1 \\ -1 & 1 \end{pmatrix} \tag{38}$$

Examples of an MSW resonance and near maximal mixing can be seen in figure (5) for an exponentially decreasing CC potential with Earth like characteristics.. Looking at the matter eigenvalues, or modified mass eigenvalues, one finds,

$$\omega_I = \omega\sqrt{\left(\cos(2\theta) - \frac{Y_e(\mathbf{r})\lambda(\mathbf{r})}{\omega}\right)^2 + \sin^2(2\theta)} \tag{39}$$

Where the resonance condition means that the first term goes to zero, implying that ω_I is also being minimized, reducing the effective matter mass difference Δm^2_I. That this is the case for the resonance location makes intuitive sense since the difference in energy between the states is becoming minimal.

Explicitly eq. (37) shows that θ_I has a spatial dependence through the matter potential. Since the evolution of the mass states can be found from the rotation of the flavour states, this adds an off-diagonal term to the time evolution,

$$i\frac{\partial \nu_F}{\partial t} = H_F \nu_F \Longrightarrow i\frac{\partial \nu_I}{\partial t} = \left(\mathcal{H}_I - U_I \frac{\partial U_I}{\partial dt}\right)\nu_I = \begin{pmatrix} -\frac{\omega_I}{2} & -\dot{\theta}_I \\ \dot{\theta}_I & \frac{\omega_I}{2} \end{pmatrix} \nu_I \tag{40}$$

What this means is that the mass basis at the production is not the eigenbasis if the density of the medium changes. This is important, for the final neutrino flavour. If a neutrino is produced as an electron in, say, the Sun, where the density is relatively smooth, then because of eq. (37) it is produced mostly as an in-medium mass state (ν_{1I}), given $\nu_\alpha = \cos(\theta_I)(\nu_{1I}) + \sin(\theta_I)(\nu_{2I})$. Since the density is smooth, the probability of $\nu_{1I} \leftrightarrow \nu_{2I}$ transitions are low, and hence the neutrino stays in the ν_{1I} mass state. However, θ_I changes its value as the resonance is crossed, leading to ν_{1I} now being identified with the x flavour neutrino. Thus if the resonance is crossed in a smooth way, a flavour will be maximally converted. If the density was a sharply changing function, however, then the original mass eigenbasis is a bad choice, and the maximal flavour change is no longer certain. Now the final neutrino flavour depends very much on the exact shape of the density function. Additionally, I note that eq. (37) shows that the MSW effect happens only for neutrinos and not antineutrinos since the sign of the vacuum Hamiltonian is opposite[4].

Therefore the way the resonance is crossed is an important factor in the flavour evolution, and the different limits are captured by the *adiabaticity* parameter γ

$$\gamma = \frac{|\omega_I|}{|\frac{\partial \theta_I}{\partial dt}|} \tag{41}$$

[4]Except for inverted ordering, in which case, the antineutrinos experience the MSW effect.

This parameter is a measure of whether the ν_I remains the eigenbasis. If the resonance is crossed in a smooth way, then $\gamma \gg 1$ and it is called an adiabatic transition. Oppositely, if $\gamma \ll 1$ then the transition is non-adiabatic[5]. In the case of the MSW resonance, it is most striking when it adiabatically crosses through the resonance, because even with small vacuum mixing, it can produce large flavour transitions, whereas for non-adiabatic the resonance may be halted or non-existent[6]. This adiabaticity is also needed for determining whether a resonance may occur. Equation (37) gives a condition for the location of the resonance, but this is a requirement not a sufficiency. In fact, the flavour states dependence on how the density changes (the adiabaticity), means that for the far majority of density functions, the exact flavour transitions do not have analytical solutions, and one must turn to numerical integration in order to solve how the phase is affected by the coherent scattering. This effect only gets worse the more interactions we add to the system, but one can still use these analytical tools to analyse where the interesting phenomena in the system start.

Although I cannot solve the system exactly, it is possible to write up the coupled differential equations that the system obeys, using eq.s (21),

$$\begin{aligned}
\frac{\partial Re\left(\rho_{ex}\right)}{\partial t} &= \frac{\omega_I}{2} Im\left(\rho_{ex}\right)\left(\cos(2\theta) - \frac{\lambda Y_e}{\omega}\right) \\
\frac{\partial Im\left(\rho_{ex}\right)}{\partial t} &= \frac{\omega_I}{2}\left(\sin(2\theta)(2\rho_{ee}-1) - Re\left(\rho_{ex}\right)\left(\cos(2\theta) - \frac{\lambda Y_e}{\omega}\right)\right) \\
\frac{\partial \rho_{ee}}{\partial t} &= \omega \sin(2\theta) Im\left(\rho_{ex}\right)
\end{aligned} \tag{42}$$

since $\lambda Y_e \gg \omega$, the imaginary and real parts of the off-diagonal are quickly oscillating into each other and never get large, whereas when the MSW resonances condition, $\omega\cos(2\theta) \simeq \lambda Y_e$, is met, the imaginary part has a chance to grow through coupling to the $\sin(2\theta)\rho_{ee}$ term. A low adiabaticity can be seen as the resonance condition stopping before the $\sin(2\theta)\rho_{ee}$ can change the off-diagonal significantly.

[5] or diabatic?

[6] In the geometric picture, the Hamiltonian vector flips so quickly that the polarization vector cannot follow it, so it flips to precess around the opposite pole of the Hamiltonian.

So far I have only included neutrinos scattering off of the medium, but the reason I included this effect was that I wanted a source which produced many neutrinos, such that a signal could be detected. If the densities become large enough, the production of neutrinos may become so large as to warrant taking neutrino-neutrino scatterings into account. This will be explored in the following section.

Neutrino-neutrino Interactions

In the SM neutrinos scatter off of each other through the neutral current only (at tree level), since each vertex has to obey lepton number and charge, which is not possible in a charged charged current for two neutrinos. These interactions are known as neutrino-neutrino interactions and the coherent parts are shown in fig. (6), where α and β are the lepton flavours. An incredible density of neutrinos is needed for this term to be relevant, and so the effects are mostly found in the cores and immediate surroundings of cosmic events such as CCSNe or BNS mergers. What's more, antineutrinos are produced in larger quantities in BNS merger remnants and coupled to the weak force with the opposite sign compared to the neutrinos, so the overall contribution to the Hamiltonian may become negative. This negative contribution can produce a resonance, as with the MSW resonance above, by cancelling other contributions. In matter densities, this is commonly called the 'Matter-Neutrino Resonance' (MNR) since the neutrino-neutrino potential is predominately counteracting the matter potential. This resonance is different from the MSW, as the neutrino-neutrino interaction makes it nonlinear in nature, and there, therefore, cannot exist an analytical solution. Indeed the flavour evolution is very dependent on both the strength of both potentials and how exactly they change as the neutrino propagates. Later on, we will see examples of how the resonances may be cut off by how the background system is generated.

The general form of the Hamiltonian can be understood from the interaction diagrams. From the top two Feynman diagrams in fig. (6) it can be seen that whatever the Hamiltonian is, the diagonal will be proportional to the number density all neutrino flavours

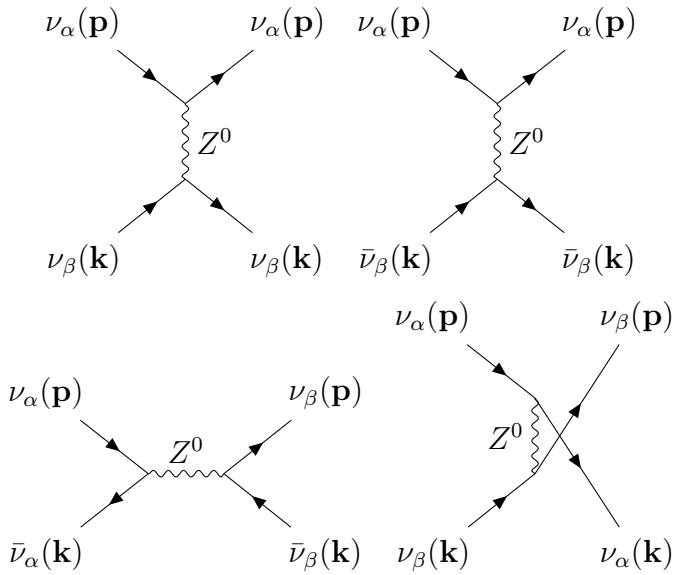

Figure 6: Neutrino-neutrino coherent forward scatterings between flavours α and β. The two upper diagrams are the diagonal NC contributions. The two lower diagrams are flavour changing NC contributions.

and also to both neutrinos and antineutrinos. This part of the neutrino-neutrino interaction is equivalent to the charged current interaction with matter seen above, excepting the case where the ν_α propagates into a medium of ν_α, because here the propagating neutrino flavour may exchange place with the same flavour in the medium. Therefore this diagram counts twice in the case of equal flavour scatterings. The bottom two diagrams show that there exist off-diagonal components of the Hamiltonian, and these will have the same proportionality. However, for coherency to be conserved in this case, one needs the background medium of neutrinos to be composed of a superposition of the initial and scattered flavour. As an example, consider an electron neutrino scattered in a muon neutrino gas converting to a muon neutrino. Then there is suddenly an electron neutrino in the gas, and the superposition collapses since we can tell that the medium has been affected. At the same time, one must not have a good enough resolution of the exact momentum distribution of the background medium, as the scattering will increase the amount of the electron neutrinos in the gas as compared to muon neutrinos in the superposition at the momentum of the incoming neutrino, due to the momentum exchange.

Since the interaction is a current-current interaction, the Hamiltonian will have the form of eq. (27), which has a Lorentz structure equal to a momentum term $(p^{\mu}_{\nu_\alpha}(p_{\nu_\beta})_{\mu})$. On dimensional grounds there will therefore be a momentum or direction dependence in the interaction [35]. So conceptually, the interaction should be proportional to how many neutrinos and antineutrinos there are in the system and a dependence on their momentum. In addition, it should be proportional to G_F since I am considering coherent effects, i.e. Hamiltonian-level effects.

In Ref. [33], they find the refractive, or coherent forward scattering, neutrino self interaction Hamiltonian in the mean-field approximation expressed via the single particle density matrices as,

$$\begin{aligned} H_{\nu\nu}(\boldsymbol{p}) =& \sqrt{2}G_F \int d\boldsymbol{p'} \left(G_S \left(\rho_{\boldsymbol{p'}} - \bar{\rho}_{\boldsymbol{p'}}\right) G_S + G_S \mathrm{Tr}\left[\left(\rho_{\boldsymbol{p'}} - \bar{\rho}_{\boldsymbol{p'}}\right) G_S\right]\right) \left(1 - \hat{\mathbf{p}} \cdot \hat{\mathbf{p}}'\right) \\ & - \frac{8\sqrt{2}G_F p_0}{4m_Z^2} \int d\boldsymbol{p'} p'_0 G_S \left(\rho_{\boldsymbol{p'}} + \bar{\rho}_{\boldsymbol{p'}}\right) G_S \cdot \left(1 - \hat{\mathbf{p}} \cdot \hat{\mathbf{p}}'\right)^2 \end{aligned} \tag{43}$$

where I have explicitly kept the momentum dependence, since the integral is over momentum space, and G_S is a matrix of coupling constants, which in the case of SM physics is equal to an identity matrix. The last integral is mostly related to effect in the early universe, where lepton symmetry is high, meaning that the first term cancels out. The trace in the first integral reflects the fact that equal flavour scattering gives twice the contribution to the Hamiltonian. Since it is proportional to identity, it provides an overall phase. Therefore I neglect these two terms in this thesis as I am concerned with oscillations in the later universe .

As can be seen, diagonal and off-diagonal components of the neutrino-neutrino interaction is indeed proportional to the number density of both neutrinos and antineutrinos, since the total density matrix is proportional to the number density, and that it has a velocity dependence between the states[7]. The velocity dependence can also be seen to

[7]This velocity dependence should really be expressed in the mass basis, as the massive states do not necessarily propagate in the same direction after the neutrino is produced.

completely disappear for a completely isotropic medium or remove any coherent effect if the neutrinos are propagating in the same direction. However, in the case of BNS mergers, the isotropy of neutrinos is very low, and so the angular term is in theory very important, and in an azimuthally symmetric, three dimensional system it reduces to $\hat{\mathbf{p}} \cdot \hat{\mathbf{p}} = \cos(\Theta_{ij})$, where Θ_{ij} is the angle between the neutrinos $\angle(\hat{\mathbf{p}}, \hat{\mathbf{p}})$. So removing the angular effects is a poor assumption, because of the complex geometries and momentum distributions involved, but the computational complexity becomes intractable. If the angular distribution is incorporated, the entire system will have to be evolved self-consistently, meaning every possible trajectory through the system becomes linked.

In this thesis I will ignore angular effects, meaning that any 'test' neutrino will experience a continuous stream of background neutrinos from the same direction. This is known as the single angle approximation and the angle can be arbitrary, but is taken to be $\frac{\pi}{2}$ for simplicity. The mean-field background neutrinos have the same history as the 'test' neutrino, as can be seen from the 'test' neutrino being in the Hamiltonian, weighted by the neutrino number density [6]. In addition, only the magnitude of the momentum becomes important. Therefore the self interaction will have the following form for this thesis,

$$\begin{aligned} \mathcal{H}_{\nu\nu}(p) &= \sqrt{2} G_F \int dp' \left(P(\mathbf{x}, p, t) - \bar{P}(\mathbf{x}, p', t) \right) \\ &= \sqrt{2} G_F \int \left(dn_{\nu,p'} \rho(\mathbf{x}, p, t) - dn_{\bar{\nu},p'} \bar{\rho}(\boldsymbol{x}, p', t) \right) \\ &= \mu \left[\rho(\mathbf{x}, p', t) - \zeta \bar{\rho}(\boldsymbol{x}, p', t) \right] \end{aligned} \tag{44}$$

Where $\mu = \sqrt{2} G_F n_\nu$ is the strength of the unoscillated neutrino-neutrino and $\zeta = \frac{n_\nu}{n_{\bar{\nu}}}$ is the relative number density of antineutrinos to neutrinos at a point $\boldsymbol{x}$. This is where the mean-field approximation comes into play, as μ and ζ gives the unoscillated background of neutrinos to the oscillation of the single neutrino. The strength then varies as the 'test' neutrino oscillates, changing the flavour population.

To symmetrize the Hamiltonian I remove the trace from eq. (44),

$$H_{\nu\nu} = \frac{\mu}{2}\begin{pmatrix} \delta\rho - \zeta\delta\bar{\rho} & 2(\rho_{ex} - \zeta\bar{\rho}_{ex}) \\ 2(\rho_{ex} - \zeta\bar{\rho}_{ex})^* & -(\delta\rho - \zeta\delta\bar{\rho}) \end{pmatrix} \tag{45}$$

Where $\delta\rho = (\rho_{ee} - \rho_{xx})$. This form will is useful for studying the relations between the neutrino-neutrino Hamiltonian and the matter and vacuum Hamiltonians.

Matter-Neutrino Resonance

As I mentioned at the beginning of the subsection, the sign of the neutrino interaction potential depends on the relative size of the neutrino and antineutrino number densities. This may lead to a cancellation of the matter term dominating the diagonal, generating a resonance as in the MSW case. This resonance is the MNR and differs from the MSW as it is nonlinear in the neutrino itself. Let us look closer at the Hamiltonian with all the effects above incorporated,

$$\begin{aligned} \mathcal{H} = & \frac{\omega}{2}\begin{pmatrix} -\cos(2\theta) + \frac{Y_e\lambda}{\omega} & \sin(2\theta) \\ \sin(2\theta) & \cos(2\theta) - \frac{Y_e\lambda}{\omega} \end{pmatrix} + \frac{\mu}{2}\begin{pmatrix} \delta\rho - \zeta\delta\bar{\rho} & 2(\rho_{ex} - \zeta\bar{\rho}_{ex}) \\ 2(\rho_{ex} - \zeta\bar{\rho}_{ex})^* & -(\delta\rho - \zeta\delta\bar{\rho}) \end{pmatrix} \\ = & \frac{1}{2}\begin{pmatrix} -\omega\cos(2\theta) + Y_e\lambda + \mu F & \omega\sin(2\theta) + \mu Q \\ \omega\sin(2\theta) + \mu Q^* & \omega\cos(2\theta) - Y_e\lambda - \mu F \end{pmatrix} \end{aligned} \tag{46}$$

with $F = (\delta\rho - \zeta\delta\bar{\rho})$, $Q = 2(\rho_{ex} - \zeta\bar{\rho}_{ex})$. Following the same procedure as for the MSW resonance, the effective mixing angle becomes,

$$\tan(2\theta_M) = \frac{\omega\sin(2\theta) + \mu Q}{\omega\cos(2\theta) - Y_e\lambda - \mu F} \tag{47}$$

This gives me the condition for where (mostly) the matter and neutrino potentials cancel, driving the in-medium mixing angle to maximal mixing, and thus give the location of the MNR,

$$\omega\cos(2\theta) - \mu F(r) = Y_e(r)\lambda(r) \tag{48}$$

However, there is also the numerator, which now may change as the neutrino density matrix changes. As I noted in subsection on MSWs, the adiabaticity (eq. (41)) is important for whether a resonance can occur at all. If the system has no phase additional derivatives, then at a resonance the adiabaticity condition is given by [36],

$$\gamma_R > \frac{2\omega_M^2 \sin(2\theta_M)}{\left|\frac{\partial\lambda(r)Y_e(r)}{\partial r} + \frac{\partial F}{\partial r}\right|}|_{r=R} \tag{49}$$

If these conditions are fulfilled then an MNRs will occur.

Consider a system with an exponentially decreasing negative neutrino potential and a constant CC potential [37], as seen in figure (7). During the MNR the population changes as in the MSW due to cancellation of diagonals, but in the case of the MNR, this change in population also changes the neutrino-neutrino potential. In fact, it changes such as to maintain the resonance if it can, since this maintains the lowest energy difference possible between the in-medium mass states. However, this is a contest between rates of change in populations, since the neutrino-neutrino interaction couples the neutrino and antineutrino, and the evolution goes as,

$$\dot{\rho}_{ee} = -\omega \sin(2\theta) Im\left(\rho_{ex}\right) + 2\mu\zeta Im\left(\bar{\rho}_{ex}^{*}\rho_{ex}\right) \tag{50}$$

$$\dot{\bar{\rho}}_{ee} = \omega \sin(2\theta) Im\left(\rho_{ex}\right) + 2\mu Im\left(\bar{\rho}_{ex}^{*}\rho_{ex}\right) \tag{51}$$

When $\mathcal{H}_{\rm CC} < |\mathcal{H}_{\nu\nu}|$ and $\mathcal{H}_{\nu\nu} < 0$, then $\zeta > 1$, which means that the neutrino population changes faster than the antineutrino population. This allows the neutrino potential to grow in size while still being negative. This is, in fact, the essence of the MNR - the neutrino-antineutrino population will change to compensate for the matter potential, in order to minimize the in-medium energy splitting. This is exactly what figure 7 shows. However, for $\mathcal{H}_{\rm CC} > |\mathcal{H}_{\nu\nu}|$ and $\mathcal{H}_{\nu\nu} < 0$, the neutrino potential cannot reduce in magnitude, because if it tries to lower to antineutrino population, then the neutrino population will lower faster, which increases the magnitude of the neutrino potential. Effectively, this means that the neutrino potential only changes if it is already larger than, and oppositely signed to, the

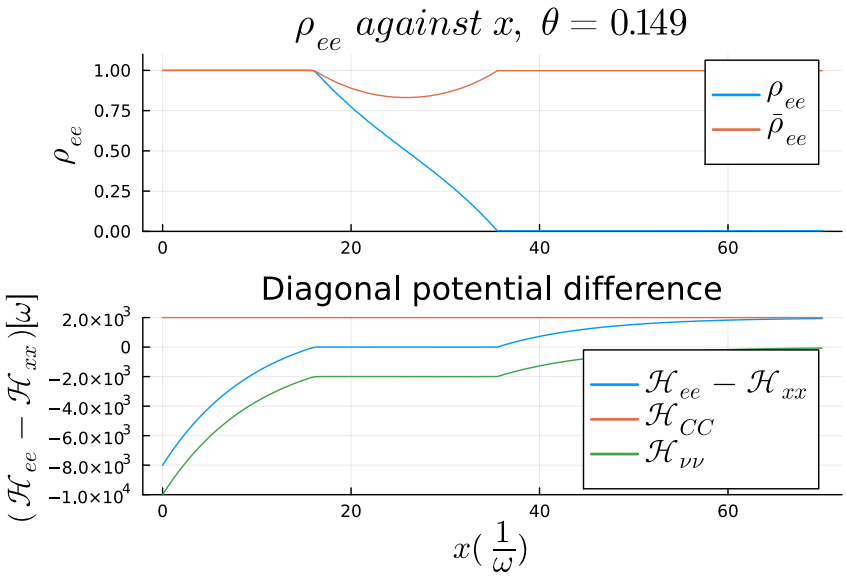

Figure 7: Matter-Neutrino Resonance (MNR) in system of exponentially decaying neutrino-neutrino interaction with constant CC interaction. The green line is the neutrino potential, the blue line is the total diagonal difference and the orange line is the CC potential. The system is scaled relative to the vacuum frequency ω in the $(\Delta m^2_{13}, \theta_{13})$ sector. The neutrino-neutrino potential goes as $\frac{10^4 \cdot \exp(-\frac{\omega x}{10})}{1-\zeta}(\rho - \zeta\bar{\rho})$ and the CC potential as $2 \cdot 10^3\omega$, where ζ is the relative occupation number of antineutrinos to neutrinos $\zeta = \frac{n_{\bar{\nu}}}{n_\nu} = \frac{4}{3}$ and ρ $(\bar{\rho})$ is the (anti) neutrino density matrix.

CC potential. Figure 8 shows the case of an exponentially decreasing CC potential against a negative neutrino potential. Since the CC potential is dropping below the neutrino potential, the neutrino potential needs to drop in magnitude to follow the CC potential and so there is no resonance. This shows an additional condition for the MNR, namely that $\mathcal{H}_{\nu\nu}$ must have the opposite sign to the CC potential but also larger in magnitude.

In order to understand the phenomenon of why the neutrino potential starts to 'follow' the CC potential, it may help to look at the derivative of the density matrix elements, as I did in the MSW case. Since the neutrino is governed by the Von Neumann eq. (21), I can write

$$\frac{\partial \rho_{ee}}{\partial r} = -i\left((\mathcal{H}_F)_{ex}\rho^*_{ex} - (\mathcal{H}_F)^*_{ex}\rho_{ex}\right) = -i\left(\omega\sin(2\theta)Im(\rho_{ex}) - 2\mu\alpha Im\left(\rho_{ex}\bar{\rho}^*_{ex}\right)\right) \tag{52}$$

Now if I expand on how $Im\left(\rho_{ex}\right)$ and $Im\left(\rho_{ex}\bar{\rho}^*_{ex}\right)$ change, then I find that the whole

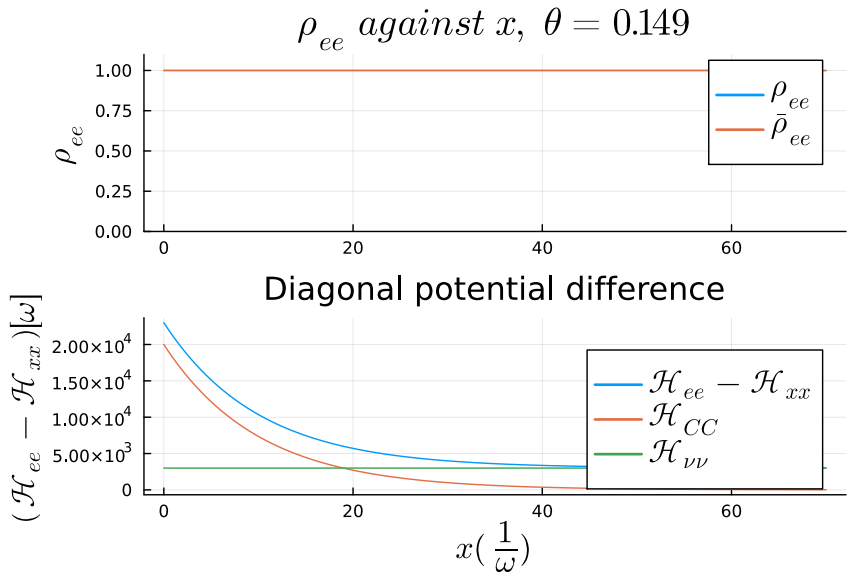

Figure 8: System of exponentially decaying CC interaction with constant neutrino-neutrino interaction. The green line shows the absolute value of the neutrino potential, the blue line is the total diagonal difference and the orange line is the CC potential. The system is scaled relative to ω in the $(\Delta m^2_{13}, \theta_{13})$ sector. The CC potential is $10^4 \cdot \exp\left(-\frac{\omega x}{10}\right)$ and the neutrino-neutrino potential is $\frac{2\cdot10^3\omega}{1-\zeta}(\rho - \zeta\bar{\rho}) < 0$, where ζ is the relative number density of antineutrinos to neutrinos $\zeta = \frac{n_{\bar{\nu}}}{n_\nu} = \frac{4}{3}$ and ρ $(\bar{\rho})$ is the (anti) neutrino density matrix.

system is governed by nine coupled, non-linear, ordinary differential equations in r. This is, therefore, a bit difficult to untangle, and is left for further study. One can, however, find the approximate flavour evolution from the beginning of the resonance in the adiabatic case. Consider a flavour generated in a dense medium. This can be identified with an in-medium mass state, if the flavour is produced far from the resonance. If the state adiabatically goes through the system, then $(\nu_I)_1$ is conserved and so one can find the probability from the inner product,

$$P_{(\nu_{ii})\to\nu_e} = |\langle\nu_e|\nu_{1i}\rangle|^2 = \frac{1}{2}\left(1+\frac{1}{\sqrt{1+|\tan(2\theta_i)|}}\right) \simeq \frac{1}{2}\left(1+\frac{\zeta^2+R^2-1}{2R}\right) \tag{53}$$

where $R = \frac{\lambda Y_e}{\mu}$ is the ratio of the matter and neutrino-neutrino potentials [36].

There exists yet a further resonance, which is due to the neutrino-vacuum interaction, called bipolar conversions, where the neutrinos and antineutrino oscillate together [38], but these will not be covered further in this thesis. These are the coherent forward interactions which a neutrino or antineutrino will meet during its propagation out of dense stellar events. One could now take into account the angular dependence of the neutrino interaction, or the collisional, second order perturbation, effects on the flavour evolution. However, another route may be the effect of new physics on the propagation. It is known that the SM falls short at high and low energies, and as such, new interactions may occur. At low energies in particular, neutrino oscillations are an excellent probe of such new physics, since slight modifications of the phase or effective masses have noticeable effects at large scales. This will be the study of the following section.

Non-Standard Interactions

The SM is extremely accurate when describing particle interactions with the SM forces, and thus seems a good effective theory. As mentioned in the introduction at both high and low energies additional interactions may occur, such as was anticipated for TeV Super Symmetric particles. Conversely, new physics may also appear at low energy scales, and

indeed the observation of neutrino masses may imply the existence of more operators than are currently in the SM [39], since the mass mechanism is still unknown. In [40] they argue that there exists just one dimension-5[8] operator which maintains the SM gauge symmetries and this operator produces neutrino masses and mixings. Further perturbatively expanding the operators of the SM, one can find new effective dimension-6 four-fermion interactions, which may perturb the neutrino oscillation through additional scatterings. Such new operators may be approximated in a Fermi interaction, with a coupling g proportional to the Fermi interaction, and the strength of the interaction relative to the weak scale is determined by the hermitian parameter $\epsilon^{fV}_{\alpha\beta}$. These types of interactions are generally called Non-Standard Interactions (NSIs). Typically, all of the different NSI models have the current-current interaction form of modified effective CC and NC interactions [40].,

$$\mathcal{L}_{\text{CC NSI}} = -\epsilon^{fV}_{\alpha\beta} 2\sqrt{2} G_F \left(\bar{\nu}_\alpha \gamma_\mu P_L l_\beta\right) \left(\bar{f}' \gamma^\mu P_x f\right) \tag{54}$$

$$\mathcal{L}_{\text{NC NSI}} = -\epsilon^{fV}_{\alpha\beta} 2\sqrt{2} G_F \left(\bar{\nu}_\alpha \gamma_\mu P_L \nu_\beta\right) \left(\bar{f} \gamma^\mu P_x f\right) \tag{55}$$

where $f = \{e, u, d\}$ are the first generation (common matter) fermions, the V in $\epsilon^{fV}_{\alpha\beta}$ refers to the vector part of the interaction and P_x is the left/right chiral projector.

There are mostly two approaches to including the NSIs, either in terms of an effective coupling to a heavy (around electroweak scale) X particle or a light mediator Z' such that $g_{Z'}/m_{Z'} \sim G_F$. In either case, the effective NSI theory should come from fundamental theory, and here a problem arises since the active neutrino is part of an SU(2)-doublet, meaning that anything that couples to the left handed neutrino, should couple to the electron. The bounds on such theory would be very stringent, so stringent that any effect on oscillation would not be measurable with current prospects. However, there exists SM extensions which compensate for this, such as a $SU(2)_L$-scalar doublet-singlet mixing which finds off-diagonal couplings as high as $\epsilon_{\mu\tau} = 0.3$ [41] or in Ref. [24], where they argue that a neutrino may be coupled to the new mediator Z' through a new heavy fermion

[8] dimension-5 meaning that 5 fields are interacting

in a $U(1) \times SU(2) \times U'(1)$ symmetry, which seems a natural extension of the seesaw mechanism, where the charged leptons do not couple to Z'[9]. The mediator mass is much below the electroweak scale, and it does not couple to the charged leptons, hence the effect on neutrinos may have gone unnoticed since it would have to be constrained by the detection of neutrinos. This type of mediator would however experience different scatterings than what I am considering in this thesis. See [40] for a status report of current NSI constructions, experiments and limits. Additionally, one may also have NSIs between active neutrinos, generally known as Non-Standard neutrino Self Interactions (NSSI), but these will not be covered in this thesis, since they add to the non-linearity, further increasing the computational complexity. CC NSIs affect production and detection at tree level, but will not be considered further, as the bounds on these interactions are strongly constrained [39].

Instead, I focus on the change in the matter potential which the (anti)neutrino may experience due to coherent forward scattering off of the common matter due to point-like NC NSIs. In the formalism of the time evolution of the density matrix, this essentially becomes an additional term in the CC Hamiltonian,

$$\frac{\partial \rho}{\partial t} = \mathcal{H}_{\text{vacuum}} + [\mathcal{H}_{\text{CC}} + \mathcal{H}_{\text{NSI}}] = \mathcal{H}_{\text{vacuum}} + \mathcal{H}_{\text{matter}} = \mathcal{H}_{\text{vacuum}} + \lambda(r) Y_e(r) \begin{pmatrix} 1 + \epsilon_{ee} & \epsilon_{ex} \\ \epsilon_{ex}^* & \epsilon_{xx} \end{pmatrix} \tag{56}$$

Where the $1 + \epsilon_{ee}$ is the standard matter effect together with the NSI effect and I lump the NSI and CC interactions into a combined matter Hamiltonian. Along the diagonal, oscillation experiments are only sensitive to the phase difference, and hence I can subtract the trace,

$$\frac{\partial \rho}{\partial t} = \mathcal{H}_{\text{vacuum}} + [\mathcal{H}_{\text{CC}} + \mathcal{H}_{\text{NSI}}] = \mathcal{H}_{\text{vacuum}} + \frac{\lambda(r) Y_e(r)}{2} \begin{pmatrix} 1 + \delta\epsilon & 2\epsilon_{ex} \\ 2\epsilon_{ex}^* & -(1 + \delta\epsilon) \end{pmatrix} \tag{57}$$

[9] At least at tree level.

Couplings	Allowed Ranges (90% C.L) for LMA $\oplus$ LMA-D
$\delta\epsilon^{uV} = \epsilon^{uV}_{ee} - \epsilon^{uV}_{\mu\mu}$	$[-1.1, -0.79] \oplus [-0.063, 0.36]$
$\epsilon^{uV}_{e\mu}$	$[-0.058, 0.013]$
$\delta\epsilon^{dV} = \epsilon^{dV}_{ee} - \epsilon^{dV}_{\mu\mu}$	$[-1.3, -0.91] \oplus [-0.072, 0.38]$
$\epsilon^{dV}_{e\mu}$	$[-0.058, 0.014]$
$\delta\epsilon^{eV} = \epsilon^{eV}_{ee} - \epsilon^{eV}_{\mu\mu}$	$[-3.0, -1.8] \oplus [-0.21, 1.0]$
$\epsilon^{eV}_{e\mu}$	$[-0.15, 0.14]$

Table 2: Current NC NSI bounds from oscillation and scattering data [39]. LMA is Large Mixing Angle, and LMA-D refers to the ambiguity in the $\sin(2\theta_{12})$ quadrant placement once NSIs are included.

with $\delta\epsilon = \epsilon_{ee} - \epsilon_{xx}$. The Hamiltonian strength couplings $\epsilon_{\alpha\beta}$ can be decomposed into the electron and quark couplings, and so are related to Lagrangian $\epsilon^{fV}_{\alpha\eta}$ by the sum over possible NSI interactions with f fermions,

$$\epsilon_{\alpha\beta} = \sum_f \epsilon^{fV}_{\alpha\beta} \frac{n_f(\mathbf{r})}{n_e(\mathbf{r})} = \sum_f \epsilon^{fV}_{\alpha\beta} \frac{Y_f(\mathbf{r})}{Y_e(\mathbf{r})} \tag{58}$$

Thus there may be a factor difference of about 3 between the Lagrangian picture and Hamiltonian picture, for Earth-like matter individual quarks are about 3 times as numerous as electrons. The most recent NSI bounds (May 2023) are given by [39], whereof I include the $(ee - \mu\mu)$-sector in Table (2). These bounds contain scattering limits, which rule out low mass NSIs since the energy-scale must be above that of the experiments. So in practise, the bounds are looser than given in the table. Combining the different bounds via eq. (58) and letting $Y_e \sim [0.1, 0.4]$ in a BNS merger remnant system. If I fix the electron fraction[10] to be $Y_e \sim \frac{1}{4}$ and combine the NSI bounds, then the NSIs of the order $\mathcal{O}(1 - 10)$ for the diagonal component and the off-diagonal component is in the order of $\mathcal{O}(0.1 - 1)$.

In the following, I introduce mediators which couple through the neutrino into the SM in the effective Fermi four-fermion manner of eq. (54) and consider their coherent forward effects on neutrino oscillations and possible resonances which may occur. These interaction can be both Lepton Flavour Violating (LFV) and Lepton Flavour Conserving (LFC), and

[10]Typical electron fraction values in the BNS merger remnant system are $Y_e \sim [0.1, 0.4]$.

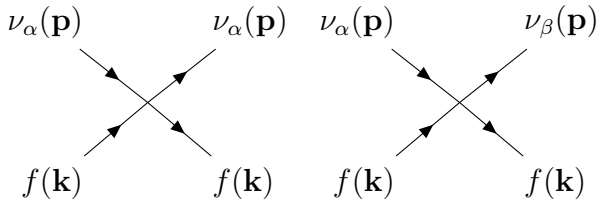

Figure 9: Effective generic NSI couplings. The left shows Lepton Flavour Conserving diagonal contributions, and the right shows Lepton Flavour Violating off-diagonal contributions.

hence a take the form in fig. (9).

I let the matter Hamiltonian be as in eq. (57),

$$\mathcal{H}_{\text{CC}} + \mathcal{H}_{\text{NSI}} = \frac{\lambda(r)Y_e(r)}{2}\begin{pmatrix} 1+\delta\epsilon & 2\epsilon_{ex} \\ 2\epsilon_{ex}^* & -(1+\delta\epsilon) \end{pmatrix} \tag{59}$$

Following [6], the NSI part of the Hamiltonian can be decomposed into its fermionic parts,

$$\mathcal{H}_{\text{NSI}} = \sqrt{2}G_F n_B(r)\left(Y_e\epsilon^{eV} + Y_u\epsilon^{uV} + Y_d\epsilon^{dV}\right) \tag{60}$$

where ϵ^{fV} are hermitian matrices constructed from $\epsilon^{fV}_{\alpha\beta}$ with real coupling strengths for NSIs with fermion f. By requiring that the medium is electrically neutral, I can make the following relations between the fermion fractions,

$$n_B = n_p + n_n = \frac{n_u + n_d}{3} \qquad 0 = \frac{2}{3}n_u - \frac{1}{3}n_d - n_e \tag{61}$$

$$3 = Y_u + Y_d \qquad 0 = \frac{2}{3}Y_u - \frac{1}{3}Y_d - Y_e \tag{62}$$

Therefore eq. (60) can be rewritten in the form,

$$\mathcal{H}_{\text{NSI}} = \lambda(r)\left(Y_e(r)\epsilon^{eV} + (1+Y_e(r))\epsilon^{uV} + (2-Y_e(r))\epsilon^{dV}\right) \tag{63}$$

Removing the trace of the fermionic NSI matrices, $\delta\epsilon^{fV} = \epsilon^{fV}_{ee} - \epsilon^{fV}_{xx}$, $\mathcal{H}_{\rm NSI}$ becomes,

$$\begin{aligned}\mathcal{H}_{\rm NSI} =& \frac{\lambda(r)Y_e(r)}{2}\begin{pmatrix}\delta\epsilon^{eV} & 2\epsilon^{e}_{ex}\\ 2(\epsilon^{e}_{ex})^* & -\delta\epsilon^{eV}\end{pmatrix} + \frac{\lambda(r)(1+Y_e(r))}{2}\begin{pmatrix}\delta\epsilon^{uV} & 2\epsilon^{u}_{ex}\\ 2(\epsilon^{u}_{ex})^* & -\delta\epsilon^{uV}\end{pmatrix}\\ &+ \frac{\lambda(r)(2-Y_e(r))}{2}\begin{pmatrix}\delta\epsilon^{dV} & 2\epsilon^{d}_{ex}\\ 2(\epsilon^{d}_{ex})^* & -\delta\epsilon^{dV}\end{pmatrix}\end{aligned} \tag{64}$$

The MSW resonance seen in the Sun follows SM oscillation theory quite well, so following [6] I impose that the NSI should go to zero at this electron fraction, $\mathcal{H}_{\rm NSI}(R_S) = 0$ for $Y_e(R_S) = Y_\odot = 0.7$. Since the MSW effect is a diagonal cancellation effect, the diagonal component of the NSI must go to zero,

$$0 = Y_\odot\delta\epsilon^{eV} + (1+Y_\odot)\delta\epsilon^{uV} + (2-Y_\odot)\delta\epsilon^{dV} \tag{65}$$

which I term the *solar constraint*. This gives the internal relation that,

$$\delta\epsilon^{eV} = -\frac{Y_\odot(\delta\epsilon^{uV} - \delta\epsilon^{dV}) + \delta\epsilon^{uV} + 2\delta\epsilon^{dV}}{Y_\odot} \tag{66}$$

With this constraint, $\mathcal{H}_{\rm NSI}$ becomes,

$$\mathcal{H}_{\rm NSI} = \frac{\lambda(\mathbf{r})}{2}\begin{pmatrix}\frac{Y_\odot - Y_e}{Y_\odot}\delta\epsilon^{n} & 2(3+Y_e)\epsilon_0\\ 2(3+Y_e)\epsilon_0^* & -\frac{Y_\odot - Y_e}{Y_\odot}\delta\epsilon^{n}\end{pmatrix} \tag{67}$$

where $\epsilon_0 = \epsilon^{e}_{ex} = \epsilon^{u}_{ex} = \epsilon^{d}_{ex}$. Comparing eq. (67) and the NSI contribution to eq. (59), the following relation can be found,

$$\delta\epsilon^{n} < \left(\frac{Y_\odot Y_e}{Y_\odot - Y_e}\right)\delta\epsilon \tag{68}$$

From which the bounds in Table 2. can be recomputed to $\delta\epsilon^{d}$, which is constrained by the solar NSI going to zero. This gives $\delta\epsilon^{n}$ to be of the order of $\mathcal{O}(1-5)$ and bounds on the off diagonals are of the order $\mathcal{O}(0.5)$.

I can now write the flavour Hamiltonian as the combination of vacuum, neutrino-neutrino, CC and NSI Hamiltonians,

$$\begin{aligned}\mathcal{H}_F &= \frac{\omega}{2}\begin{pmatrix} -\cos(2\theta) & \sin(2\theta) \\ \sin(2\theta) & \cos(2\theta) \end{pmatrix} + \frac{\lambda}{2}\begin{pmatrix} Y_e + \frac{Y_\odot - Y_e}{Y_\odot}\delta\epsilon^n & 2(3+Y_e)\epsilon_0 \\ 2(3+Y_e)\epsilon_0^* & -\left(Y_e + \frac{Y_\odot - Y_e}{Y_\odot}\delta\epsilon^n\right) \end{pmatrix} + \frac{\mu}{2}\begin{pmatrix} F & Q \\ Q^* & -F \end{pmatrix} \\ &= \frac{1}{2}\begin{pmatrix} -\omega\cos(2\theta) + \lambda\Phi + \mu F & \omega\sin(2\theta) + 2(3+Y_e)\epsilon_0 + \mu Q \\ \omega\sin(2\theta) + 2(3+Y_e)\epsilon_0^* + \mu Q^* & \omega\cos(2\theta) - \lambda\Phi - \mu F \end{pmatrix}\end{aligned} \tag{69}$$

where $\Phi = Y_e + \frac{Y_\odot - Y_e}{Y_\odot}\delta\epsilon^n$, which may be both positive and negative, depending on the electron fraction. From this I can find the in-medium mixing angle,

$$\tan(2\theta_{\text{NSI}}) = \frac{\omega\sin(2\theta) + 2(3+Y_e)\epsilon_0 + \mu Q}{\omega\cos(2\theta) - \lambda\Phi - \mu F} \tag{70}$$

And we see that an MNR type may still occur for,

$$\omega\cos(2\theta) - \lambda\Phi = \mu F \tag{71}$$

The matter potential is always positive for the SM, but $\lambda\Phi$ may be both positive an negative, which opens up for new areas for resonances, as well as inverted MNRs as we will see in the following section. In addition, the off-diagonal NSIs may affect the adiabaticity at which resonances may occur. Both of these effects will be explored in the following section, where I numerically solve different systems for this Hamiltonian.

Numerical Implementation of NSIs in Flavour Evolution

The flavour evolution of neutrinos is a highly debated subject and is a sector of the SM which is continuously and thoroughly being developed. The influence of neutrinos on many astrophysical environments warrants their full investigation, but the theory of flavour evolution is in general not possible to solve analytically, especially once the non-linear nature of the neutrino-neutrino interaction is included. As such, the flavour dynamics must be solved numerically, and this section will explore the effects that Non-Standard Interactions may have on resonances, or subversion of resonances, in the flavour evolution. I will explore this in two stages.

First I will consider a 'toy model', where I create a system with smooth density functions. Here I include all of the effects I described in the theory section, but in a way that is constructed to affect the resonances. I then perturb these resonances by introducing the NSIs. The toy model will allow me to predict what effects the NSI might have, and thereby let me know what I need to look for in a real system, as well as allowing me to ensure that my code is doing what I am anticipating. This sets the stage for studying the actual system which I wish to understand more fully.

Secondly, I will look at the flavour evolution in the aftermath of a simulated Binary Neutron Star Merger event. Here I use my knowledge from the toy model to find out resonances that will occur and find the evolution in the absence of NSIs. Turning on the NSIs can completely alter the types of resonances a neutrino experiences, even allowing for a symmetric MSW. Moreover, it can change the total and relative occupation numbers of neutrinos and antineutrinos, averaging over the contribution from all initial trajectories. In particular, the trajectory is dependent only broadly on how the neutrino is placed, not the particular initial position, and on how many resonances are crossed during the evolution.

I end this section with an analysis of the implications of NSIs on the flavour evolution in such a BNS merger in the context of a parameter scan of the NSIs.

Toy Model for Flavour Evolution

The theory section culminated in a Hamiltonian which describes propagation through dense media, and all of the effects and resonances which may happen, additionally impacted by possible NSI effects. I now turn to solve the flavour evolution numerically in two different systems. I first implement these NSIs in the 'toy model', the same system as was explored for MNRs in the neutrino-neutrino interaction subsection, in figures (7) and (8). Either an exponentially decreasing neutrino potential dominates over a constant CC interaction, or the reverse [37], and crucially I do not consider the constraint on the NSI disappearing in the Sun. This means that I fix $\delta\epsilon$ and ϵ_0, so the NSIs will therefore not be able to change sign, as they only scale proportional to the CC potential, which remains positive throughout. For the diagonal, both potential orderings are just a rescaling of the vacuum and CC potentials since the NSIs are scaled relative to the CC Hamiltonian, so if the CC diagonal is changing, so is the NSI. The additional NSI off-diagonal terms do not just scale the off-diagonal, since the off-diagonals are purely from the vacuum or neutrino-neutrino interaction terms, and the NSI off-diagonal may be constant or changing depending on the setup. I use the Hamiltonian in eq. (57) with the addition of the neutrino-neutrino Hamiltonian,

$$\begin{aligned}\mathcal{H} &= \mathcal{H}_{\text{vacuum}} + [\mathcal{H}_{\text{CC}} + \mathcal{H}_{\text{NSI}}] + \mathcal{H}_{\nu\nu} \\ &= \frac{\omega}{2}\begin{bmatrix} -\cos(2\theta) & \sin(2\theta) \\ \sin(2\theta) & \cos(2\theta) \end{bmatrix} + \frac{\lambda(r)Y_e(r)}{2}\begin{pmatrix} 1+\delta\epsilon & 2\epsilon_0 \\ 2\epsilon_0 & -(1+\delta\epsilon) \end{pmatrix} + \frac{\mu}{2}\begin{pmatrix} F & Q \\ Q^* & -F \end{pmatrix}\end{aligned} \tag{72}$$

where both ϵ_0 and $\delta\epsilon$ are real single-valued numbers, rather than functions of of position. Since the system was explored in the neutrino-neutrino subsection, I already know what to expect, and add NSIs in order to remove or start resonances, as I see possible.

I'll start with the neutrino-neutrino interaction initially dominating the CC interaction. In this setup, I saw an MNR occuring, but no MSW effect, since the CC term never went to the vacuum level. Adding the NSI shifts the diagonal potential, such that the new MNR

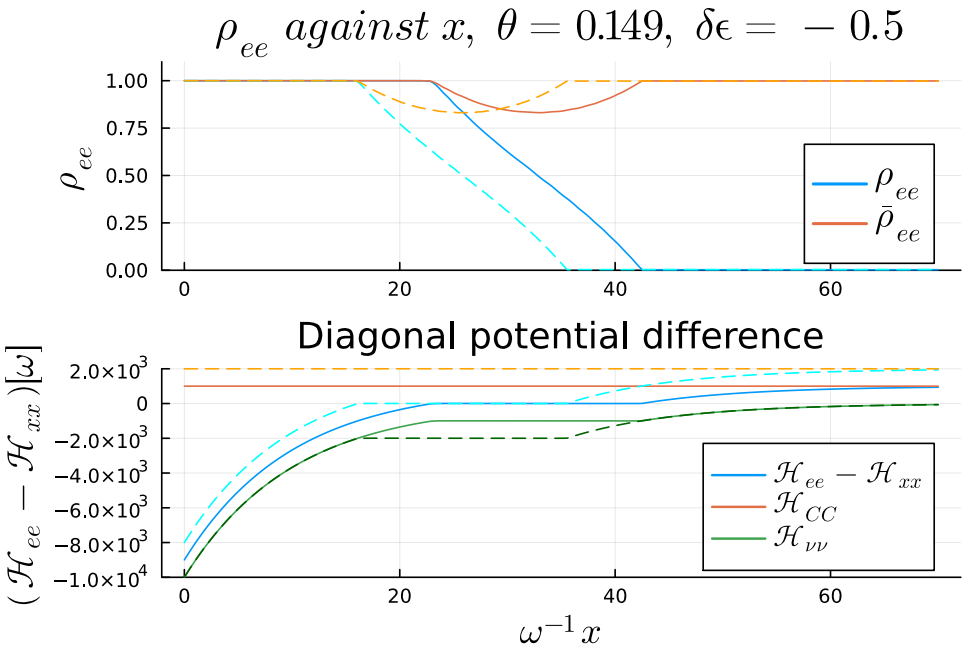

Figure 10: Diagonal NSIs have the effect of shifting, where the NSI contribution corresponds to $\delta\epsilon = -0.5$. The dotted line show the original system with $\delta\epsilon = 0$.

condition becomes,

$$\tan(2\theta_{\text{toy}}) = \frac{\omega \sin(2\theta) + \lambda\epsilon_0 + Q}{\omega \cos(2\theta) - \lambda(1 + \delta\epsilon) + \mu F} \tag{73}$$

where $\lambda = \sqrt{2} G_F n_e(x)$, i.e. the density of electrons in the system, and $n_e(x)$ will either be constant or exponentially decaying. The MNR location is therefore simply shifted by the $\lambda\delta\epsilon$ as compared to no NSI, see figure. (10).

In the region where $\delta\epsilon = -1$, the system is solely described by neutrino-neutrino and vacuum potentials, but the vacuum oscillations are not suppressed as extremely as for a CC potential (see fig. (8)). This is because Q and F are of relatively similar size, so the effective mixing angle stays more or less the same, although the effective frequency is changed. The difference in effective mixing angle between having no NSI and an NSI which cancels the matter potential can be seen in fig. (11). That the neutrino potential in and of itself is not enough to suppress the oscillations indicates that a large neutrino potential is not enough in and of itself to suppress possible resonances.

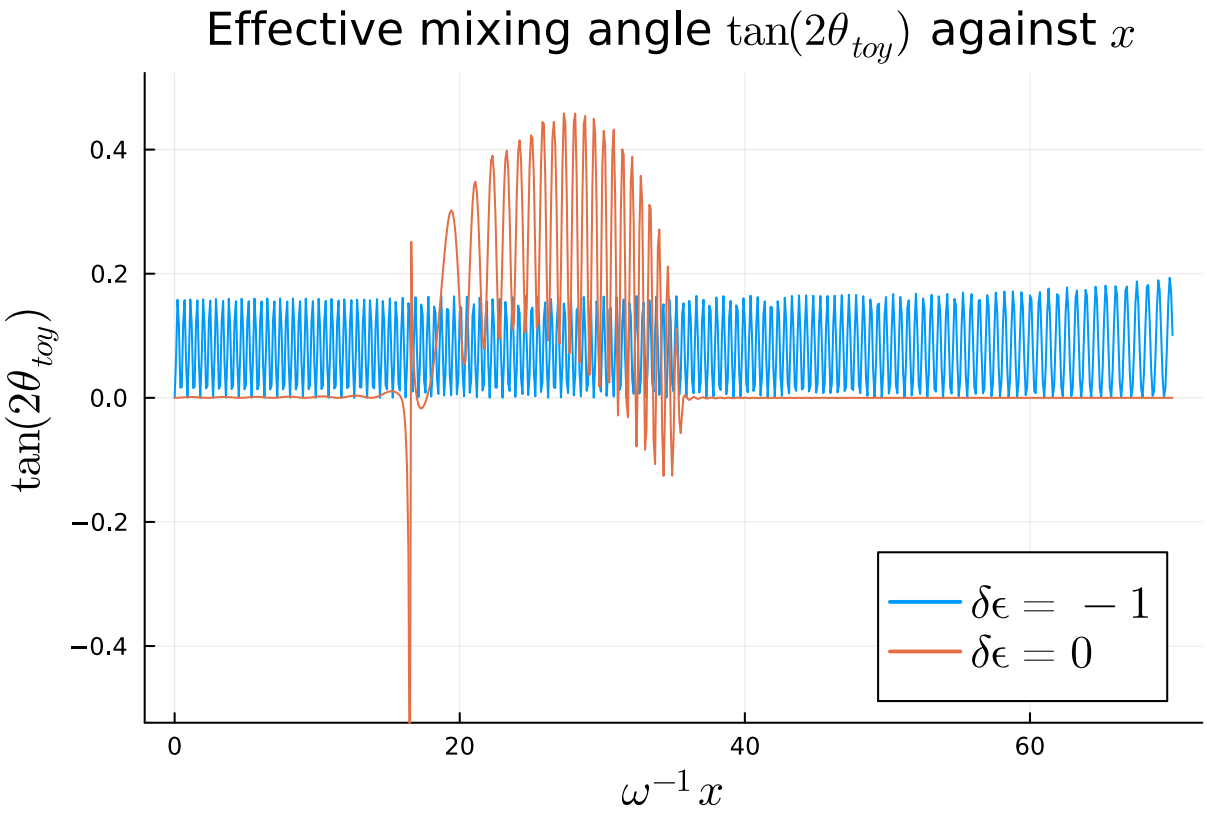

Figure 11: The difference in effective mixing angle, $\tan(2\theta_{\text{toy}})$ between having no matter potential and constant matter potential with $\delta\epsilon = -1,\ \epsilon_0 = 0$, in a decaying neutrino-neutrino potential.

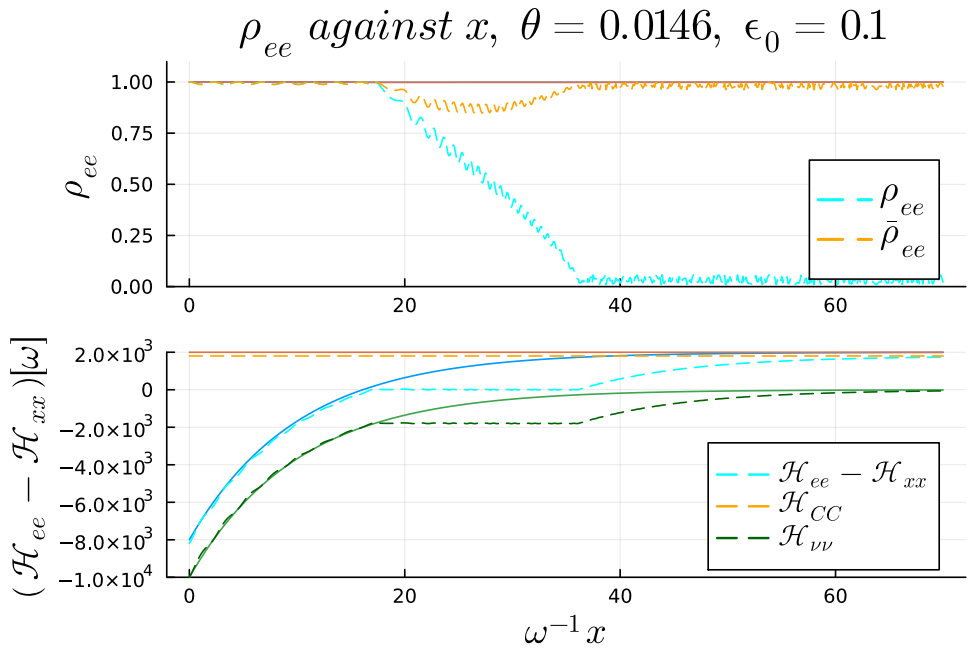

Figure 12: MNR occurring the in a system with modified mixing angle $\theta_{\text{modified}} = 0.0146$, due to an additional off-diagonal NSI. The full lines show ρ_{ee} and $\bar{\rho}_{ee}$ without NSI (both of which are 1 for the duration of the evolution), and the dotted lines are with NSI.

The off-diagonal contribution ϵ_0 changes how large the adiabaticity of the system should be before a resonance can occur. Indeed it shows that there exists a cut-off for which the MNR cannot happen anymore, and as the cut-off is approached, the MNR is reduced in magnitude. Figure (12) shows instead a modified mixing angle of $\theta_{\text{modified}} = 0.0146$ for which the MNR does not occur, but with the addition of NSIs it can reoccur. The same applies for NSIs removing the MNR by effectively changing the regular mixing angles given in Table 1. This requires some relation between the diagonals and the off-diagonals.

Now let me consider the case of falling CC potential with NSI. First of all, the MNR does not occur nor is there any MSW effect. However, there is some sort of resonance as can be seen in figure (13), since the neutrino potential is still large. That the neutrino potential suppresses the MSW from happening is important to keep in mind for later. If the CC was also decaying, then there may be an effect of the NSI on the bipolar resonance, since it may change the off-diagonal, meaning it could affect whether such a resonance could occur.

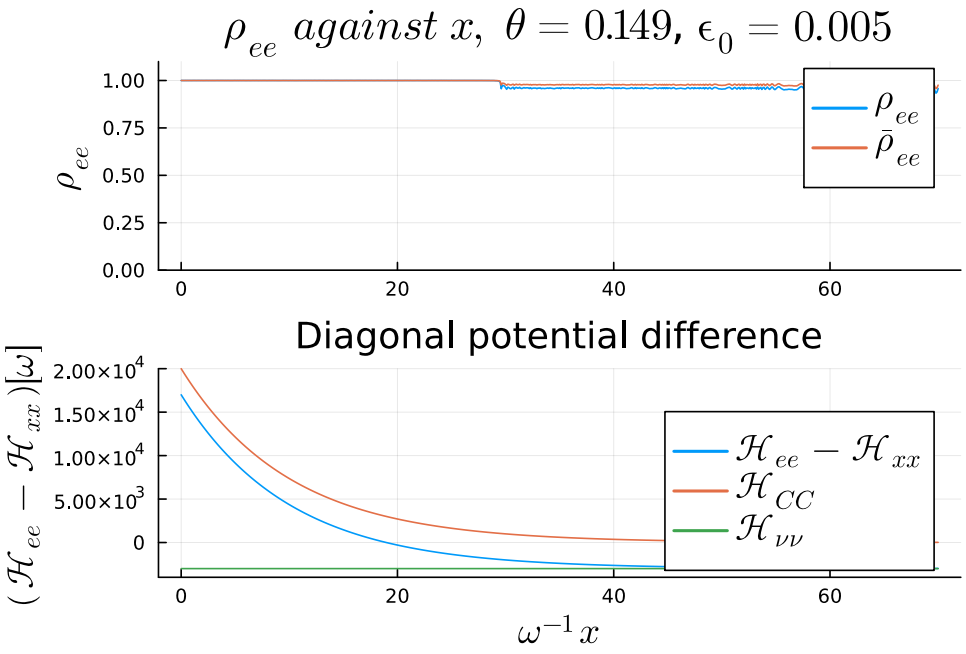

Figure 13: Exponentially decaying CC potential with $\epsilon_0 = 0.005$. There is a suppressed resonance, although the location does not match any of the conditions found in the theory section. In the MSW resonance condition is region, the neutrino potential is still $|\mathcal{H}_{\nu\nu}| = 1000\omega$ and the neutrino potential is suppressing the MSW from happening.

All in all, these effects show that the resonances will be perturbed by NSI and gives an idea of what to look for in a real system, namely,

1. The resonance location is shifted by $\delta\epsilon$

2. MNRs can be turned on or off by ϵ_0

3. The effective mixing angle for a large neutrino potential system is relatively large.

Non-Standard Interactions in a Binary Neutron Star Merger Remnant

Now I have built all the theory and code necessary to study the behaviour of neutrino oscillations in a Compact Binary Merger (CBM), specifically, I will consider the collision of two neutron stars from Ref. [1]. In general such mergers have neutron-rich ejecta, which are excellent sites for r-processes and heavy element production. Additionally, the mergers are rich in neutrinos and antineutrinos and r-processes are affected by the number of electron neutrinos and antineutrinos through beta reactions. Therefore the flavour evolution of the neutrinos and antineutrinos is important to consider for the production of heavy elements in such a system. Furthermore, the neutrino sector is furthermore a place where new physics may emerge, and a study of the effects of new non-standard mediators on flavour evolution is the main goal of this subsection. In general, the NSIs change the SM flavour evolution, and in parts of the NSI parameter space the final flavour population are completely inverted w.r.t. the SM results.

I will split my analysis into four parts. First I will go through the BNS merger remnant system. Then I will consider how neutrinos would oscillate on the background of the remnant with SM physics. This I will do for a select few trajectories, to capture the different types of oscillations I expect to occur in the system. Then I consider the effects that NSIs would have on said trajectories. Next I gather this in a more general view, where I consider the average of many trajectories, since flavour evolution is dependent on the geometry of the system. This is done for both SM and NSI potentials. Finally, I perform a parameter scan over possible NSI configurations, and analyse how the sectors of the parameter space can be decomposed in terms of a few trajectories.

Binary Neutron Star Merger Remnant

The synthesis of elements that are heavier than Iron is thought to be produced in the so-called r- and s-processes, where neutrons bombard nuclei at, respectively, 'rapid' or 'slow' rates. The nuclei climb the element ladder via β-decays, as they become unstable isotopes.

This may occur in neutron-dense environments, such as the collapse of stellar cores, otherwise known as Core Collapse SuperNovae (CCSNe), or a Compact Binary Merger (CBM), such as NS-NS systems (known as Binary Neutron Stars (BNS)), NS-BH or BH-BH. The binary merger loses energy by conversion of angular momentum into gravitational waves, and thus they are good candidates for multimessenger astronomy, as was confirmed by the gravitational detection of the GW170818 event [44]. The result of a binary merger is a merger remnant, where a Central object, which may be a hypermassive NS or another BH, is surrounded by various ejecta of the merger. The cross section of a remnant of such a system can be seen in figure (14). Neutrinos are emitted in large amounts, either through a neutrino-driven jet or from the decompression of the torus. The neutrino driven winds and outer layers of the ejecta are neutron-rich and so may be sites of r-processes. In particular, for BNS systems the neutron-rich material allows for very strong r-processes in the viscous and dynamic ejecta [1], compared to the wind. However, the r-process depends on the proton-to-neutron ratio. Neutrinos and antineutrinos emerging from the remnant may undergo beta reactions with the ejecta if they are the right flavour for such a reaction to occur. This changes the proton-to-neutron ratio, and thus the flavour evolution of the neutrinos is important for the elements which may be generated in this system. However, neutrino oscillations are not in general included in such hydrodynamical simulations, as the computational complexity increases significantly. Therefore the neutrino population only changes through interactions with other particles, such as inverse beta decay [1]. So one can approximate that the neutrino population is more or less constant until it hits the dynamic ejecta. As we will see, the effects of flavour conversions are substantial.

For this thesis I will be considering a hydrodynamical simulation of CBM remnant resulting from of a BNS merger with a BH central object in the post-merger phase from Ref. [1]. The system is assumed to be axially symmetric and therefore a 2D simulation is taken to be equivalent to a 3D simulation. The specific simulation is "M3A8m3a5_yyms" where M3A8 refers to a central 3 solar mass black hole of spin parameter 0.8, m3a5 is a 0.3 solar mass torus of viscosity parameter 0.05 and yy refers to the time slice in the $\mathcal{O}(10-50)$ ms. I will in particular be looking at the time slice at 20 ms. Initially, the

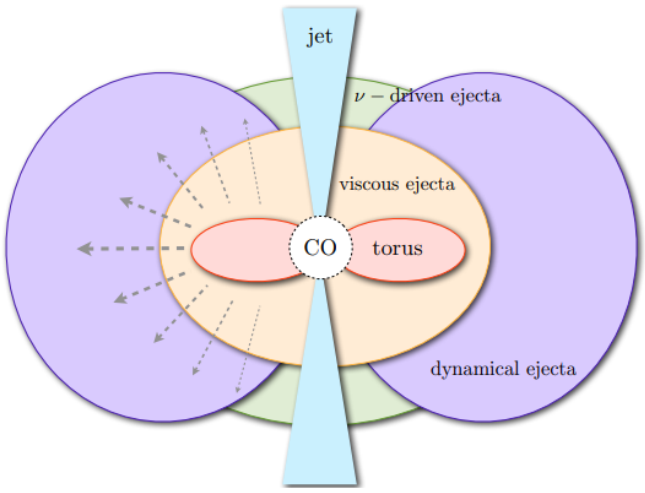

Figure 14: Cross section of a Compact Binary Merger Remnant, with a Compact Object (CO) in the center, surrounded by a torus, ejectra and outstreaming jets. From ref [43].

torus region is optically thick in the $\mathcal{O}(10-20)$ ms range, trapping neutrinos, but as it decompresses, neutrinos may emerge, cooling the disk.

Figures (15 - 18) show the cross section of various important parameters of the system, such as the baryon density, neutrino number density and relative neutrino-antineutrino number densities.

I follow Ref. [44] and define a surface where I assume that the average neutrino starts free streaming, i.e. the following medium is no longer opaque, so the neutrinos decouple from the medium and require that the subsequent scatterings are coherent. This surface is the *neutrinosphere* and is defined by $\frac{F_{\nu_\alpha}}{n_{\nu_\alpha}} = \frac{1}{3}$, where F_{ν_α} is the size of the neutrino flavour flux, and n_{ν_α} is the neutrino flavour number density, of the α neutrino at a point in space. The neutrinosphere for both neutrinos and antineutrinos can be seen in figures (15 - 18). After this point, it passed it is assumed that the mean free path is large enough to justify that on average no incoherent scattering happens. The remnant has a max nucleon density of $10^{35} cm^{-3}$ in the torus and so the mean free path of neutrinos in the densest part is of the order 1-10 km. At the neutrinosphere, the mean free path is much above this value, in the thousands of km, so I safely assume that the neutrinos are unperturbed on their path out of the remnant. The surface of the neutrinosphere in the cross-section can be seen in

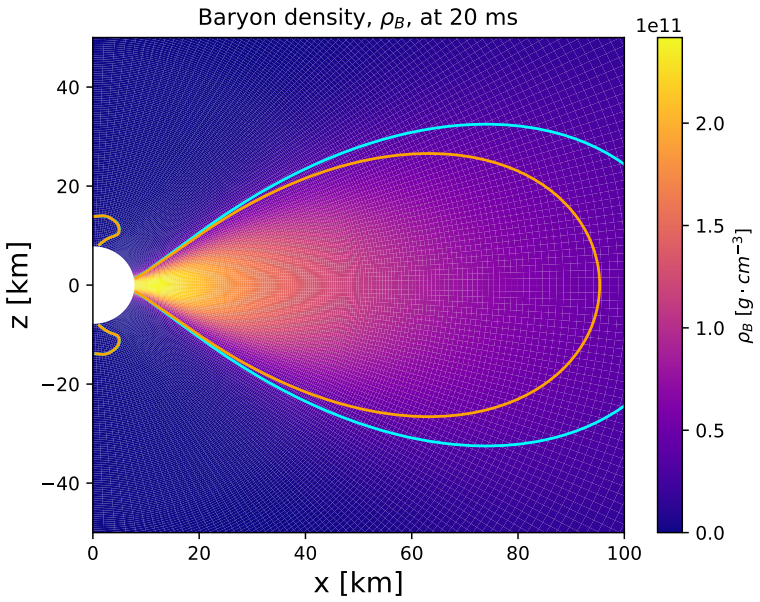

Figure 15: Baryon density for the BNS merger remnant of Ref. [1] at 20 ms after merging. Adapted from Ref. [44].Orange lines shows the antineutrinosphere, and the cyan line shows the neutrinosphere.

figure 15. It is worth mentioning that they consider dynamic ejecta, where the r-processes occur, begins at around 150 km from the central object.

This sets up the system in which I will explore how the flavour oscillation evolve. Let me first consider the effects that SM physics has on flavour oscillations.

Standard Model Flavour Oscillations

The Hamiltonian I will consider for the SM oscillation is eq. (46), where the vacuum term is for 1 MeV electron neutrinos and antineutrinos in the 1-2 neutrino sector with values from Table 1. The CC and unoscillated neutrino potentials (λY_e, μ) are computed from the BNS remnant simulation data, and shows that the jet is dominated by antineutrinos (figure 17), and that the baryon density is large in the torus, which shows a mean free path of around 10 km, i.e. incoherent scattering should occur in this region.

As I saw in the theory section, the resonance location is mainly determined by the cancellation of the Hamiltonian diagonal. Since the system is not spherically symmetric,

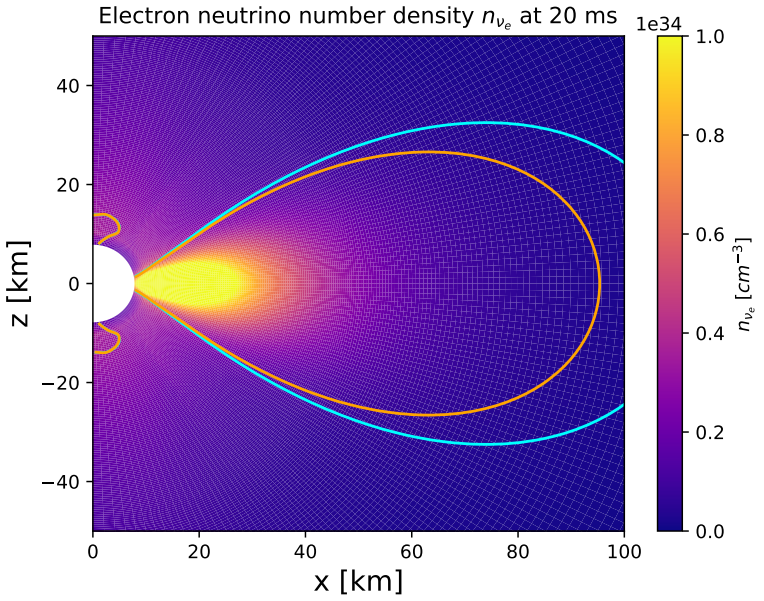

Figure 16: Electron neutrino number density for the BNS merger remnant of Ref. [1] at 20 ms after merging. Adapted from Ref. [44]. Orange lines shows the antineutrinosphere, and the cyan line shows the neutrinosphere.

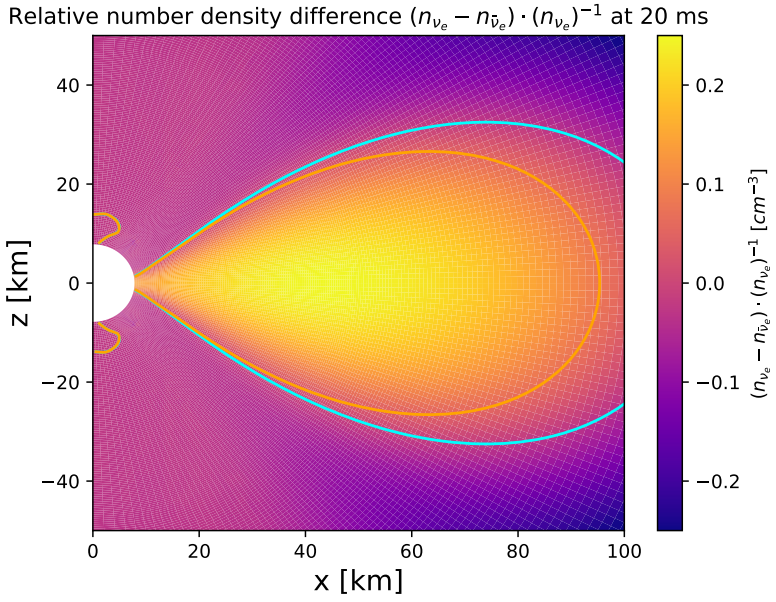

Figure 17: relative neutrino-antineutrino number density for the BNS merger remnant of Ref. [1] at 20 ms after merging. Adapted from Ref. [44]. Orange lines shows the antineutrinosphere, and the cyan line shows the neutrinosphere.

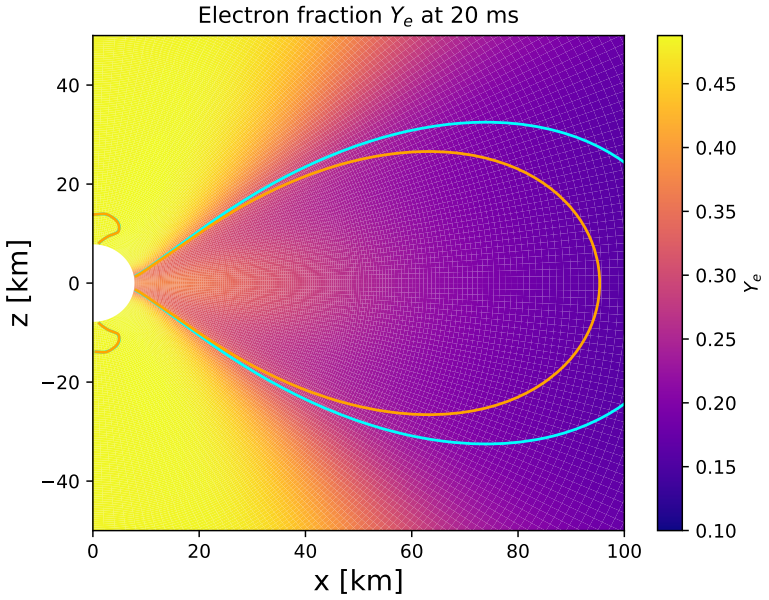

Figure 18: Electron neutrino number density for the BNS merger remnant of Ref. [1] at 20 ms after merging. Adapted from Ref. [44]. Orange lines shows the antineutrinosphere, and the cyan line shows the neutrinosphere.

the flavour evolution will in general be very trajectory dependent. Therefore a heatmap of the diagonal difference is a good place to start to have an idea of what the flavour evolution will be like for different trajectories. I consider the inner most part of the remnant close to the central object, as this is where the potentials are the most extreme. Figure. 19 shows this diagonal potential difference due to the vacuum, CC and neutrino potentials and also potential trajectories. From the figure I can see that the jet is governed by the negative neutrino potential, and that the torus is CC dominated. This shows that there exists possibilities for seeing resonances, as some MNR criteria are fulfilled, but to see whether they occur I need to numerically solve the flavour evolution of neutrinos crossing the regions where the potential changes sign. I cannot cover all trajectories, so I begin with disregarding trajectories which cross back across the neutrinosphere and trajectories that start other places than the neutrinosphere, and so I am left with radially forward peaked trajectories. Here I find similarities between two types of trajectory. Either the neutrino propagates away from the remmnant, or it propagates through the torus and then

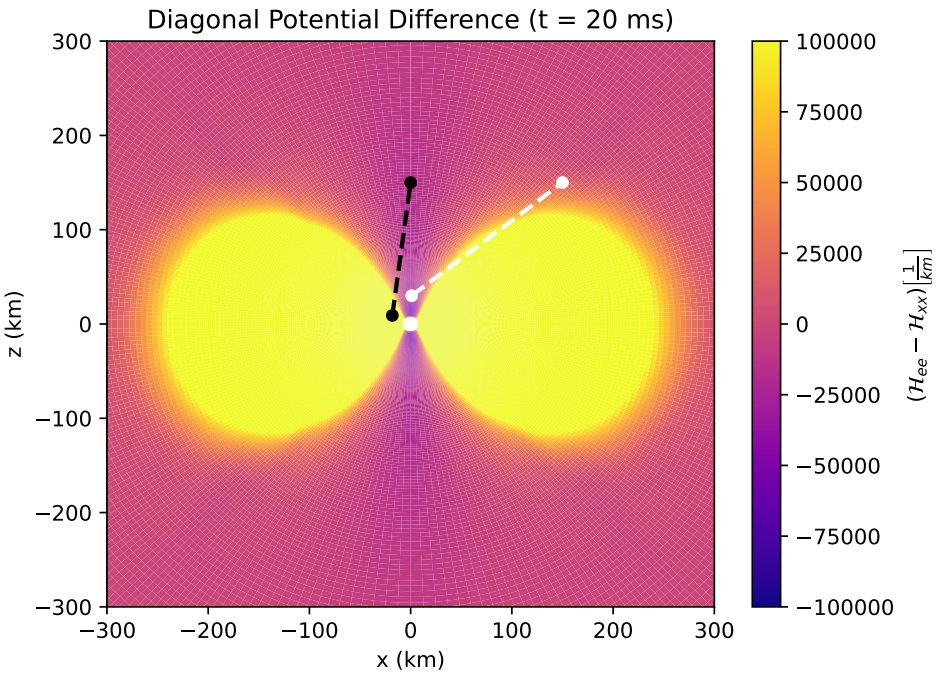

Figure 19: A heatmap of the diagonal potential difference at 20 ms, with two trajectories. The (x,y) coordinates of the trajectories are: black = {(-18,9),(0,150)}, white = {(1,30),(150,150)}. I have put an upper bound on the potential, so as to be able to see the regions where resonance effects may occur.

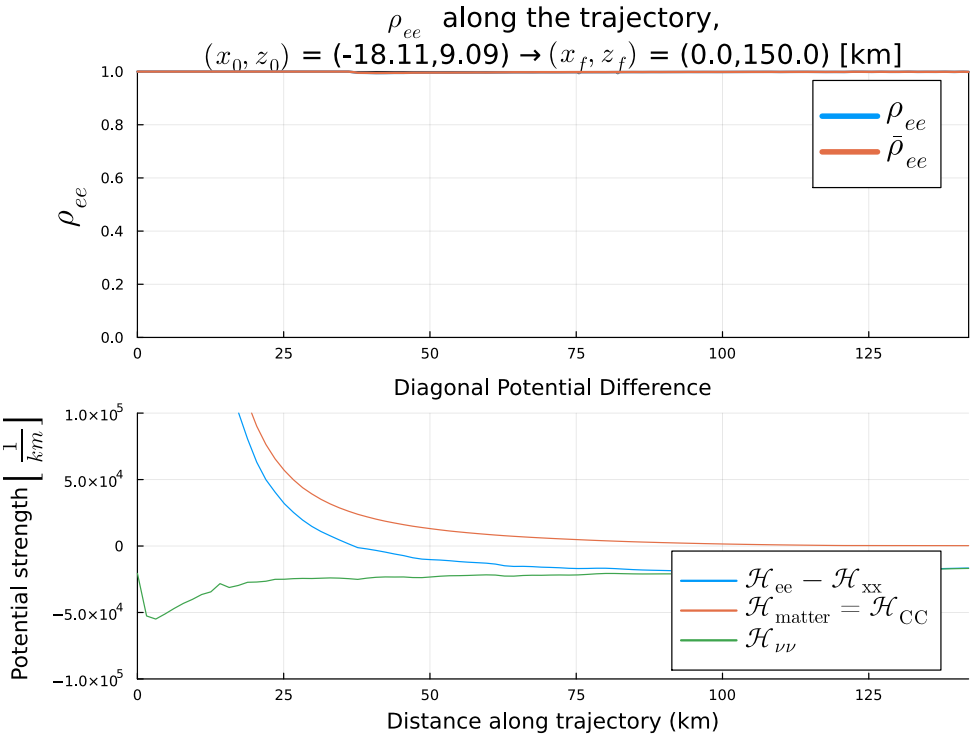

Figure 20: The electron neutrino and antineutrino populations, ρ_{ee}, as a function of the distance along their trajectory. This trajectory shows that trajectories which go directly away from the remnant experience a suppression in their flavour oscillation due to the large CC and neutrino potentials.

away. So I consider two neutrinos, where the first one starts at the neutrinosphere and goes away from the torus, effectively going from the positive CC potential into the negative neutrino potential. The flavour evolution can be seen in fig. 20, and shows that the flavour is mostly unperturbed, except at around 15 km along the trajectory. Here the diagonal potential difference goes to zero and an MNR condition is reached, and it looks like there is suppressed MNR occurring. However, the MNR is not possible in the scenario, since the $\mathcal{H}_{CC} > \mathcal{H}_{\nu\nu}$ to begin with. Instead what is occurring is just an extremely brief stint of vacuum oscillation.

The second neutrino starts in the jet and goes through the torus and away from the remnant. Not starting at the neutrinosphere can be here justified by no flavour evolution occurring from the CC-region into the neutrino-potential-region (as can be seen in figure 20) and the trajectory leading back to the neutrinosphere. The flavour evolution can be

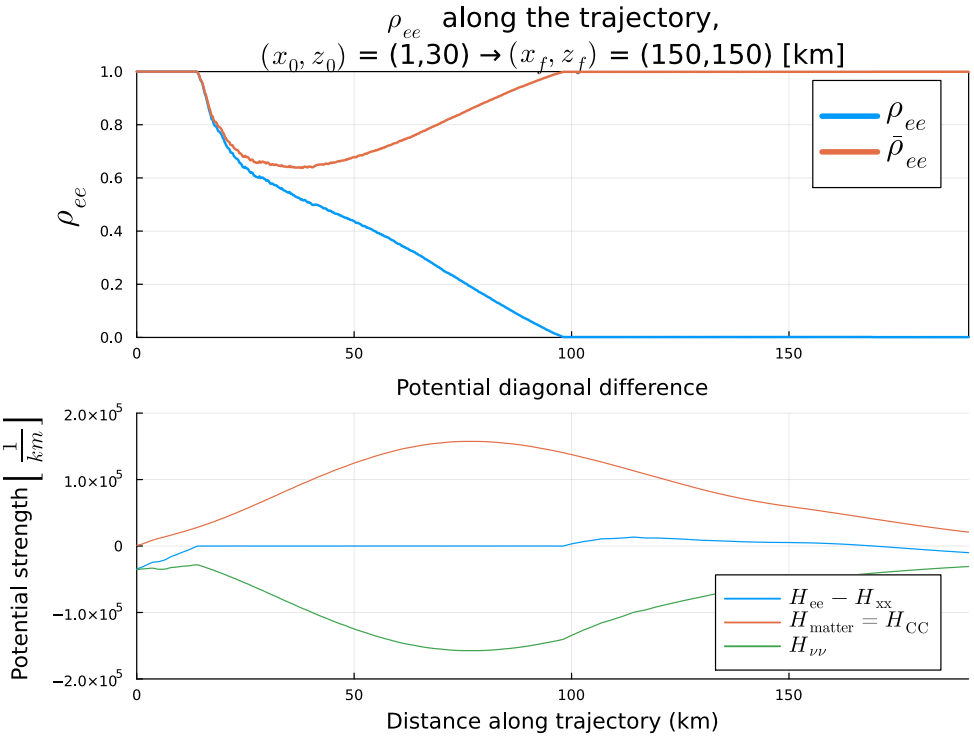

Figure 21: The electron neutrino and antineutrino populations, ρ_{ee}, as a function of the distance along their trajectory. This trajectory shows that trajectories which go through the outer torus region experience an MNR.

seen in figure 21. Since the trajectory goes through a $\mathcal{H}_{\text{CC}} < \mathcal{H}_{\nu\nu}$ region, a standard[11] MNR occurs. It is elongated by the CC potential changing derivative during the MNR, but still completes. In addition, I could let the neutrinos go further out in the system to where the CC and vacuum potentials cancel, and here the MSW resonance should happen. I assume the system looks much like my toy model here, with a small CC potential and large neutrino potential, and so I neglect to investigate this further as I am mostly concerned with the effects which occur close the remnant, but an MSW should happen at around 850 km from the center of the torus.

These two trajectories are representative for the rest of the trajectories in the system, that tells me that 1. Crossing from CC into neutrino potential dominated areas has no effect on the flavour evolution and 2. MNRs are possible for trajectories which cross through

[11] as opposed to the symmetric MNR found in [36], where both neutrino and antineutrino occupation numbers fall together.

the torus. This means that the relative neutrino-antineutrino occupation number will be affected in the plane of the torus. Both of these suggest that neutrino flavour evolution has an impact on the neutrino flavour occupation number in the outer layers of the remnant, where the r-processes occur. Firstly, the CC suppression will affect the regions above the torus plane, and the MNR will affect the torus plane. Any possible MSW only affects neutrinos far away and the MNR was trying to increasing in magnitude, therefore both the neutrino populations are affected, whilst the antineutrinos are stable. For a complete MNR (like fig. 21), the neutrino population is maximally reduced. This is again, for a single energy and single trajectory, and there exist trajectories where the resonances are cut off, so really I should average many trajectories to find the actual result. Now let me introduce NSIs and see how they perturb these trajectories.

Effects of Non-Standard Interactions on Flavour Oscillations

Adding in the NSIs, the Hamiltonian I now consider is exactly the one I found in eq. (69), with vacuum, CC, neutrino-neutrino and NSIs, where the NSIs obey the solar constraint. As I saw in the toy model, the NSIs will most likely change the position of any MNRs, so figure 22 shows the new heatmap of the diagonal potential difference in the case of $\delta\epsilon^n = -0.9$ and $\epsilon_0 = 10^{-4}$. In the inner region of the torus the electron fraction is low ($Y_e \sim 0.1$) which makes the combined matter Hamiltonian proportional to $\lambda\Phi = \lambda(Y_e - \frac{Y_\odot - Y_e}{Y_\odot}\delta\epsilon^n) \sim -\lambda 0.6$. So the torus is dominated by the NSI part, but as the electron fraction increases towards the jet area or the outer regions of the torus, Φ changes sign to be positive. Figure 23 shows the second trajectory with the NSIs turned on. The flavour evolution is perturbed heavily, and the final population is actually the opposite of the SM case. Let me look at the resonances one at a time. The first resonance is a failed MNR, which starts since the trajectory starts in the jet region, crosses into the region where Φ grows positive, meaning that the neutrino potential is dominating the matter potential. However, the matter potential becomes negative as the trajectory crosses towards the $\Phi \sim 0$ region. This means that the neutrino potential must decrease again, which it can

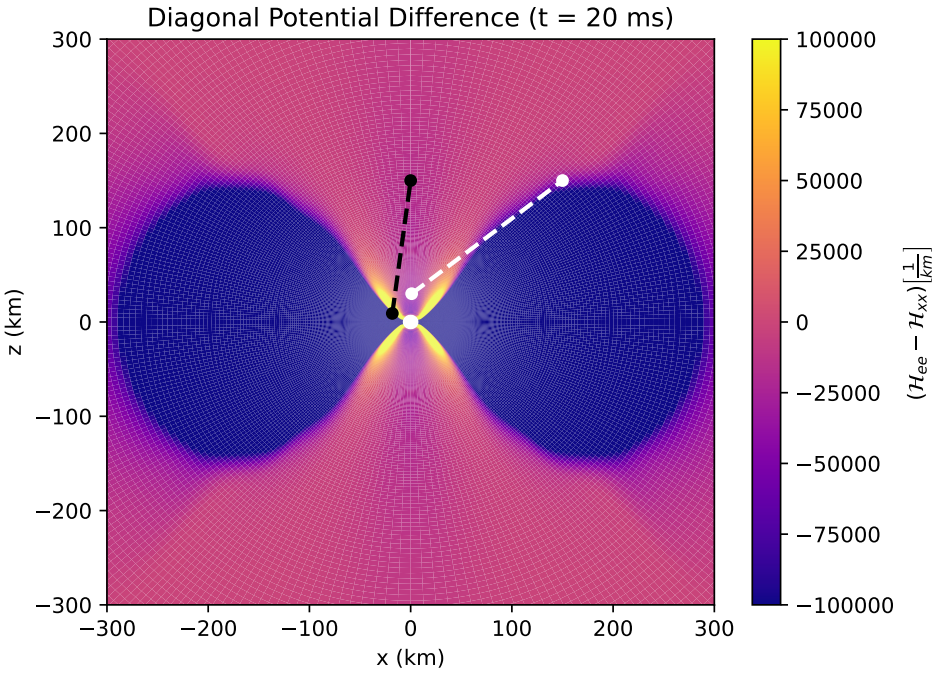

Figure 22: A heatmap of the diagonal potential difference with NSIs turned on for $\delta\epsilon^n = -0.9$ at 20 ms, with two trajectories. The (x,y) coordinates of the trajectories are: black = {(-18,9),(0,150)}, white = {(1,30),(150,150)}. I have put an upper bound on the potential, so as to be able to see the regions where resonance effects may occur.

only do by increasing the neutrino-antineutrino fraction. As trajectory crosses into the $\Phi < 0$ region the total diagonal goes to zero, and both the neutrino and antineutrino experience an abrupt MSW. The MSW is commonly only allowed for neutrinos, but the effective mixing angle is,

$$\tan(2\theta_{\text{NSI}}) = \frac{\omega \sin(2\theta) + 2(3 + Y_e)\epsilon_0 + \mu Q}{\omega \cos(2\theta) - \lambda\Phi - \mu F} \tag{74}$$

Since the total matter potential can change sign the vacuum term can also be cancelled for antineutrinos. So in the case of NSIs, a new Symmetric MSW effect may take place. This effect happens whenever the diagonal difference of the matter Hamiltonian changes sign, which is more or less whenever the dark purple areas change to lilac or yellow in figure (22). Here the observation in the toy model of MSW not occurring because of large background neutrino potential is to be noted, since the MSW suddenly can occur. The last resonance is a fulfilled MNR, which may occur since the neutrino potential has changed sign after the Symmetric MSW and can counteract the negative matter potential.

Since the symmetric MSW happens for the total diagonal goes to zero, then the same will happen in the first trajectory, as can be seen in figure (24)

Two things are worth noting. The first is that the second trajectory starting in the jet is no longer a good approximation, since it would experience a symmetric MSW effect before reaching the jet, and then it would experience another MSW again. Thus the full flavour evolution for trajectory two starting at the neutrinosphere would be a sort of well, as can be seen in figure (25). Thus this trajectory ends up with its original population. The second is that, in the case of no off-diagonal term, the adiabaticity of the MSW is too small, and one only sees the initially failed MNR in both trajectories. Thus both trajectories end up as their original population.

The figures 20 - 25 show that the NSIs have a large impact on the flavour evolution in both types of trajectories, and so impact both the total and relative neutrino-antineutrino population, as compared to the SM effects.

These effects were for a single set of NSI parameters $(\delta\epsilon^n, \epsilon_0) = (-0.9, 10^{-4})$ and just

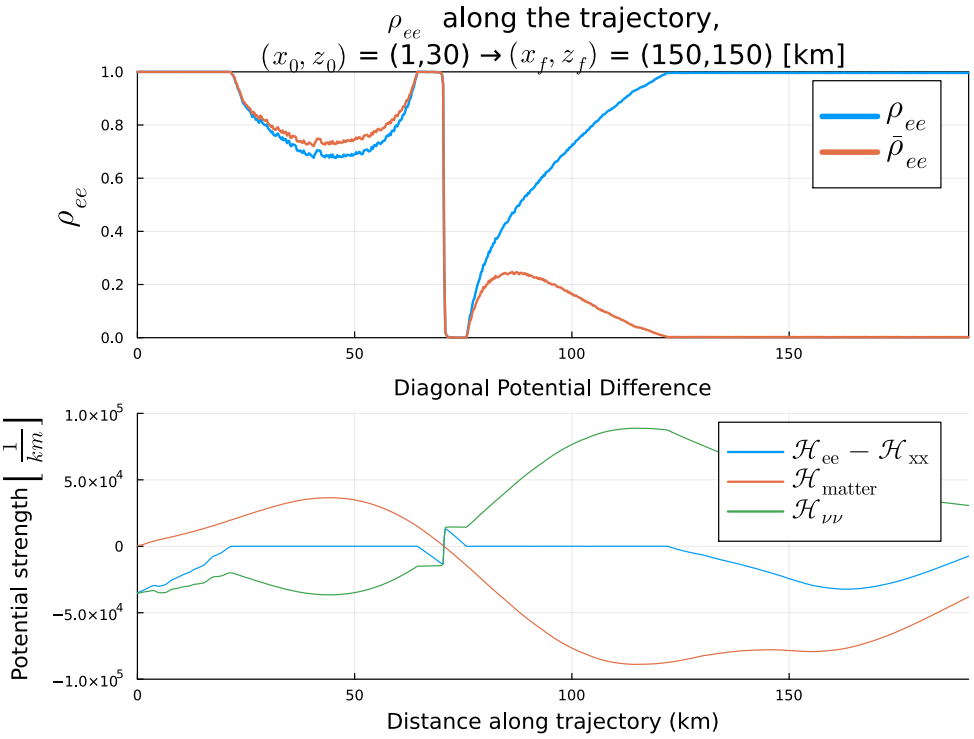

Figure 23: Flavour evolution of the second trajectory [(1,30) to (150,150)] with NSIs: $\delta\epsilon = -0.9$ and $\epsilon_0 = 10^{-4}$. Three resonances occur: First a failed MNR due to the matter potential decreasing. Secondly a symmetric MSW. Thirdly a standard MNR, but for a negative matter potential. Here $\mathcal{H}_{\text{matter}} = \mathcal{H}_{\text{CC}} + \mathcal{H}_{\text{NSI}}$ is the combined CC and NSI contributions to the matter Hamiltonian.

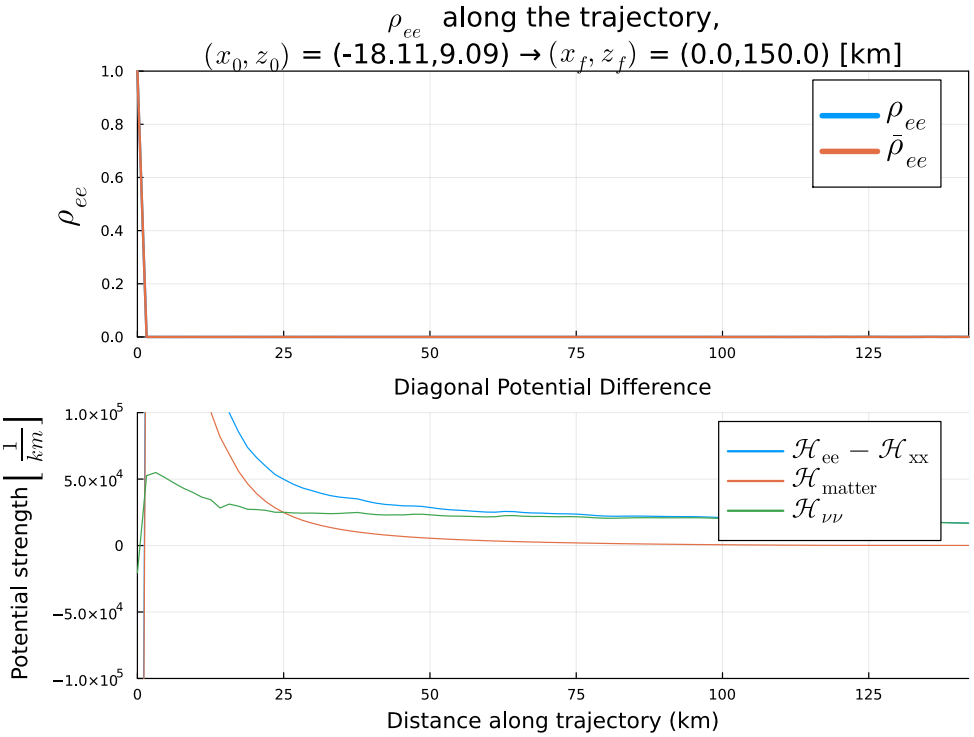

Figure 24: Flavour evolution of the first trajectory [(-18.11,9.09) to [(0,150)]] with NSIs: $\delta\epsilon^n = -0.9$ and $\epsilon_0 = 10^{-4}$. One resonance occurs: An initial symmetric MSW. Here $\mathcal{H}_{\text{matter}} = \mathcal{H}_{\text{CC}} + \mathcal{H}_{\text{NSI}}$ is the combined CC and NSI contributions to the matter Hamiltonian.

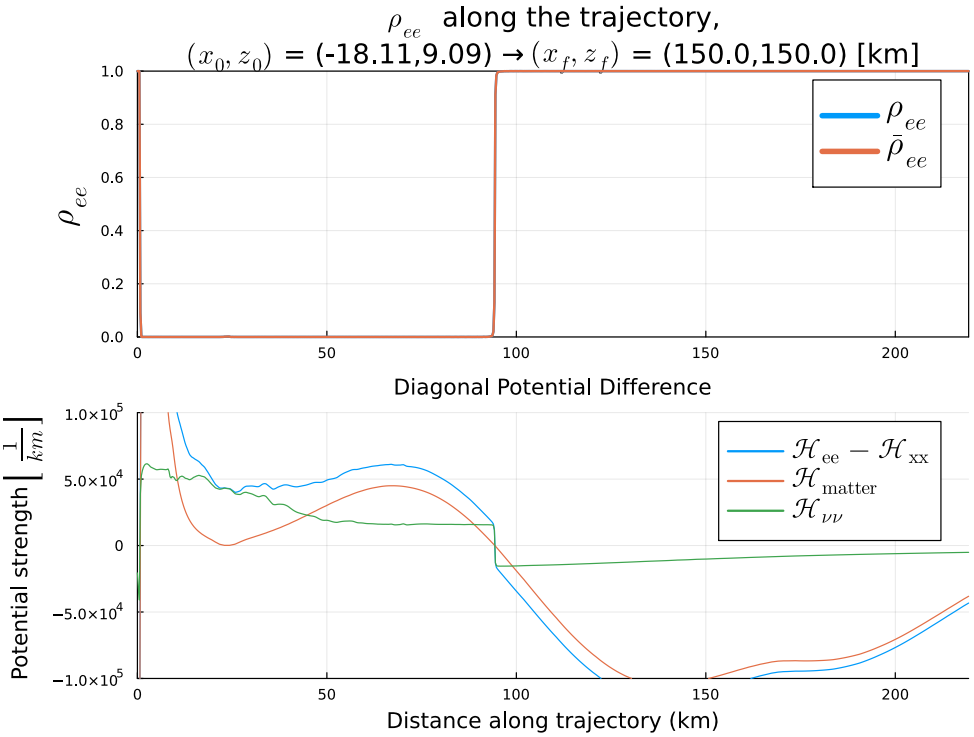

Figure 25: The second trajectory, but starting from the neutrinosphere [(-18.11,9.09) to (150,150)], with NSIs: $\delta\epsilon^n = -0.9$ and $\epsilon_0 = 10^{-4}$. The flavour evolution experiences two symmetric MSW effects and becomes a well, as opposed to the two MNRs and single symmetric MSW experienced in the case of figure (21).

two trajectories. First of all, the $\delta\epsilon^n$ parameter can control how large the dark purple region in figure 22 is which as an impact on whether the initial symmetric MSW happens. So a parameter scan over possible NSI combinations is necessary. Secondly, in order to have an idea of the overall effect that the NSIs might have on the neutrinos as they exit the inner remnant region and arrive at the r-process region in the dynamic ejecta, I cannot just consider the effect of a single neutrino trajectory or two. I will have to consider the average effect of neutrinos propagating from along the entire neutrinosphere. To begin with, I explore the impact of the neutrinosphere, and then the NSI combinations in the following subsubsection.

Average Flavour Population from the Neutrinosphere

Since the flavour evolution is dependent on the trajectory, it would be wise to consider the final population averaged over many trajectories from along the neutrinosphere. Then I can average the neutrino flavour population at any point (x,y) to find the total effect of the flavour evolution. This will incorporate the weight of how many neutrinos undergo certain resonances. For example, if I consider the point (150,150) [km], many trajectories along the neutrinosphere will undergo no resonances, and a small amount of trajectories undergo SM standard MNRs (figure 21), flipping the electron neutrino population. The average neutrino population will then only be slightly reduced by the MNR-type trajectories. I require that the trajectories do not cross back over the neutrino sphere, which ensures they do not go into an incoherent scattering regime. I pick out 16 points[12], which symmetrically span the upper half of the torus, and consider four endpoints in (x,y) [km] : along the z-axis (0,150), slightly to the right of the torus (150,150), to the right and further out (150,250) and lastly a point far outside of the primary resonance regions (550,405). These points have been chosen to show the overall effect of propagating in the system. Either above the plane of the torus to points (0,150) or (150,250), or near the plane of the torus to points (150,150) or (550,405). The points can be seen in figure 26. I numerically evolve

[12]The chosen points are in the Appendix and go from the inner region of the torus to the outer edge.

End points	$\overline{\rho_{ee}}$	$\overline{(\bar{\rho}_{ee})}$	$d = \overline{(\rho_{ee} - \bar{\rho}_{ee})}$	$s = \overline{(\rho_{ee} + \bar{\rho}_{ee})}$
$(0, 150)$	0.9981	0.9984	$3 \cdot 10^{-4}$	1.997
$(150, 150)$	0.6410	0.9697	-0.3287	1.611
$(250, 150)$	0.9958	0.9969	$1 \cdot 10^{-3}$	1.993
$(550, 405)$	0.7473	0.9938	-0.2465	1.741

Table 3: The average neutrino and antineutrino populations at different end points in the remnant at 20 ms, for 16 symmetric points along the neutrinosphere. s and d are respectively the sum and difference of the end point neutrino-antineutrino populations.

a neutrino from each on the 16 points on the neutrinosphere to an endpoint and look at the final population the neutrino and antineutrino population. The average I compute as $\overline{\rho_{ee}} = \frac{1}{N}\sum_i \rho_{ee}(r_i)$, with N the number of trajectories and $\rho_{ee}(r_i)$ the final population from initial point r_i. The results for the final population can be seen in Table 3, where the final populations and their sum and difference are given. These results can be split into two. The average trajectory for the two points (0,150) and (150,250) do not cross any resonances and hence their oscillation is suppressed by the CC potential, as in figures (20). For (150,150) and (550,405), about a third of the trajectories go through an MNR resonance as in figure 21 and hence the population of the neutrinos is reduced.

For completeness, I add that only picking points along the neutrinosphere in 2d misses that I am going beyond the axial symmetry of the system. As soon as I consider an endpoint outside of the z-axis, I have to take into account the oscillations. This is however beyond the current scope of the project.

Averaging over several initial positions shows me that the neutrinos and antineutrino population have been perturbed by the oscillations, in such a way that some trajectories must have gone through the torus region. Since I know that the SM MNR must come from crossing from a negative neutrino potential into a positive CC potential, then this contribution must come from the torus on the opposing side to the end point. This is a trend which I see again when I include the combined effect of NSIs and averaging the trajectories, and points at a dependence on the initial region and endpoint, rather than the exact trajectory.

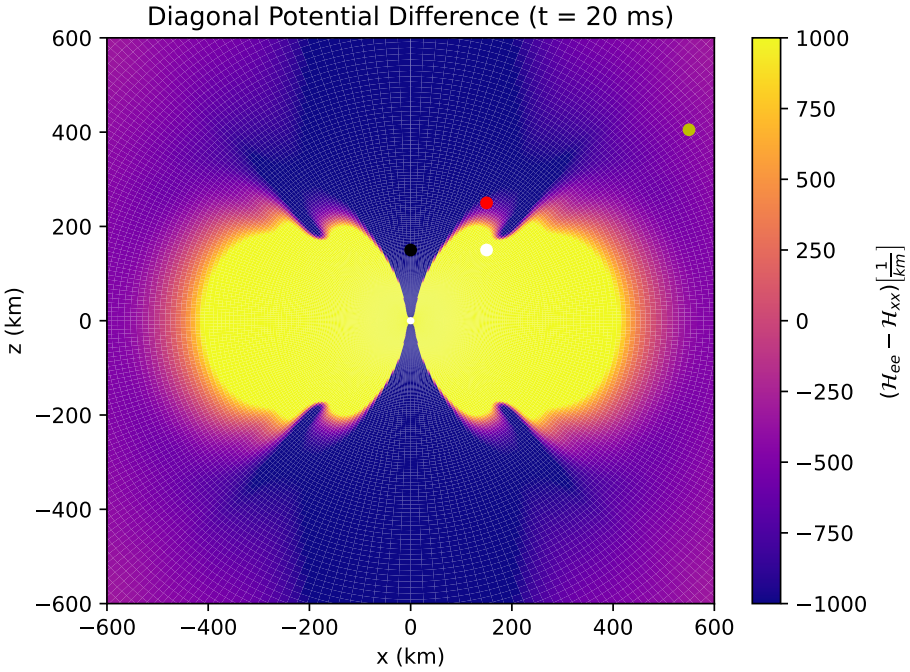

Figure 26: Diagonal potential difference heatmap with SM potentials, with endpoints for the flavour evolution of 16 symmetric points along the neutrinosphere. The endpoints are: black = $[0, 150]$, white = $[150, 150]$, red = $[150, 250]$ and yellow = $[550, 405]$. The neutrinosphere lies far inside of the yellow region, as can be seen by comparison with figure 15.

Parameter Scan of the Non-Standard Interactions

In the theory subsection NSI I computed the bounds of the $\delta\epsilon^n$ and ϵ_0 to be around $\mathcal{O}(5)$ and $\mathcal{O}(0.5)$, respectively. The parameter scan will go much below this. I will compute a range of NSIs from $\delta\epsilon^n = [-1, 5, 0.4]$ and $\delta\epsilon^n = [10^{-6}, 10^{-4}]$ with steps of 0.1 and 10^{-5} respectively. This will give me a rather poor resolution, but it will give a rough estimate of what I can expect to happen as I change the values. I analyse the flavour outcomes of a single one of the endpoints above in detail. For the rest of the endpoints, I include the graphs for completeness, with explanations in the descriptions. In particular, I am interested in whether the NSIs give me a different total and relative population of neutrinos as compared to the SM oscillations. Therefore I compute the average total and relative populations and divide it by the SM final outcomes found in Table 3.

I will focus on the parameter scan for the endpoint (150,150), as I saw flavour conversions for this endpoint in the previous subsection. The scans can be seen in figures (27) and (28) which respectively show the relative and total populations. The first thing to notice is that the effect of the off-diagonal NSI ϵ_0 is saturated quickly, and afterwards does not have a large effect on most of the parameter space. Therefore I'll split this into three sectors based on the magnitude and sign of diagonal: $\{[\delta\epsilon^n < -0.9], [-0.9 < \delta\epsilon^n < -0.3], [-0.1 < \delta\epsilon^n < 0.4]\}$. The relative population is defined such that if antineutrinos dominate the sign becomes negative so the regions in figure 27 which are blue, have more antineutrinos than neutrinos and red regions are more abundant in neutrinos.

The $[\delta\epsilon^n < -0.9]$ region has a negative matter potential which dominates the entire remnant region (the dark purple region in figure (22) grows when $\delta\epsilon^n$ is large and negative.). This means that any resonance is suppressed, except at very small ϵ_0 where the symmetric MSW is halted and the system experiences an MNR[13]. Once ϵ_0 reaches a critical value, a double symmetric MSW effect happens for this entire region. Hence the difference is ~ 0, since both neutrinos and antineutrinos are affected and the total population is higher than the SM, as the MSW is maximally changing the populations. Thus the region is very

[13]See figure (36) in the Appendix for an example.

uniform in structure.

As the diagonal is lowered, the negative matter potential can dip below the neutrinosphere, so that the symmetric MSW effect does not occur at the beginning of each trajectory. This is why the region $[-0.9 < \delta\epsilon^n < -0.3]$ has a peculiar structure. The region is denser in neutrinos than antineutrinos, so I am seeing something akin to a combination of figures (23 - 25), where, in the inner region of the remnant, the relative population inverted with respect to the SM evolution due to a symmetric MSW and an MNR resonance. The total population is also diminishing, meaning that it is not exactly just an inversion I am seeing, as otherwise the total population would stay the same. Instead, these are interrupted MNRs, culminating in the MNRs occurring at $\delta\epsilon^n = -0.4$ being completely interrupted, so the symmetric MSW is the dominating effect[14], making the relative populations zero and the total plummet. I note, however, that although there is a plummet, it only halves the total population, since the MNRs only occur for trajectories originating in the torus opposite the endpoint.

As $\delta\epsilon^n$ passes zero and goes toward 0.4, the number of trajectories which experience MNRs are more pronounced, as the positive matter potential increases in size, thereby increase the number of trajectories which undergo MNRs, hence, the relative population increases in favour of antineutrinos (more blue.) in this sector.

I am able to explain the sectors of the parameter scan using the flavour oscillations I found in the Effects of Non-Standard Interactions of Flavour Oscillations subsection, which suggests that those trajectories are good predictions for many different trajectories. Indeed it seems that for a given set of NSI parameters, one can equate variations of the flavour evolutions found in figures (23 - 25), with different regions of the remnant. Let me consider $\delta\epsilon^n \sim -0.7$ as an example. The parameter scan figures suggest that some relative population inversion is occurring, with respect to the SM evolution case, and also that the total population is somewhat diminished. The actual trajectories can be split into the three flavour evolutions of the Effects of Non-Standard Interactions of Flavour Oscillations subsection, almost exactly. Any trajectory which starts in the region of the main left part

[14]See figure **??** in the Appendix.

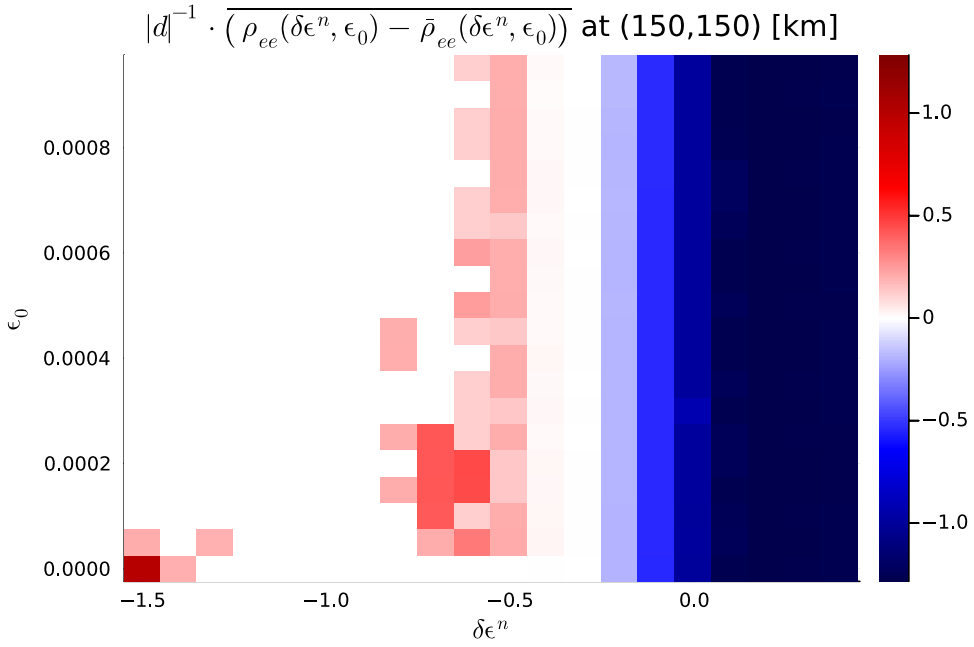

Figure 27: Parameter scan over different values of $(\delta\epsilon^n, \epsilon_0)$ for the averaged neutrino-antineutrino relative population with an endpoint at $(150, 150)$. The plots can be split into three overall sectors. The left sector is dominated by a symmetric MSW. The middle sector is a combination of symmetric MSW and MNRs. The right sector has an increased number of MNRs and looks most like the SM case.

of the torus will experience an evolution as in figure (25) and on the main part of the right torus their evolution is as figure (24). Neutrinos emerging from around the central object will in general experience an evolution like figure (23) MNR. This suggests that the overall trajectory is not so important for the flavour evolution, but the initial starting region is. For one thing, this lessens computational complexity, as I can rely on a smaller sample of trajectories representing a larger surface on the neutrinosphere, with some appropriate weighting based on how big the represented surface is. This also indicates that the single-angle approximation, while still woefully inadequate, can be slightly justified, since many trajectories and momentum directions can be lumped together, based on the region in which it starts. This lessens the computational complexity, but the full treatment is still far beyond current computational limits.

This was just a single endpoint, and already one can see that the effect of NSIs is rich in

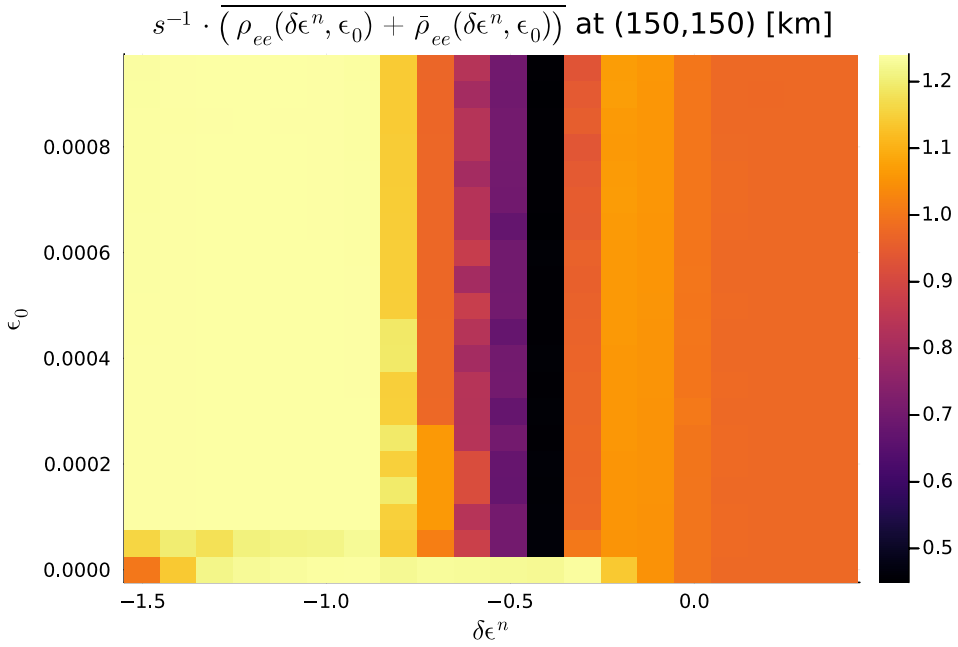

Figure 28: Parameter scan over different values of $(\delta\epsilon^n, \epsilon_0)$ for the averaged neutrino-antineutrino total population with an endpoint at $(150, 150)$. The plots can be split into three overall sectors. The left sector is dominated by a symmetric MSW. The middle sector is a combination of symmetric MSW and MNRs. The right sector has an increased number of MNRs and looks most like the SM case.

different flavour outcomes and on the total flavour flux. I include parameter scans for the other endpoints with explanations of the general behaviour in the caption for completeness, but will not go into a further analysis of these points. These can be found from figure 29 through to figure 34, with limited analysis in the captions. However, these points represent the general behaviour of the system and that is why their parameter scans are included. There is a larger dependence on the off-diagonal for regions so far from the remnant as can be seen from figure 34. This point is however so far outside the remnant that the overall population should start to decrease from beta reactions which should be taken into account.

This ends the section on NSI effects in the BNS merger remnant provided by ref. [1]. I defined a region from which the neutrinos could escape their production region, the neutrinosphere, and evolved these neutrino states along different trajectories in the system. I started with the SM effects on the oscillation and saw that MNRs and MSW effects are both occurring within the system, although at different radii, the MSW occurring beyond the start of the dynamic ejecta, where the neutrinos are expected to undergo inverse beta decay. I then added NSI effects I found that the NSIs can have large effects on the flavour evolutions of different neutrino trajectories through the system. In particular, I found examples where the final neutrino and antineutrino populations may be inverted with regard to the SM oscillations. As the system has a complex geometry, I averaged over many different initial trajectories from the neutrinosphere for both the SM and NSI cases, to find what the relative and total population would be at specific points within the system. Finally,a parameter scan revealed that many kinds of final flavour populations were possible, and very much dependent on the endpoints in the system.

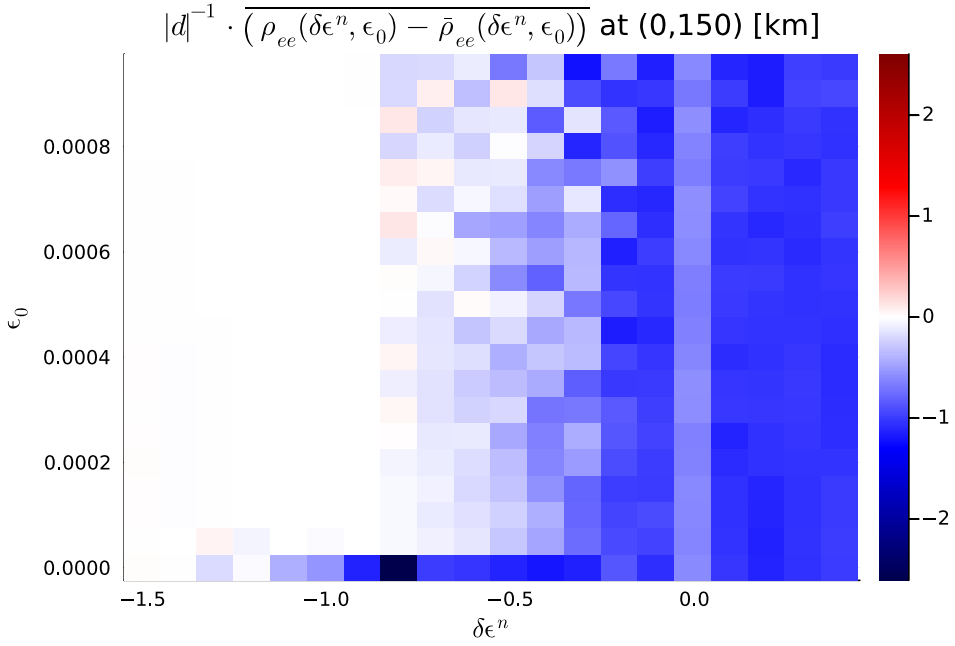

Figure 29: Parameter scan over different values of $(\delta\epsilon^n, \epsilon_0)$ for the averaged neutrino-antineutrino relative population with an endpoint at $(0, 150)$. The SM relative difference in population is given in table 3, and is very close to zero. This remains true throughout this plot, although it seems like a lot of variation is occurring. This is an artefact of the already low SM difference. The white region is a difference on the order of 10^{-7} and the blue region is of the order 10^{-3}, so both or basically in regards to any flavour difference of notice.

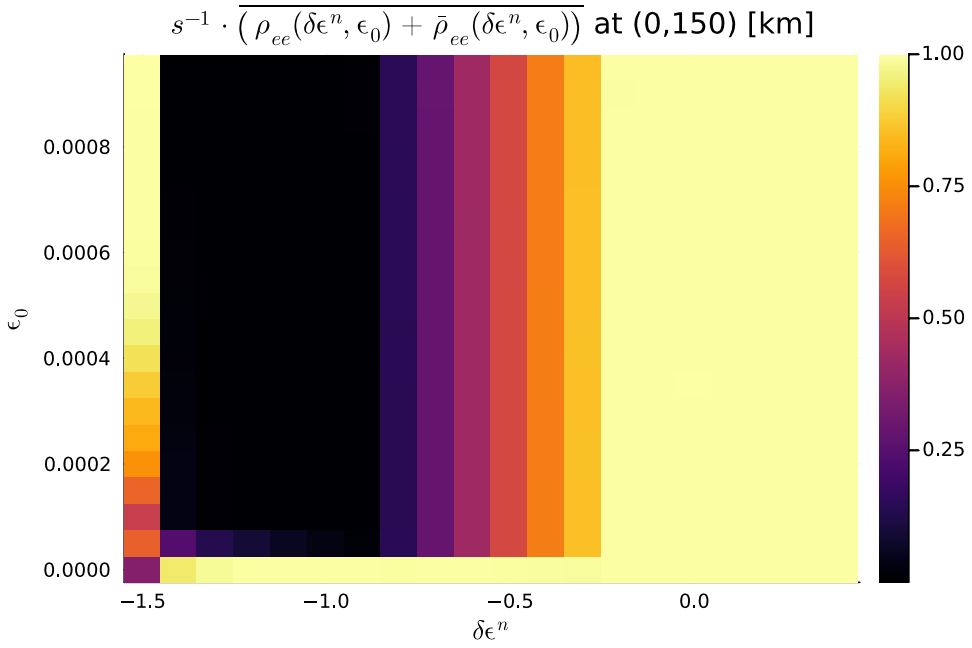

Figure 30: Parameter scan over different values of $(\delta\epsilon^n, \epsilon_0)$ for the averaged neutrino-antineutrino total population with an endpoint at $(0, 150)$. In general the high $(\delta\epsilon^n, \epsilon_0)$ region shows a single symmetric MSW effect, hence the decrease in overall population. As $\delta\epsilon^n$ is lowered the negative matter potential drops below parts of the neutrinosphere, so the total population starts to rise as they have overall supressed oscillations as in figure 20.

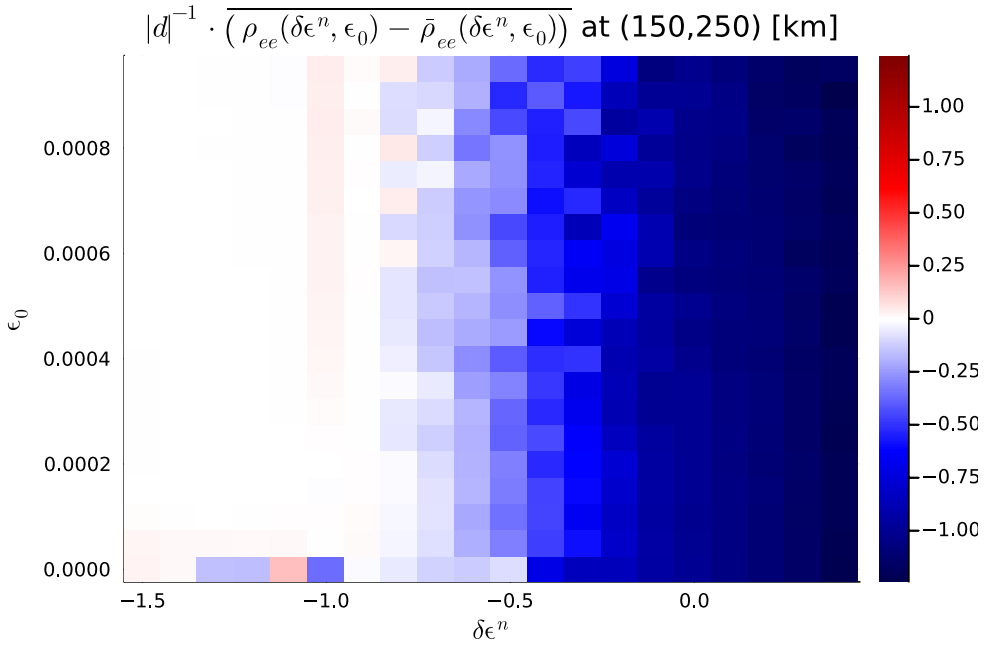

Figure 31: Parameter scan over different values of $(\delta\epsilon^n, \epsilon_0)$ for the averaged neutrino-antineutrino relative population with an endpoint at $(150, 250)$. The SM relative difference in population is given in table 3, and is very close to zero. This remains true throughout this plot, although it seems like a lot of variation is occurring. This is an artefact of the already low SM difference. The white region is a difference on the order of 10^{-7} and the blue region is of the order 10^{-3}, so both or basically in regards to any flavour difference of notice.

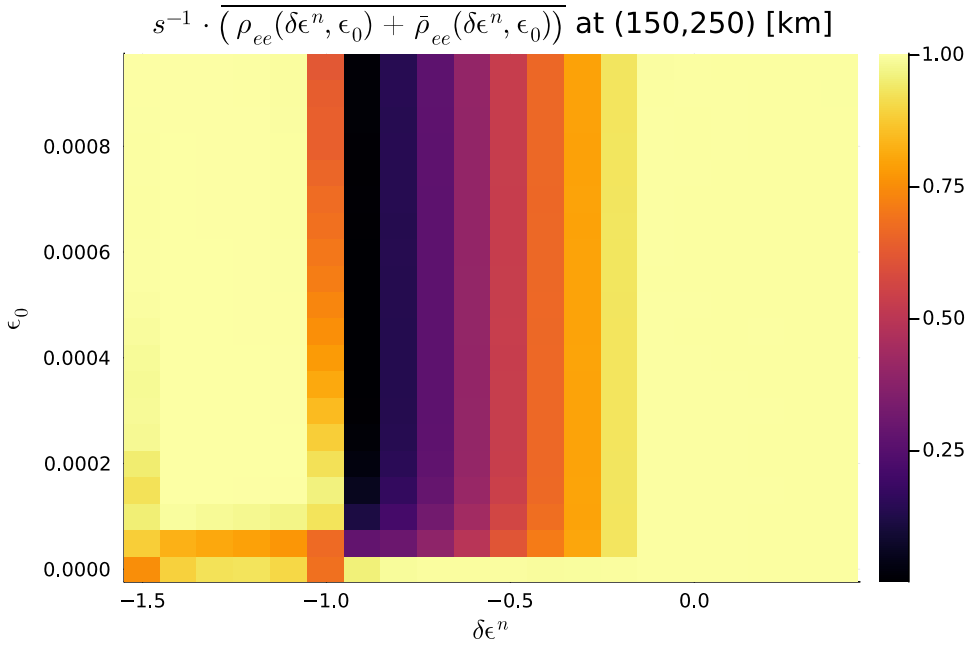

Figure 32: Parameter scan over different values of $(\delta\epsilon^n, \epsilon_0)$ for the averaged neutrino-antineutrino total population with an endpoint at $(150, 250)$. The endpoint $(150, 250)$ is within the negative matter potential for high $\delta\epsilon^n$, and as it lowers to $\delta\epsilon^n = -0.9$, the point is such that the negative matter potential is crossed three times. This means that either one or three symmetric MSWs are experienced, and so the total neutrino population drops substantially. See figure (38) in the appendix for an example of the three symmetric MSWs.

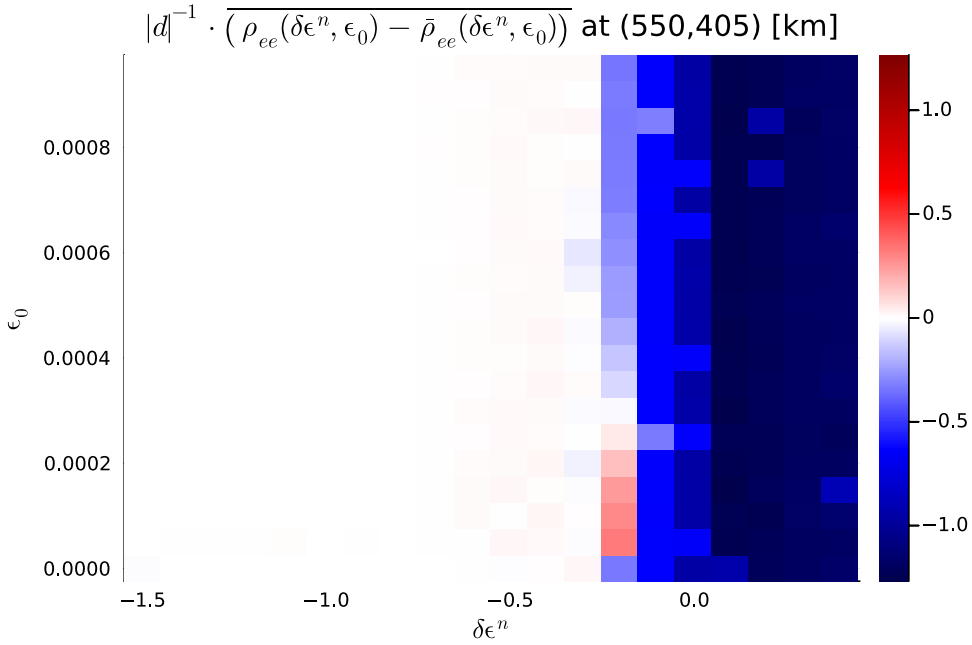

Figure 33: Parameter scan over different values of $(\delta\epsilon^n, \epsilon_0)$ for the averaged neutrino-antineutrino relative population with an endpoint at $(550, 405)$. The left sector of $\delta\epsilon^n > -0.3$ shows no difference in relative populations, and here the relative population difference for SM was ~ -0.24. The left sector shows stable relative population because all flavour conversions are halted MSWs, hence their populations are large. In the right sector are unfinished MNRs due to the MNR starting later.

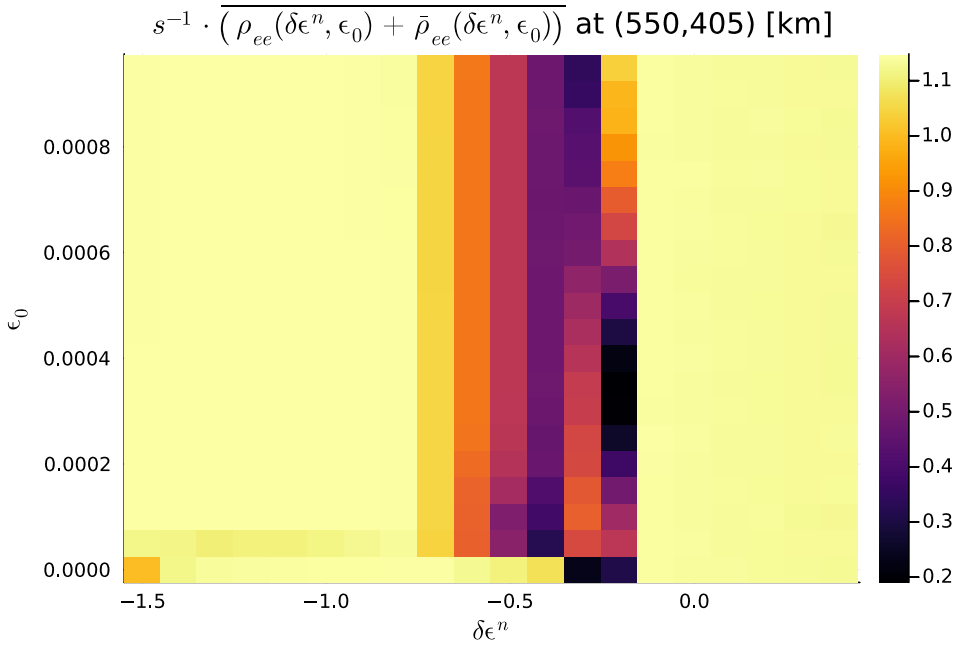

Figure 34: Parameter scan over different values of $(\delta\epsilon^n, \epsilon_0)$ for the averaged neutrino-antineutrino total population with an endpoint at $(550, 405)$. The left sector shows stable total population because all flavour conversions are halted MSWs, hence their populations are large. The middle sector is more complicated and warrants further study. The right sector shows unfinished MNRs, due to the MNR starting later.

Conclusion

Neutrinos are produced copiously in Compact Binary Mergers (CBM) and their remnants and are also environments where the otherwise weakly interacting neutrinos may interact with the abundant matter and neutrino backgrounds. This influences the flavour conversion as the neutrinos propagate away from these events and may result in different types of flavour resonances where the neutrinos can undergo flavour conversions. These CBM remnants are thought to be excellent candidates for heavy element production through the r-process, whereby nuclei are bombarded with neutrons which creates an unstable chain of heavy isotopes with increasing proton number. This process is very dependent on the proton-to-neutron ratio in the outer layers, the dynamical ejecta, of the merger. This is significantly influenced by the neutrino flavour since the neutrino may undergo beta reaction in the dynamical ejecta, changing the proton-to-neutron ratio. In modelling merger phenomena, it is common to leave out neutrino flavour conversions for computational ease, however, resonances in flavour conversions may change the neutrino population completely which changes the proton-to-neutron ratio. Therefore it is important to consider what types of resonances may occur during the propagation from the remnant to the outer layers. The main bulk of the theory section was dedicated to building the Hamiltonian for such Standard Model (SM) types of resonances. In addition, ever since the discovery of neutrino flavour oscillations, the neutrino sector of the SM has been undergoing continuous development, and many theories for effective low energy phenomena are being put forth, so-called Beyond The Standard Model physics or New Physics. The neutrinos have low interaction rates, and so they are still relatively unconstrained, and any interaction with new particles may have gone unnoticed. The effects of such undiscovered particles interacting in a Fermi point-like interaction with neutrinos and antineutrinos, and the effects of these interactions on neutrino flavour evolution, have been studied in this thesis.

In particular, I considered the coherent effects of new effective interactions through mediators which couple the different neutrino flavours to common matter, electron, and up- and down-quarks, found in astrophysical phenomena. These interactions are known as

Non-Standard Interactions (NSIs). The NSIs were first studied in a toy model, where they had such effects as shifting resonance locations, suppressing resonances or altering the final outcome of a resonance. They were studied in a toy model to find out how to approach a more realistic system.

A more realistic system came in the form of a simluated CBM remnant, a Binary Neutron Star (BNS) merger remnant, providing the background data for evolving the neutrinos. The geometry of such a system is complicated, and as such I made some assumptions. I defined a surface, the neutrinosphere, from which neutrinos are emitted, assumed that the neutrinos would propagate much faster than the remnant would change, and hence only considered linear trajectories which did not recross the emitting surface. From this, I constructed trajectories which would represent the general flavour evolution and found that both Matter-Neutrino-Resonances (MNR) and Mikheyev–Smirnov–Wolfenstein (MSW) resonances occurred in the system. The MNR flipped the neutrino flavour population, leaving the antineutrino unaltered. These trajectories I then disturbed by including NSIs and saw that the flavour evolution was heavily altered. In particular, a new resonance was possible, which was a Symmetric MSW resonance, MSW because it was the MSW resonance and symmetric because it worked for both neutrinos and antineutrinos, due to a sign change in the matter potential. Furthermore, the NSI MNRs were shown to change the SM MNRs, ending with a maximally converted antineutrino flavour population and leaving the neutrinos population unaltered, with the opposite populations for the SM case.

Since the geometry of the remnant is complicated, I averaged the result of many different trajectories starting from the emitting surface and going to a few endpoints to see what the overall effect of oscillations would be, for systems with only SM and then included NSIs afterwards. This showed that the overall region in which the trajectory started and the endpoints were the most important factors for the evolution. Finally, I analysed a parameter scan over possible NSI values, $(\delta\epsilon^n, \epsilon_0)$ in the range $\delta\epsilon^n = [-1, 5, 0.4]$ and $\epsilon_0 = [10^{-6}, 10^{-3}]$ for the endpoint $(150, 150)$. The scan could be segmented into overall sectors, which could be decomposed in terms of three types of trajectories: One which

experienced a single symmetric MSW, flipping both the neutrino and antineutrino flavour population. The second experienced a failed MNR, a symmetric MSW and a full MNR, where the symmetric MSW flipped the final outcome of the MNR, with respect to the SM case. The third trajectory went through a double symmetric MSW, ending up in the original configuration again. Variations on these systems described the overall final relative and total neutrino and antineutrino populations. In addition I provide NSI parameter scans for other endpoints of interest within the system, with brief explanations of their sectors.

All in all, the NSIs considered in this thesis have a large, and varied impact on the overall neutrino flavour evolution in the BNS merger remnant, in many sectors of the NSI parameter space. Although the final results are varied they may be described by a few simple resonances, namely symmetric MSW and MNR resonances, although the geometry affects if the resonances can be sustained. The final flavour evolution will in turn affect the neutron-rich matter in the dynamic ejecta and thereby affect the r-processes.

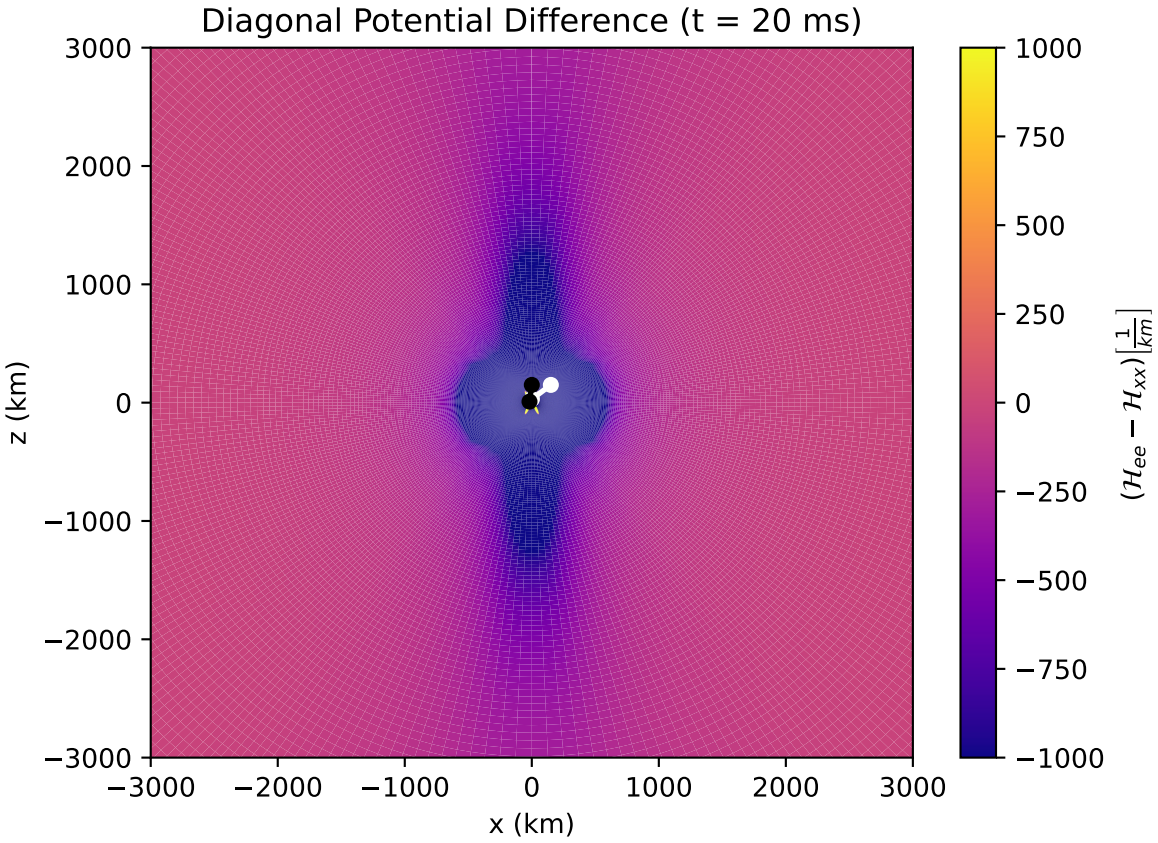

Figure 35: Diagonal Potential Difference at $3 \cdot 10^3$ km distance, with the two original trajectories still visible. The symmetric MSW is expected to occur at the change from dark purple to lilac, at around 600 km from the remnant at the earliest. The MNR effects that have been studied in subsubsection end at around 400 km, so before this region is reached.

Appendix

x	z
-112.56	0.91
-90.14	29.91
-62.57	31.47
-44.78	25.82
-34.73	20.67
-25.65	14.81
-18.11	9.09
-11.66	4.04
112.55	0.91
90.15	29.91
62.57	31.47
44.78	25.82
34.73	20.67
25.65	14.81
18.11	9.09
11.66	4.04

These figures refer to the parameter scan subsection.

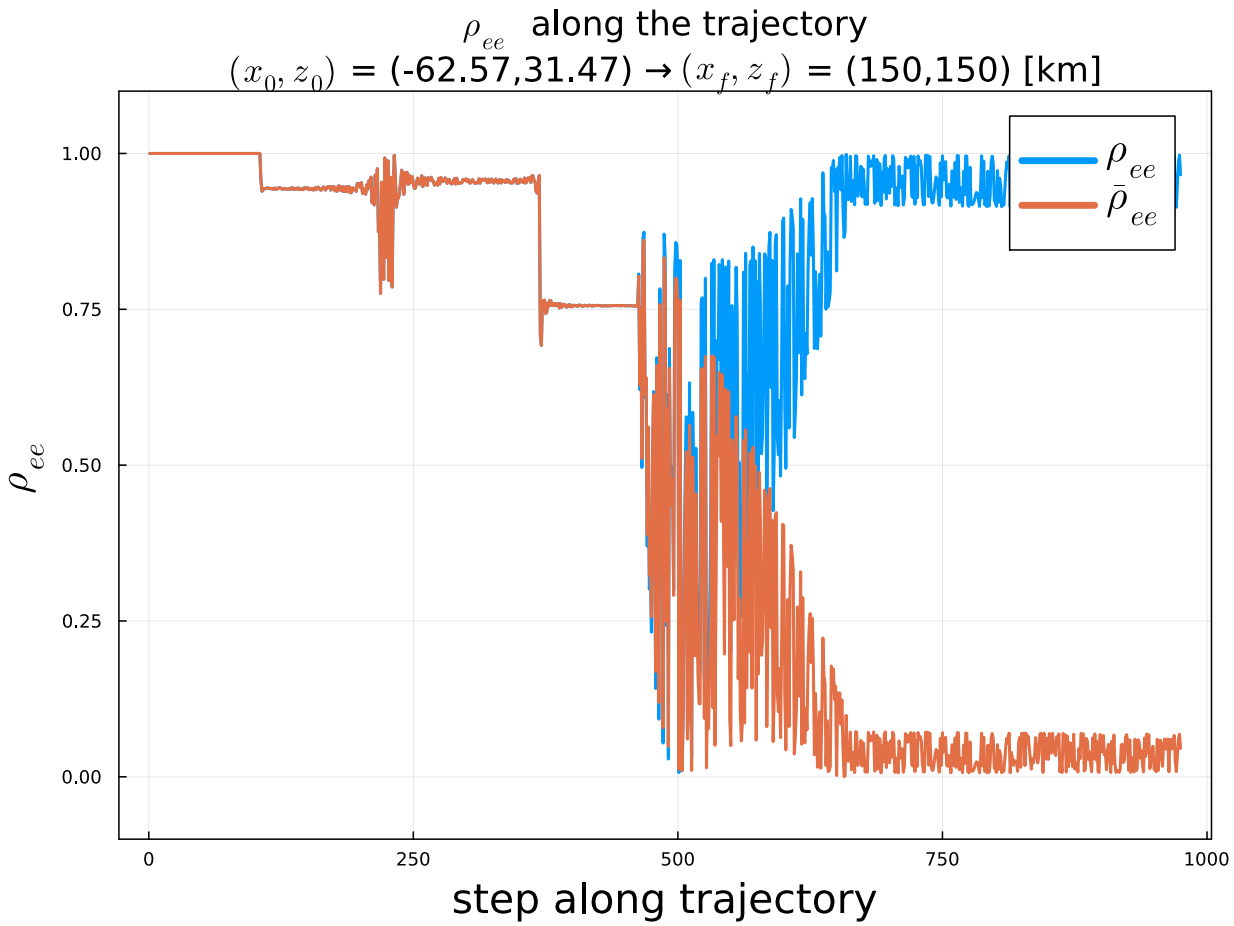

Figure 36: Example of trajectory in lower left corner of parameter scan for (150,150)$\delta\epsilon^n = -1.5$ and $\epsilon_0 = 10^{-6}$. Two halted MSW effects and a final MNR. The x-axis is not distance along trajectory in km, but the step along the trajectory, although it has the same scale as figures in subsection

.

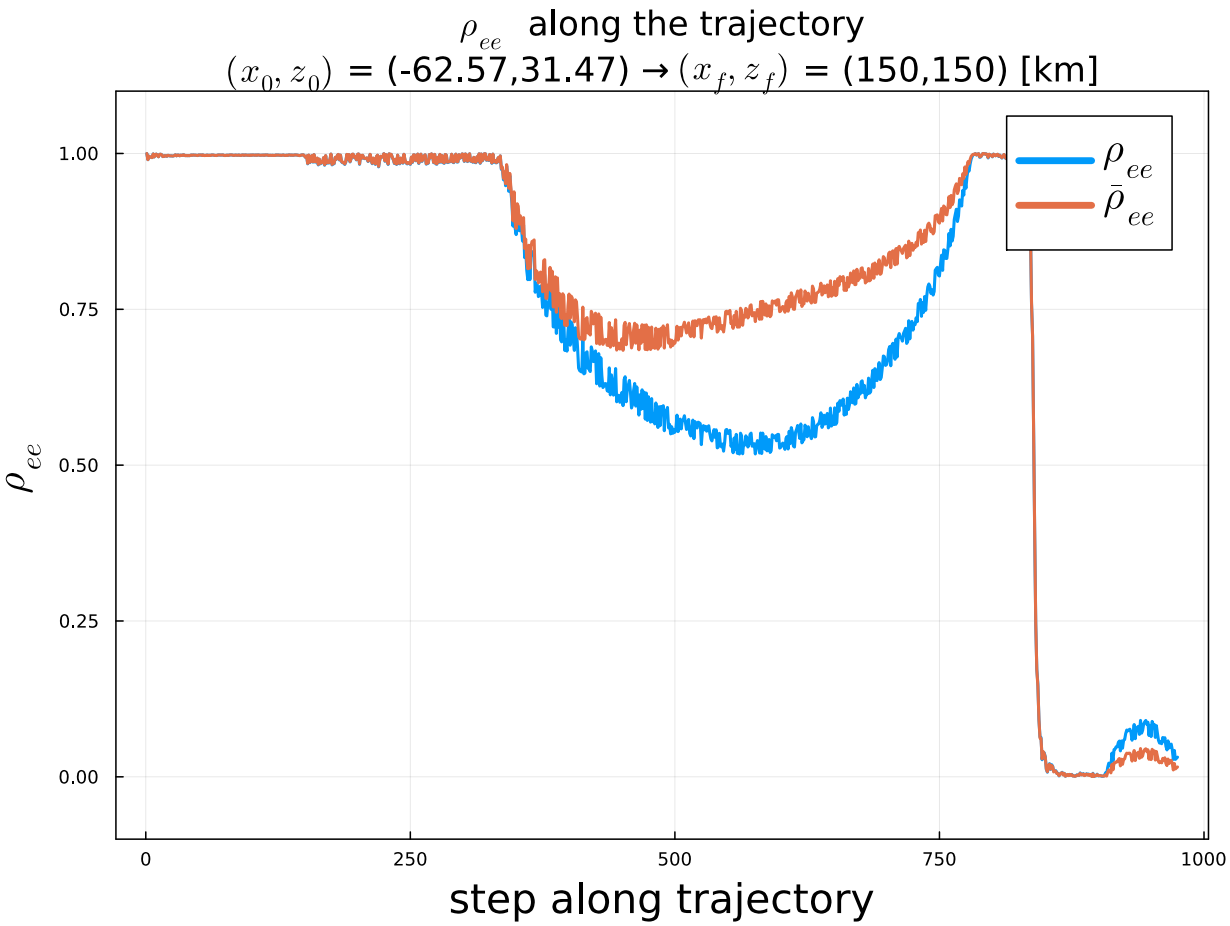

Figure 37: Example of trajectory in center of parameter scan for (150,150)$\delta\epsilon^n = -0.4$ and $\epsilon_0 = 10^{-4}$. Two reversed MNR effects and a middle MSW. The x-axis is not distance along trajectory in km, but the step along the trajectory, although it has the same scale as figures in subsection .

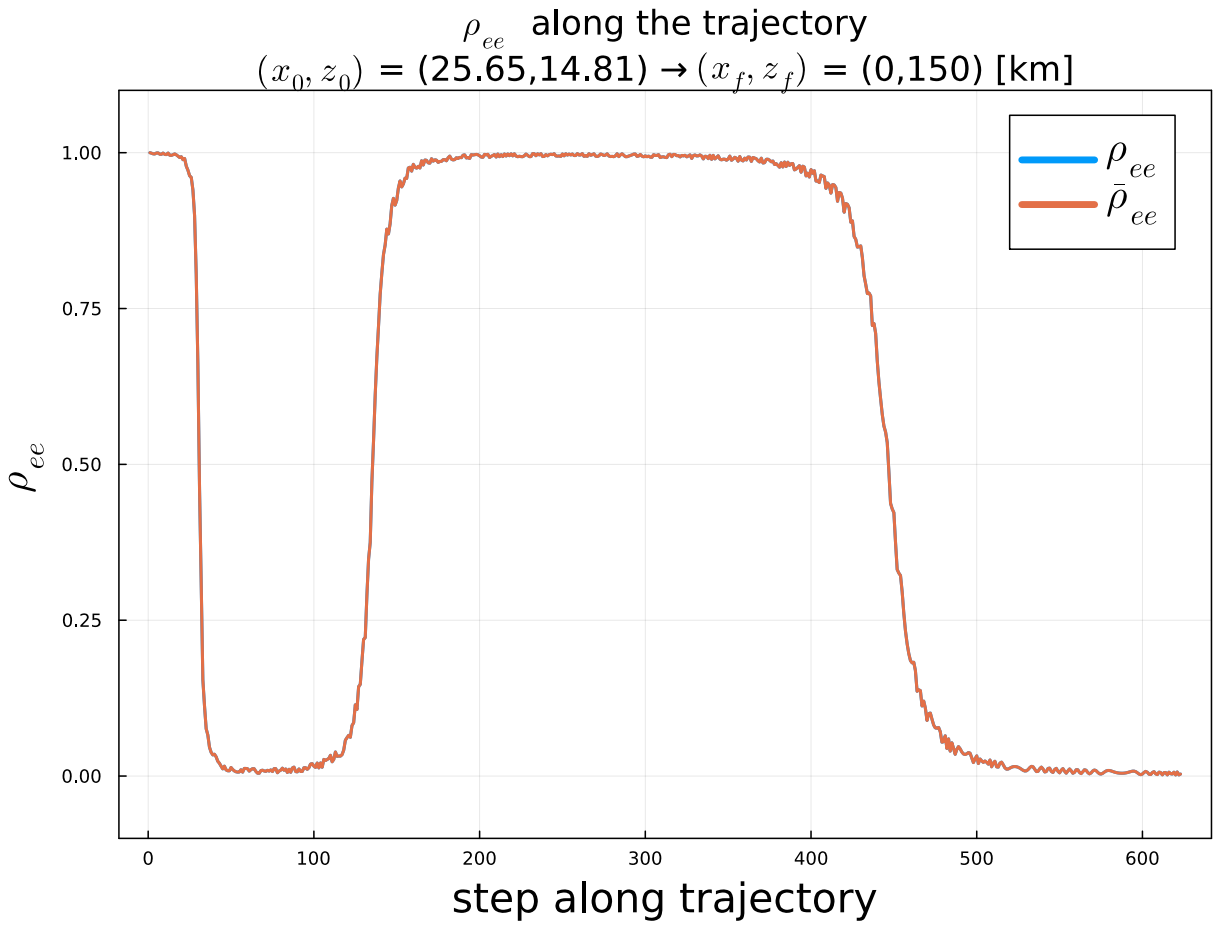

Figure 38: Three symmetric MSW in for the $(150, 250)$ endpoint, starting from (25.65,14.81)

References

[1] O. Just, A. Bauswein, R. A. Pulpillo, S. Goriely, and H. T. Janka, "Comprehensive nucleosynthesis analysis for ejecta of compact binary mergers," 6 2014. [Online]. Available: http://arxiv.org/abs/1406.2687http://dx.doi.org/10.1093/mnras/stv009

[2] A. Chatelain and M. C. Volpe, "Neutrino propagation in binary neutron star mergers in presence of nonstandard interactions," 10 2017. [Online]. Available: http://arxiv.org/abs/1710.11518http://dx.doi.org/10.1103/PhysRevD.97.023014

[3] E. Vitagliano, I. Tamborra, and G. Raffelt, "Grand unified neutrino spectrum at earth: Sources and spectral components," *Reviews of Modern Physics*, vol. 92, 12 2020.

[4] A. Y. Smirnov, "Neutrino conversion and neutrino astrophysics *," 1998.

[5] A. S. Dighe and A. Y. Smirnov, "Identifying the neutrino mass spectrum from a supernova neutrino burst," 1999.

[6] C. J. Stapleford, D. J. Väänänen, J. P. Kneller, G. C. McLaughlin, and B. T. Shapiro, "Nonstandard neutrino interactions in supernovae," 5 2016. [Online]. Available: http://arxiv.org/abs/1605.04903http://dx.doi.org/10.1103/PhysRevD.94.093007

[7] "p1072."

[8] Y.-L. Zhu, A. Perego, and G. C. McLaughlin, "Matter neutrino resonance transitions above a neutron star merger remnant," 7 2016. [Online]. Available: http://arxiv.org/abs/1607.04671http://dx.doi.org/10.1103/PhysRevD.94.105006

[9] A. Malkus, A. Friedland, and G. C. McLaughlin, "Matter-neutrino resonance above merging compact objects," 3 2014. [Online]. Available: http://arxiv.org/abs/1403.5797

[10] S. Shalgar, "Multi-angle calculation of the matter-neutrino resonance near an accretion disk," 7 2017. [Online]. Available: http://arxiv.org/abs/1707.07692http://dx.doi.org/10.1088/1475-7516/2018/02/010

[11] A. Malkus, J. P. Kneller, G. C. McLaughlin, and R. Surman, "Neutrino oscillations above black hole accretion disks: disks with electron-flavor emission," 7 2012. [Online]. Available: http://arxiv.org/abs/1207.6648http://dx.doi.org/10.1103/PhysRevD.86.085015

[12] M.-R. Wu, H. Duan, and Y.-Z. Qian, "Physics of neutrino flavor transformation through matter-neutrino resonances," 9 2015. [Online]. Available: http://arxiv.org/abs/1509.08975http://dx.doi.org/10.1016/j.physletb.2015.11.027

[13] A. Vlasenko and G. C. McLaughlin, "Matter-neutrino resonance in a multi-angle neutrino bulb model," 1 2018. [Online]. Available: http://arxiv.org/abs/1801.07813http://dx.doi.org/10.1103/PhysRevD.97.083011

[14] J. Y. Tian, A. V. Patwardhan, and G. M. Fuller, "Neutrino flavor evolution in neutron star mergers," 3 2017. [Online]. Available: http://arxiv.org/abs/1703.03039http://dx.doi.org/10.1103/PhysRevD.96.043001

[15] D. Vaananen and G. C. McLaughlin, "Uncovering the matter-neutrino resonance," 10 2015. [Online]. Available: http://arxiv.org/abs/1510.00751http://dx.doi.org/10.1103/PhysRevD.93.105044

[16] H. Duan, G. M. Fuller, and Y. Z. Qian, "Collective neutrino flavor transformation in supernovae," *Physical Review D - Particles, Fields, Gravitation and Cosmology*, vol. 74, 2006.

[17] T. Ohlsson and H. Snellman, "Three flavor neutrino oscillations in matter," 2000.

[18] H. Duan, "Flavor oscillation modes in dense neutrino media," 9 2013. [Online]. Available: http://arxiv.org/abs/1309.7377http://dx.doi.org/10.1103/PhysRevD.88.125008

[19] C. Volpe, D. Väänänen, and C. Espinoza, "Extended evolution equations for neutrino propagation in astrophysical and cosmological environments," *Physical Review D - Particles, Fields, Gravitation and Cosmology*, vol. 87, 6 2013.

[20] Y.-Z. Gian and G. M. Fuller', "Neutrino-neutrino scattering and matter-enhanced neutrino flavor transformation in supernovae," 1995.

[21] H. Duan, G. M. Fuller, and Y.-Z. Qian, "Collective neutrino oscillations," 1 2010. [Online]. Available: http://arxiv.org/abs/1001.2799http://dx.doi.org/10.1146/annurev.nucl.012809.104524

[22] G. Fantini, A. G. Rosso, F. Vissani, and V. Zema, "The formalism of neutrino oscillations: an introduction," 2 2018. [Online]. Available: http://arxiv.org/abs/1802.05781

[23] Y.-Z. Qian and G. M. Fuller, "Neutrino-neutrino scattering and matter-enhanced neutrino flavor transformation in supernovae," 1994.

[24] Y. Farzan and M. Tortola, "Neutrino oscillations and non-standard interactions," 10 2017. [Online]. Available: http://arxiv.org/abs/1710.09360

[25] S. Davidson, E. Nardi, and Y. Nir, "Leptogenesis," 2 2008. [Online]. Available: http://arxiv.org/abs/0802.2962http://dx.doi.org/10.1016/j.physrep.2008.06.002

[26] C. Giunti and W. K. Chung, *Fundamentals of Neutrino Physics and Astrophysics*, 2007, vol. 1.

[27] B. Pontecorvo, "Inverse beta processes and nonconservation of lepton charge," *Zh. Eksp. Teor. Fiz. 34 (1957)*, p. 247, 1957.

[28] R. Davis, "A review of the homestake solar neutrino experiment," *Progress in Particle and Nuclear Physics*, vol. 32, pp. 13–32, 1 1994.

[29] Q. R. Ahmad and et al, "Direct evidence for neutrino flavor transformation from neutral-current interactions in the sudbury neutrino observatory," *Physical Review Letters*, vol. 89, 2002.

[30] E. Akhmedov, "Quantum mechanics aspects and subtleties of neutrino oscillations," 1 2019. [Online]. Available: http://arxiv.org/abs/1901.05232

[31] R. L. Workman and et al (Particle Data Group)., "Prog. theor. exp. phys., 083c01," 2022.

[32] I. Padilla, "Neutrino flavor conversion in dense astrophysical environments," 2022.

[33] G. Sigl and G. Raffelt, "General kinetic description of relativistic mixed neutrinos," *Nuclear Physics B*, vol. 406, pp. 423–451, 9 1993.

[34] L. Johns and Z. Xiong, "Collisional instabilities of neutrinos and their interplay with fast flavor conversion in compact objects," 8 2022. [Online]. Available: http://arxiv.org/abs/2208.11059http://dx.doi.org/10.1103/PhysRevD.106.103029

[35] S. Shalgar, "Insights into coherent forward scattering of neutrinos," 2022.

[36] D. Vaananen and G. C. McLaughlin, "Uncovering the matter-neutrino resonance," 10 2015. [Online]. Available: http://arxiv.org/abs/1510.00751http://dx.doi.org/10.1103/PhysRevD.93.105044

[37] A. Malkus, A. Friedland, and G. C. McLaughlin, "Matter-neutrino resonance above merging compact objects," 3 2014. [Online]. Available: http://arxiv.org/abs/1403.5797

[38] S. Hannestad, G. G. Raffelt, G. Sigl, and Y. Y. Y. Wong, "Self-induced conversion in dense neutrino gases: Pendulum in flavour space," 2007.

[39] P. Coloma, M. C. Gonzalez-Garcia, M. Maltoni, J. P. Pinheiro, and S. Urrea, "Global constraints on non-standard neutrino interactions with quarks and electrons," 5 2023. [Online]. Available: http://arxiv.org/abs/2305.07698

[40] P. S. B. Dev, K. S. Babu, P. B. Denton, P. A. N. Machado, C. A. Argüelles, J. L. Barrow, S. S. Chatterjee, M.-C. Chen, A. de Gouvêa, B. Dutta, D. Gonçalves, T. Han, M. Hostert, S. Jana, K. J. Kelly, S. W. Li, I. Martinez-Soler, P. Mehta, I. Mocioiu, Y. F. Perez-Gonzalez, J. Salvado, I. M. Shoemaker, M. Tammaro, A. Thapa, J. Turner, and X.-J. Xu, "Neutrino

non-standard interactions: A status report," 7 2019. [Online]. Available: http://arxiv.org/abs/1907.00991http://dx.doi.org/10.21468/SciPostPhysProc.2.001

[41] D. V. Forero and W.-C. Huang, "Sizable nsi from the $su(2)_l$ scalar doublet-singlet mixing and the implications in dune," 8 2016. [Online]. Available: http://arxiv.org/abs/1608.04719http://dx.doi.org/10.1007/JHEP03(2017)018

[42] D. Xiao, Z.-G. Dai, and P. Meszaros, "Prompt neutrino emission of gamma-ray bursts in the dissipative photospheric scenario revisited: Possible contributions from cocoons," 6 2017. [Online]. Available: https://arxiv.org/abs/1706.01293

[43] I. Tamborra and S. Shalgar, "New developments in flavor evolution of a dense neutrino gas," 11 2020. [Online]. Available: http://arxiv.org/abs/2011.01948http://dx.doi.org/10.1146/annurev-nucl-102920-050505

[44] G. Sigurðarson, I. Tamborra, and M.-R. Wu, "Resonant production of light sterile neutrinos in compact binary merger remnants," 9 2022. [Online]. Available: http://arxiv.org/abs/2209.07544http://dx.doi.org/10.1103/PhysRevD.106.123030

[45] P. S. B. Dev, K. S. Babu, P. B. Denton, P. A. N. Machado, C. A. Argüelles, J. L. Barrow, S. S. Chatterjee, M.-C. Chen, A. de Gouvêa, B. Dutta, D. Gonçalves, T. Han, M. Hostert, S. Jana, K. J. Kelly, S. W. Li, I. Martinez-Soler, P. Mehta, I. Mocioiu, Y. F. Perez-Gonzalez, J. Salvado, I. M. Shoemaker, M. Tammaro, A. Thapa, J. Turner, and X.-J. Xu, "Neutrino non-standard interactions: A status report," 7 2019. [Online]. Available: http://arxiv.org/abs/1907.00991http://dx.doi.org/10.21468/SciPostPhysProc.2.001

[46] P. Coloma, M. C. Gonzalez-Garcia, M. Maltoni, J. P. Pinheiro, and S. Urrea, "Global constraints on non-standard neutrino interactions with quarks and electrons," 5 2023. [Online]. Available: http://arxiv.org/abs/2305.07698

[47] S. Mertens, "Direct neutrino mass experiments," 5 2016. [Online]. Available: http://arxiv.org/abs/1605.01579http://dx.doi.org/10.1088/1742-6596/718/2/022013

[48] J. Bjorken and S. Drell, *Relativistic Quantum Mechanics*, 1964.

[49] M. Schwartz, *Quantum Field Theory and the Standard Model*, 2014.